ABSTRACT

LIN, CHUNG-YI. Determination of the Fracture Parameters in a Stiffened Composite Panel. (Under the direction of Dr. F. G. Yuan)

A modified J-integral, namely the equivalent domain integral, is derived for a three-dimensional anisotropic cracked solid to evaluate the stress intensity factor along the crack front using the finite element method. Based on the equivalent domain integral method with auxiliary fields, an interaction integral is also derived to extract the second fracture parameter, the T-stress, from the finite element results. The auxiliary fields are the two-dimensional plane strain solutions of monoclinic materials with the plane of symmetry at x_3=0 under point loads applied at the crack tip. These solutions are expressed in a compact form based on the Stroh formalism. Both integrals can be implemented into a single numerical procedure to determine the distributions of stress intensity factor and T-stress components, T_{11}, T_{13}, and thus T_{33}, along a three-dimensional crack front.

The effects of plate thickness and crack length on the variation of the stress intensity factor and T-stresses through the thickness are investigated in detail for through-thickness center-cracked plates (isotropic and orthotropic) and orthotropic stiffened panels under pure mode-I loading conditions. For all the cases studied, T_{11} remains negative. For plates with the same dimensions, a larger size of crack yields larger magnitude of the normalized stress intensity factor and normalized T-stresses. The results in orthotropic stiffened panels exhibit an opposite trend in general. As expected, for the

thicker panels, the fracture parameters evaluated through the thickness, except the region near the free surfaces, approach two-dimensional plane strain solutions. In summary, the numerical methods presented in this research demonstrate their high computational effectiveness and good numerical accuracy in extracting these fracture parameters from the finite element results in three-dimensional cracked solids.

DETERMINATION OF THE FRACTURE PARAMETERS IN A STIFFENED COMPOSITE PANEL

by

CHUNG-YI LIN

A dissertation submitted to the Graduate Faculty of
North Carolina State University
in partial fulfillment of the
requirements for the Degree of
Doctor of Philosophy

MECHANICAL ENGINEERING

Raleigh
2000

Approved By:

Dr. Jeffrey W. Eischen

Dr. Kerry S. Havner

Dr. Eric C. Klang

Dr. Fuh-Gwo Yuan
Chair of Advisory Committee

BIOGRAPHY

Chung-yi Lin was born in Tainan, Taiwan in November 1967. He graduated from Taipei Municipal Chien-Kuo Senior High School in June 1985 and received a Bachelor of Science degree in mechanical engineering from National Tsing Hua University at Hsinchu, Taiwan in June 1990. Before attending State University of New York at Buffalo in August 1993, he served in Taiwan's Army for two years as a second lieutenant and worked as a research assistant in the Department of Engineering and System Science (the former Department of Nuclear Engineering) at National Tsing Hua University. He completed his Master of Science project, *Finite Element Analysis of Solid Contact of Rough Surfaces by ANSYS 5.0A*, under the direction of Dr. Andres Soom of Mechanical and Aerospace Engineering at SUNY-Buffalo, in June 1995. In the following years, Chung-yi Lin held several engineering positions across different industries in Taiwan. That included a CAE Engineer providing ANSYS technical support and training in the Taiwan Auto-Design Company at Taipei; a Senior Engineer performing thermal-stress analysis on various IC packages in the Advanced Semiconductor Engineering, Inc. at Kaohsiung; and a Foreman in the China Steel Corporation at Kaohsiung, where he assisted test-running of a newly built production line and supervised three shifts of workers. These industrial experiences motivated him to pursue higher education in the mechanical engineering field, for which he entered the doctorate program of Mechanical Engineering at North Carolina State University in August 1997. His research at NCSU focused on computational fracture mechanics for anisotropic materials.

ACKNOWLEDGMENTS

First and foremost, I am indebted to my advisor, Dr. F. G. Yuan for his guidance during these last three and half years. My research has benefited greatly from his exceptional knowledge and experience, as well as the "open door" policy he has always maintained. I would like also to thank the remainder of my committee – Dr. J. W. Eischen, Dr. K. S. Havner, and Dr. E. C. Klang – for the roles they have played in my education, both on my committee and in the classroom. Thanks also go to Dr. S. Yang of the Mars Mission Research Center at NCSU for his knowledgeable advice and discussions on this dissertation.

Support for this research is from NASA Langley Research Center under Grant No. 98-0548. The computing support from North Carolina Supercomputing Center is greatly appreciated. The computations presented herein required a huge amount of CPU time. Without allocations from NCSC, many of the cases would not yet be completed.

For almost the past three decades, I have been privileged to have many great teachers throughout the different schools I have attended. Their contributions to my education are substantial. I would like to say, "thank you very much!" I will always remember the impact each of you had on my academic success.

I would like also to recognize some of my fellow graduate students for all sorts of help and international friendships. These include Parsaoran Hutapea, Fei Liang, Xiao Lin, and Benjamin Shipman.

Last but definitely not least, I would like to thank my family for their never-ending support, love and encouragement. Special appreciation goes to my parents, who always stand behind my idea of pursuing higher education. I am very grateful to my wife Chieh-sheng. Words cannot express how much her support and love have meant to me. Our daughter Angela gives me so much happiness and amusement. Her presence in my life has also fortified my determination to complete the graduate work.

TABLE OF CONTENTS

List of Tables vi

List of Figures vii

Nomenclature x

1 Introduction 1

2 Equivalent Domain Integral (EDI) 8

2.1 Mathematical Formulation 8

2.2 Numerical Implementation 12

2.2.1 The Jacobian Matrix 13

2.2.2 The Stress Tensor and Stress-Work Density 14

2.2.3 The Derivatives of the s-Function 14

2.2.4 The Derivatives of the Displacements 15

3 Interaction Integral 19

3.1 Auxiliary Fields for T_{11} 21

3.2 Auxiliary Fields for T_{13} 28

4 Stress Intensity Factor and T-Stress 32

4.1 Stress Intensity Factor 32

4.2 T-Stress 33

5 Models 35

5.1 Plates 35

5.2 Stiffened Panels 36

6 Results 43

6.1 Isotropic Plates 43

6.1.1 Crack Length 44

6.1.2 Plate Thickness 46

6.2 Orthotropic Plates 47

6.2.1 Crack Length 48
6.2.2 Plate Thickness 49
6.3 Stiffened Panels 51
7 Summary and Conclusions 69
References 72
Appendices 76
A. ANSYS Program 77
B. FORTRAN Program 86

List of Tables

Table 6.1 Material properties of the orthotropic plate 48

List of Figures

Figure 1.1 An arbitrary path on which a line integral is to be calculated 6

Figure 1.2 The cracked stiffened panel to be analyzed in the dissertation. (Courtesy of NASA Langley Research Center) 7

Figure 2.1 A small cylindrical volume around a segment of crack front, with the local coordinate system shown 17

Figure 2.2 A domain enclosing a segment of crack front 17

Figure 2.3 The schematic finite element mesh near a segment of the crack front 18

Figure 2.4 A 20-node element with the associated s-functions 18

Figure 3.1 Auxiliary line load on a three-dimensional crack: (a) uniform forces f_1 normal to crack front; (b) uniform forces f_3 parallel to crack front 31

Figure 3.2 Locations of the integration points inside an element 31

Figure 5.1 A through-thickness center-cracked plate subjected to a uniform far-field displacement 38

Figure 5.2 One-eighth of the plate to be generated as a finite element model 38

Figure 5.3 Finite element mesh of a one-eighth center-cracked plate (a/w=0.1) 39

Figure 5.4 Mesh refinement near crack front region 39

Figure 5.5 Radius of the outer surface of Ring #12 equals to $100e_0$ 40

Figure 5.6 Sizes of element layers in terms of the half thickness t 40

Figure 5.7 Configuration and dimensions of a center-cracked panel with stiffeners 41

Figure 5.8 The finite element model of a one-fourth center-cracked stiffened panel (a'/w'=0.1) 41

Figure 5.9 Enlarged finite element mesh showing definition of the crack aspect ratio a'/w' (a'/w'=0.1) 42

Figure 5.10 Mesh refinements near the crack front of the stiffened panel (a'/w'=0.1) 42

Figure 6.1 Normalized stress intensity factors through half of the thickness for isotropic plates of t=0.165 in. (t/w=0.00825) with various a/w ratios. 54

Figure 6.2 Normalized stress intensity factors at center of the thickness (x_3/t=0) for isotropic plates with two different thicknesses 54

Figure 6.3 Normalized T_{11} stresses through half of the thickness for isotropic plates of t=0.165 in. (t/w=0.00825) with various a/w ratios 55

Figure 6.4 Normalized T_{11} stresses at center of the thickness (x_3/t=0) for isotropic plates with two different thicknesses 55

Figure 6.5 Normalized T_{13} stresses through half of the thickness for isotropic plates of t=0.165 in. (t/w=0.00825) with various a/w ratios..... 56

Figure 6.6 Normalized T_{13} stresses at quarter of the thickness (x_3/t=0.5) for isotropic plates with two different thicknesses 56

Figure 6.7 Normalized stress intensity factors through half of the thickness for isotropic plates of a/w=0.1 with various t/w ratios 57

Figure 6.8 Normalized stress intensity factors at center of the thickness (x_3/t=0) for isotropic plates of a/w=0.1 57

Figure 6.9 Normalized T_{11} stresses through half of the thickness for isotropic plates of a/w=0.1 with various t/w ratios..... 58

Figure 6.10 Normalized T_{11} stresses at center of the thickness (x_3/t=0) for isotropic plates of a/w=0.1 58

Figure 6.11 Normalized T_{13} stresses through half of the thickness for isotropic plates of a/w=0.1 with various t/w ratios..... 59

Figure 6.12 Normalized T_{13} stresses at quarter of the thickness (x_3/t=0.5) for isotropic plates of a/w=0.1 59

Figure 6.13 Normalized stress intensity factors through half of the thickness for orthotropic plates of t=0.165 in. (t/w=0.00825) with various a/w ratios 60

Figure 6.14 Normalized stress intensity factors at center of the thickness (x_3/t=0) for orthotropic plates with two different thicknesses 60

Figure 6.15 Normalized T_{11} stresses through half of the thickness for orthotropic plates of t=0.165 in. (t/w=0.00825) with various a/w ratios 61

Figure 6.16 Normalized T_{11} stresses at center of the thickness (x_3/t=0) for orthotropic plates with two different thicknesses 61

Figure 6.17 Normalized T_{13} stresses through half of the thickness for orthotropic plates of t=0.165 in. (t/w=0.00825) with various a/w ratios 62

Figure 6.18 Normalized T_{13} stresses at quarter of the thickness (x_3/t=0.5) for orthotropic plates with two different thicknesses 62

Figure 6.19 Normalized stress intensity factors through half of the thickness for orthotropic plates of a/w=0.1 with various t/w ratios 63

Figure 6.20 Normalized stress intensity factors at center of the thickness (x_3/t=0) for orthotropic plates of a/w=0.1 63

Figure. 6.21 Normalized T_{11} stresses through half of the thickness for orthotropic plates of a/w=0.1 with various t/w ratios 64

Figure 6.22 Normalized T_{11} stresses at center of the thickness (x_3/t=0) for orthotropic plates of a/w=0.1 64

Figure 6.23 Normalized T_{13} stresses through half of the thickness for orthotropic plates of a/w=0.1 with various t/w ratios 65

Figure 6.24 Normalized T_{13} stresses at quarter of the thickness (x_3/t=0.5) for orthotropic plates of a/w=0.1 65

Figure 6.25 Normalized stress intensity factors through the thickness for orthotropic stiffened panels of t=0.165 in. (t/w=0.00825) with various a'/w' ratios 66

Figure 6.26 Normalized stress intensity factors at center of the thickness (x_3/t=0) for orthotropic stiffened panels with various a'/w' ratios for two thicknesses ... 66

Figure 6.27 Normalized T_{11} stresses through the thickness for orthotropic stiffened panels of t=0.165 in. (t/w=0.00825) with various a'/w' ratios 67

Figure 6.28 Normalized T_{11} stresses at center of the thickness (x_3/t=0) for orthotropic stiffened panels with various a'/w' ratios for two thicknesses 67

Figure 6.29 Normalized T_{13} stresses through the thickness for orthotropic stiffened panels of t=0.165 in. (t/w=0.00825) with various a'/w' ratios 68

Figure 6.30 Normalized T_{13} stresses at center of the thickness (x_3/t=0) for orthotropic stiffened panels with various a'/w' ratios for two thicknesses 68

Nomenclature

Latin symbols:

A	Complex matrix containing Stroh eigenvectors
$A, A_\varepsilon, A_1, A_2$	Surfaces on a domain
a	Half crack length
a'	Half crack length calculated from the edge of the central stiffener to the crack front
B	Complex matrix containing Stroh eigenvectors
B	Stress biaxiality ratio
C	Stiffness matrix
$\mathbf{C}^0$	Reduced stiffness matrix
C_{ij}	Components of stiffness matrix
E	Young's modulus
E_X, E_Y, E_Z	Young's moduli of an orthotropic material
e	Expression for manipulation of eigenvalues of elastic constants
e_0	Radial size of finite elements attached on crack front
F	Total nodal force on one end of a panel (plate)
f	Auxiliary line load vector
f	Area under the s-function curve
f_1	Auxiliary uniform line load normal to crack front
f_3	Auxiliary uniform line load parallel to crack front
$f_{ij}^{(n)}(\theta),\ f_{ij}(\theta)$	Functions of the angle of orientation in the asymptotic equation
G	Energy release rate
G_{XY}, G_{YZ}, G_{XZ}	Shear moduli of an orthotropic material
I	Identity matrix
$I, I_1, I^{(1)}, I^{(2)}$	Values of the interaction integral
i	$\sqrt{-1}$
J	Jacobian matrix

J, J_1	Values of J-integral or the equivalent domain integral
$K, K_{\mathrm{I}}, K_{\mathrm{II}}, K_{\mathrm{III}}$	Stress intensity factors
$\overline{K}_{\mathrm{I}}$	Normalized stress intensity factor
$\mathbf{k}$	Vector for local stress intensity factors
$k_{\mathrm{I}}, k_{\mathrm{II}}, k_{\mathrm{III}}$	Local stress intensity factors
k_1, k_2, k_3	Normalization factors in Stroh formalism
$\mathbf{L}, \mathbf{L}(\theta)$	Barnette-Lothe tensors
l	Half panel (plate) length
l_c	Characteristic length of a finite element mesh
m	Expression for manipulation of reduced compliance
N_j	Shape function of the j-th node in an element
$\mathbf{n}$	unit normal vector
n_j	The j-th directional component of the unit normal vector
p_1, p_2	Expressions in Stroh eigenvectors
Q	Simplified symbol for terms in J-integral calculation
q_1, q_2	Expressions in Stroh eigenvectors
r	Distance from a crack tip; the first coordinate in a polar coordinate system
$\mathbf{S}, \mathbf{S}(\theta)$	Barnette-Lothe tensors
$\mathbf{s}$	Compliance matrix
$\mathbf{s}^0$	Reduced compliance matrix
$\mathbf{s}'$	Vector of the derivatives of the s-function
s	Spatial weighting function (also called s-function)
$s^{(j)}$	Value of the s-function on the j-th node of an element
s_{ij}	Components of compliance matrix
s'_{ij}	Components of reduced compliance matrix
T, T_{ij}	Elastic T-stress
T_{11}, T_{13}, T_{33}	Components of T-stress
$\overline{T}_{11}, \overline{T}_{13}$	Normalized T-stresses
$\mathbf{t}_{\mathrm{r}}$	Traction vector

t	Half panel (plate) thickness
$\bar{t}$	Normalized panel (plate) thickness
$\mathbf{u}$	Displacement vector
$\mathbf{u}^{\mathrm{a}}$	Auxiliary displacement vector
u_i, u_k	Components of displacement vector
u_i^{a}	Components of the auxiliary displacement field
u_∞	Far-field displacement applied on the ends of a panel (plate)
V, V_ε	Volumes of a domain
W	Stress-work density
w	Half panel (plate) width
w'	Distance between edges of two adjacent stiffeners
w_m, w_n, w_p	Integration weights
X, Y, Z	Global Cartesian coordinates in a panel (plate)
x_1, x_2, x_3	Cartesian coordinates of a local (crack front) coordinate system
y_1, y_2	Real parts of complex numbers
z_1, z_2	Imaginary parts of complex numbers

Greek symbols:

Γ	An arbitrary path around a crack tip
Δ	Length of a segment of crack front
ε^{c}	Contracted strain vector
ε	Radius of a small cylindrical volume encompassing a segment of crack front
ε_i	Components of contracted strain vector
ε_{ij}	Components of strain tensor
$\varepsilon_{ij}^{\mathrm{a}}$	Components of the auxiliary strain field
ζ	The third coordinate in an element coordinate system
η	The second coordinate in an element coordinate system
θ	Angle of orientation; the second coordinate in a polar coordinate system
μ_α	Eigenvalues of elastic constants

ν	Poisson's ratio
ν_{XY}, ν_{YZ}, ν_{XZ}	Poisson's ratios of an orthotropic material
ξ	The first coordinate in an element coordinate system
σ	Stress tensor
σ^{a}	Auxiliary stress tensor
σ^{c}	Contracted stress vector
σ_{ij}	Components of stress tensor
σ_{ij}^{a}	Components of the auxiliary stress field
σ_{∞}	Average stress applied on the ends of a panel (plate)
ς_{α}	Simplified symbol for expressions associated eigenvalues of elastic constants
ϕ^{a}	Auxiliary stress function
ϕ_1, ϕ_2	Components of auxiliary stress function
Ω_{α}	Derivative of ς_{α}

1 Introduction

The study of fracture mechanics emerged in the early twentieth century. Among a handful of researchers, Griffith's idea of "minimum potential energy" [1] provided a foundation for all later successful theoretical studies of fracture, especially for brittle materials. But it was not until after World War II that fracture mechanics developed as a discipline. Derived from Griffith's theorem, the concept of energy release rate, G, was first introduced by Irwin [2], and was in a form that is more useful for engineering applications. He defined the energy release rate, or the crack extension force tendency so that it can be determined from the stress and displacement fields in the vicinity of the crack tip rather than from considering an energy balance for the elastic solid as a whole, as Griffith suggested. Irwin also used the Westergaard stress function [3] to show that the stresses and displacements near the crack tip of an isotropic linear elastic material in mode-I plane stress could be described by a single parameter, K, that is related to the energy release rate [4], i.e.,

$$G = K^2/E\,, \tag{1.1}$$

where E is the Young's modulus. For plane strain, E is replaced by $E/(1-\nu^2)$. This crack tip characterizing parameter later became known as the stress intensity factor.

Rice [5] later defined a path-independent J-integral for two-dimensional crack problems in linear and nonlinear elastic materials. As shown in Figure 1.1, J is the line integral surrounding a two-dimensional crack tip and is defined as

$$J = \int_{\Gamma} (W dx_2 - \sigma_{ij} n_j \frac{\partial u_i}{\partial x_1} ds)\,, \qquad i,j = 1,2 \tag{1.2}$$

where Γ is a curve surrounding the crack tip, W is the stress-work density, σ_{ij} are components of the stress tensor, n_j is the j-th directional component of the unit normal vector on the path Γ, and ds is an element of arc length along Γ. It was shown that the J-integral is a more general type of energy release rate. For a linear elastic material, $G = J$.

Therefore, the stress intensity factor K can be readily obtained, according to Eq.(1.1) and the computational efficiency of the J-integral, as

$$K = \sqrt{JE}\,. \tag{1.3}$$

The J-integral is effective for evaluating K in two-dimensional crack problems. For three-dimensional problems, however, it is difficult to distinguish K at different x_3 locations, assuming the line integral is performed on the x_1-x_2 plane. Thus an alternative procedure needs to be developed to determine the distribution of K through the thickness. Parks [6] employed the virtual crack extension method to determine J from elastic-plastic finite element solutions. The method is based on an energy comparison of two slightly different crack lengths and requires only one elastic-plastic finite element solution, because the altered crack configuration is obtained by changing nodal positions. The procedure is directly applicable to two-dimensional configurations but can be extended in a straightforward manner to obtain arc-length-weighted average values of J along three-dimensional crack fronts. The three-dimensional applications, however, have significant loss of accuracy in the near-tip region where the values of field quantities (stresses, strains, and displacements) are required to determine the point-wise energy release rate along the crack front. Based on the virtual crack extension method, deLorenzi [7,8] developed a finite element method that is more general to calculate the energy release rate in two-dimensional and three-dimensional fracture problems and could include the effects of body forces and traction loading on the crack faces.

Another investigation was made by Li *et al.* [9]. They proposed a formulation which would convert area integrals to volume integrals in order to calculate point-wise values of the energy release rate along a three-dimensional crack front. Shih, Nakamura and co-workers [10,11] then developed a finite element formulation to calculate the volume domain integral. About the same time, Nikishkov and Atluri [12,13] applied a somewhat different approach but a similar numerical procedure, and named the formulation "equivalent domain integral (EDI)" which would be used by subsequent researchers [14-16]. All of those derivations involve the application of the divergence

theorem and the implementation of a spatial weighting function that is based upon the virtual crack extension method.

With the EDI method, a point-wise value of J along a three-dimensional crack front can be calculated, and therefore the value of K along the crack front can be obtained from Eq.(1.3). Another advantage is that the EDI method transforms surface integrals in a three-dimensional problem into integrals over a volume, or a domain (hence the name of equivalent domain integral), without evaluation of the stress singularities directly on the crack front.

The stress intensity factor alone is not enough to characterize the crack behavior in some cases. Other fracture parameters may be needed to describe the crack behavior more precisely. As Irwin [4] pointed out there is a mathematical expression for crack-tip stress distributions in linear isotropic solids, Williams [22] showed that the expression is in fact an infinite power series of r, where r is the distance from the crack tip. The power series, in a concise form, can be written as

$$\sigma_{ij}(r,\theta) = \sum_{n=-1}^{\infty} A_n r^{(1/2)n} f_{ij}^{(n)}(\theta)\,, \qquad i,j = 1,2 \tag{1.4}$$

where A_n are unknown constants which depend on the geometry and loading conditions, and $f_{ij}^{(n)}(\theta)$ are the known angular distributions. The mode-I stress intensity factor is included in the first term of Eq.(1.4) as

$$\sigma_{ij} = \lim_{r\to 0} \frac{K_{\mathrm{I}}}{\sqrt{2\pi r}} f_{ij}^{(-1)}(\theta)\,, \tag{1.5}$$

in which the stresses are singular at $r = 0$ and $A_1 = K_{\mathrm{I}}/\sqrt{2\pi}$. The leading term of the series of Eq.(1.4) represents $r^{-1/2}$ singularity; the second term is a constant; the third and higher-order terms are proportional to $r^{(1/2)n}$, n=1,2,3…. Larsson and Carlsson [23] first denoted this constant term as T, and later it became the so-called "elastic T-stress".

In addition to the stress intensity factor, the elastic T-stress provides another parameter to identify the severity of stress and displacement fields near a crack. Larsson

and Carlsson [23] showed that the T-stress is necessary to modify the solution of the stress state in a small-scale yielding crack problem in plane strain condition. Rice [24] showed that T is in fact a constant stress parallel to the crack flank, and included it as a second crack tip parameter to characterize suitably small plane strain yield zones. Several methods have been used to practically determine the T-stress [25]. In addition to the methods mentioned in [25], recently other methods were also used, such as the boundary layer method and the displacement field method [26], as well as the stress difference method [27]. Among those methods, the interaction integral method developed by Nakamura and Parks [28] demonstrated highly computational effectiveness since it is based on the EDI method and has the capability to compute the T-stress not only in an isotropic material but also in an anisotropic material.

Under the NASA Advanced Composite Technology Program, Langley Research Center (LaRC) has performed fracture toughness tests for various types of wing structure specimens made from stitched warp-knit fabric composites. Variations of in-plane geometry and crack length were evaluated from three kinds of specimen geometry [29]: compact tension (CT) specimen with the crack aspect ratios $0.46 \le a/w \le 0.69$; center-cracked tension (CCT) specimen with $0.26 \le 2a/w \le 0.42$; single-edge notched tension (SENT) with $0.25 \le a/w \le 0.34$.

Methods based on the equivalent domain integral and Betti's reciprocal theorem were developed by Yuan and Yang [29] to extract the fracture parameters – critical stress intensity factor and T-stress. With the limited experimental data, the results tend to show that the critical mode-I stress intensity factor provides a satisfactory characterization for engineering applications of fracture initiation in the composite of a given laminate thickness, provided the failure is fiber-dominated and the crack growth follows in a self-similar manner. In addition, the high constraint due to high tensile T-stress may be expected to inhibit the crack extension in the same plane and promote the crack turning.

Recently, LaRC performed a mode-I test on a five-stringer panel manufactured

using the stitched warp-knit composite material. The crack initially extended in a self-similar manner and then turned parallel to the stiffener direction when the crack approached stiffeners (see Figure 1.2). In this dissertation, the effects of the geometrical attributes on the fracture behavior of this panel are investigated by using three-dimensional finite element analysis and linear elastic fracture mechanics to analyze the composites. Due to the high computational efficiency, the equivalent domain integral method is used to calculate the through-thickness K_I stress intensity factor and the interaction integral method is adopted to compute the through-thickness T-stress components. The algorithms of the equivalent domain integral and interaction integral are implemented into a single computer program, which reads a set of finite element solutions from a given mesh as the input to determine the distributions of the fracture parameters along the crack front. The composites are modeled as linear, anisotropic, and homogeneous materials. For the purpose of verification and comparison, a similarly cracked plate structure without stiffeners is also analyzed with the same composite material properties as well as an isotropic material.

The derivation of the EDI method is reviewed in Chapter 2 by the approaches mostly found in [15]. The derivation of the auxiliary fields necessary in the interaction integral method for an anisotropic material is presented in Chapter 3. Chapter 4 shows the procedure to determine the stress intensity factor and components of the T-stress from the values of the equivalent domain integral and interaction integral. The finite element models used in this research are described in Chapter 5; the associated results are presented in Chapter 6. Finally, the summary and discussion is presented and suggestions for future research are made in Chapter 7.

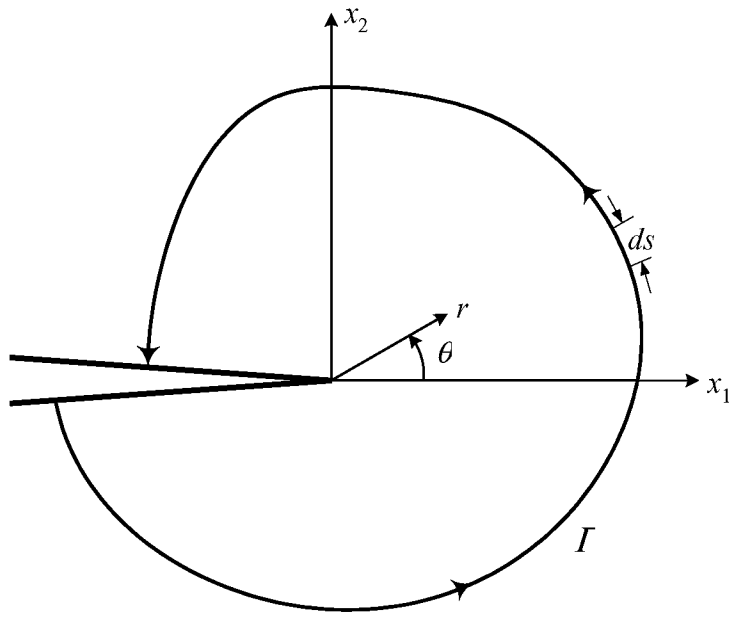

Figure 1.1 An arbitrary path on which a line integral is to be calculated.

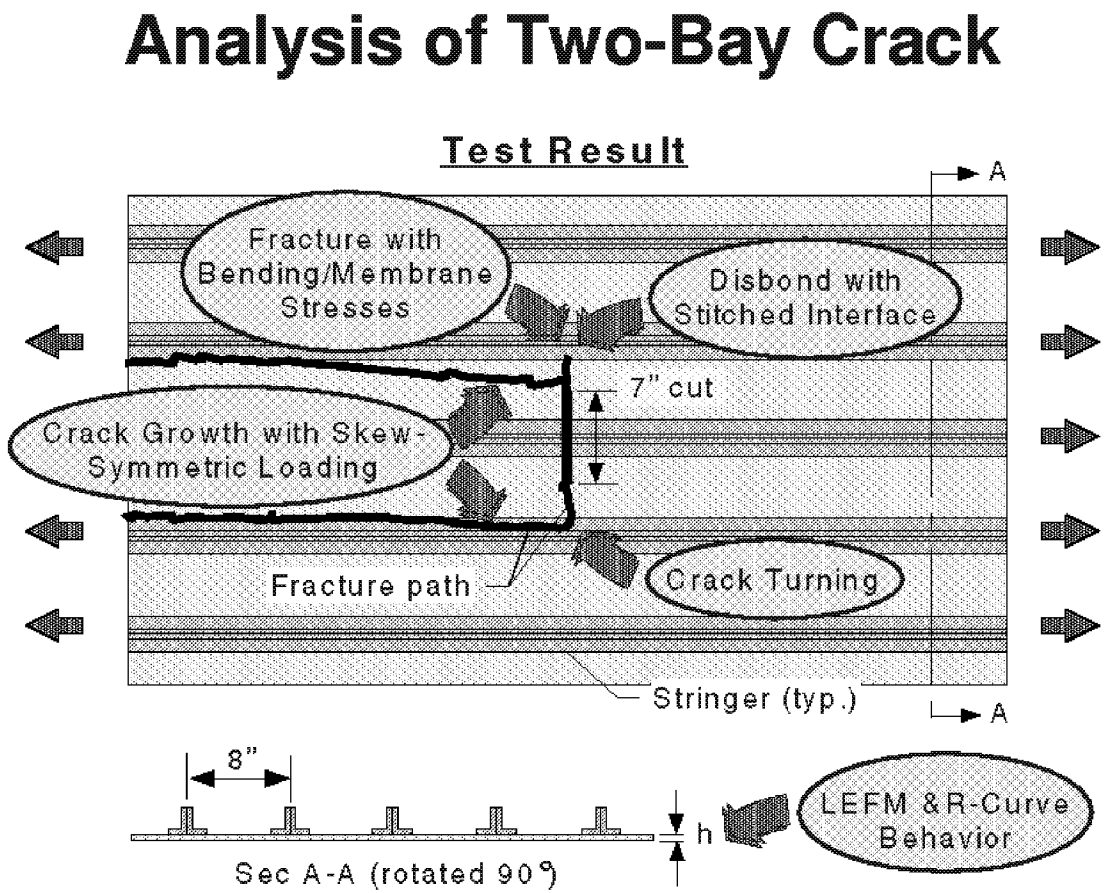

Figure 1.2 The cracked stiffened panel to be analyzed in the dissertation. (Courtesy of NASA Langley Research Center)

2 Equivalent Domain Integral (EDI)

The derivation will assume a traction-free crack in a linear elastic material, with the intention of determining the mode-I stress intensity factor K_I through the thickness.

2.1 Mathematical Formulation

Let us consider a small cylindrical volume with radius ε encompassing a segment of crack front of length Δ such that both ε and Δ approach zero, as shown in Figure 2.1. A local coordinate system is defined so that the axes x_1 and x_2 are perpendicular to the crack front, while x_1 and x_3 are lying on the crack plane. The volume is enclosed by five areas, namely the outer surface A_ε, two end surfaces $A_{\varepsilon 1}$ and $A_{\varepsilon 2}$, the top crack surface $A_{\varepsilon ct}$, and the bottom crack surface $A_{\varepsilon cb}$.

The local J-integral over the outer surface A_ε of the tube is defined as [30]

$$J = \lim_{\substack{\Delta \to 0 \\ \varepsilon \to 0}} \frac{1}{\Delta} \int (W n_1 - \sigma_{ij} \frac{\partial u_i}{\partial x_1} n_j) dA \,. \qquad i, j = 1, 2, 3 \tag{2.1}$$

In Eq.(2.1), W is the stress-work density, defined as $W = \int \sigma_{ij} d\varepsilon_{ij}$, where σ_{ij} are components of the stress tensor, and ε_{ij} are components of the strain tensor. u_i are components of the displacement vector; n_j is the j-th directional component of the unit normal vector on the surface A_ε. Since this research will be limited only to linear elastic materials, the stress-work density is simplified as $W = (\sigma_{ij}\varepsilon_{ij})/2$. Note that displacements, strains, stresses are expressed in the local crack front coordinate system.

For the purpose of simplicity in later derivations, let

$$Q = W n_1 - \sigma_{ij} \frac{\partial u_i}{\partial x_1} n_j \,. \tag{2.2}$$

Then Eq.(2.2) can be rewritten in terms of boundaries shown in Figure 2.1 to complete a

surface integral as

$$J = \lim_{\substack{\Delta \to 0 \\ \varepsilon \to 0}} \frac{1}{\Delta} \left[\int_{A_\varepsilon} Q dA + \int_{A_{\varepsilon 1} + A_{\varepsilon 2}} Q dA + \int_{A_{\varepsilon ct} + A_{\varepsilon cb}} Q dA \right]. \tag{2.3}$$

The evaluation of surface integrals in Eq.(2.3) is tedious and could lead to errors because singular terms on the crack front are included for numerical integration. Therefore, a modified form of the surface integrals is desirable, and this modified form would be the equivalent domain integral.

Now consider two tubular surfaces, A and A_ε, as shown in Figure 2.2. A is an arbitrary surface enclosing A_ε on which the J-integral is calculated. A_1 and A_2 are end surfaces connecting A and A_ε. $(A\text{-}A_\varepsilon)_{ct}$ and $(A_\varepsilon\text{-}A)_{cb}$ denote the top and bottom crack surfaces between A and A_ε, respectively. An enclosed volume $(V\text{-}V_\varepsilon)$ is surrounded by all of these surfaces, which are called collectively A_Σ, defined as

$$A_\Sigma = A - A_\varepsilon + (A - A_\varepsilon)_{ct} + (A_\varepsilon - A)_{cb} + A_1 + A_2 . \tag{2.4}$$

Based on the virtual crack extension theory, deLorenzi [8] proposed the concept of virtual node shift that forms the definition of a spatial weighting function, which is called s-function by some researchers [12-16,30]. We will adopt this name throughout this dissertation and use the symbol s to represent this spatial weighting function.

According to the configuration shown in Figure 2.2, an arbitrary but continuous s-function is defined between A and A_ε so that the function has the following properties:

$$s(x_1, x_2, x_3) = 0 \text{ on } A, A_{\varepsilon 1} \text{ and } A_{\varepsilon 2}, A_1 \text{ and } A_2; \tag{2.5a}$$

$$s(x_1, x_2, x_3) = s(x_3) \text{ on } A_\varepsilon. \tag{2.5b}$$

In order to complete the surface integrals over A_Σ, the first integral in Eq.(2.3) can be rewritten as an integral over the closed surface A_Σ and an integral over the physical boundaries $(A - A_\varepsilon)_{ct} + (A_\varepsilon - A)_{cb}$. And with the use of Eq.(2.5), Eq.(2.3) becomes

$$J = \frac{1}{f}\left[-\int_{A_\Sigma} QsdA + \int_{(A-A_\varepsilon)_{ct}+(A_\varepsilon-A)_{cb}} QsdA + \int_{A_{\varepsilon 1}+A_{\varepsilon 2}} QdA + \int_{A_{\varepsilon ct}+A_{\varepsilon cb}} QsdA \right]. \tag{2.6}$$

In Eq.(2.6) f is the area under the s-function curve on surface A_ε and is defined as

$$f = \int_{\Delta} s(x_3)dx_3 . \tag{2.7}$$

The s-function is equal to zero on both end surfaces of $A_{\varepsilon 1}$ and $A_{\varepsilon 2}$; therefore, $\int_{A_{\varepsilon 1}+A_{\varepsilon 2}} QsdA = 0$ and Eq.(2.6) remains as

$$J = \frac{1}{f}\left[-\int_{A_\Sigma} QsdA + \int_{(A-A_\varepsilon)_{ct}+(A_\varepsilon-A)_{cb}} QsdA + \int_{A_{\varepsilon ct}+A_{\varepsilon cb}} QsdA \right]. \tag{2.8}$$

In Eq.(2.8) the negative sign of the first integral, which is over an enclosed domain, comes from the opposite direction of the outer normal vector to the surface A_ε of the volume (V-V_ε) in comparison with the normal vector to the surface A_ε in Figure 2.1. The other integrals in Eq.(2.8) are actually on the crack surfaces. Therefore, we may separate integrals in Eq.(2.8) into a "domain" integral and a "crack face" integral, denoted as

$$J = \frac{1}{f}\left[(J)_{\text{domain}} + (J)_{\text{crack face}}\right], \tag{2.9}$$

where $(J)_{\text{domain}} = -\int_{A_\Sigma} QsdA$, (2.10)

and $(J)_{\text{crack face}} = \int_{(A-A_\varepsilon)_{ct}+(A_\varepsilon-A)_{cb}} QsdA + \int_{A_{\varepsilon ct}+A_{\varepsilon cb}} QsdA = \int Q_{\text{crack face}} sdA$. (2.11)

By recalling Eq.(2.2), Eq.(2.10) can be written as

$$(J)_{\text{domain}} = -\int_{A_\Sigma}\left[Wsn_1 - \left(\sigma_{ij}\frac{\partial u_i}{\partial x_1}s\right)n_j \right]dA . \tag{2.12}$$

The use of divergence theorem on Eq.(2.12) gives the following result:

$$(J)_{\text{domain}} = -\int_{V-V_\varepsilon}\left(W\frac{\partial s}{\partial x_1} - \sigma_{ij}\frac{\partial u_i}{\partial x_1}\frac{\partial s}{\partial x_j}\right)dV - \int_{V-V_\varepsilon}\left(\frac{\partial W}{\partial x_1} - \sigma_{ij}\frac{\partial \varepsilon_{ij}}{\partial x_1}\right)s\,dV\,. \tag{2.13}$$

Since the analysis is limited to linear elastic materials, it can be shown that the second integral in Eq.(2.13) is equal to zero [13]. Thus Eq.(2.13) is simplified as

$$(J)_{\text{domain}} = -\int_{V-V_\varepsilon}\left(W\frac{\partial s}{\partial x_1} - \sigma_{ij}\frac{\partial u_i}{\partial x_1}\frac{\partial s}{\partial x_j}\right)dV\,. \tag{2.14}$$

On the crack surfaces, the first and third directional components of the unit normal vector **n** are equal to zero ($n_1 = n_3 = 0$), according to the local coordinate system. The second component of **n** has the properties of $n_2 = +1$ on the bottom face and $n_2 = -1$ on the top face. Upon substituting these conditions into Eq.(2.2), we have

$$Q_{\text{crack face}} = Wn_1 - \left(\sigma_{12}\frac{\partial u_1}{\partial x_1}n_2 + \sigma_{22}\frac{\partial u_2}{\partial x_1}n_2 + \sigma_{32}\frac{\partial u_3}{\partial x_1}n_2\right). \tag{2.15}$$

Since $\sigma_{22} = \sigma_{32} = 0$ on the crack surfaces, Eq.(2.15) is then reduced to

$$Q_{\text{crack face}} = -\sigma_{12}\frac{\partial u_1}{\partial x_1}n_2\,. \tag{2.16}$$

For a traction-free crack surface, $\sigma_{12} = 0$. Thus the value of Q in Eq.(2.16) is equal to zero, and all integrals in Eq.(2.11) vanish.

Therefore, for a traction-free crack in a linear elastic material, the equivalent domain integral for the determination of K_{I}, in terms of displacements, strains, and stresses, can be conveniently expressed as

$$J_1 = -\frac{1}{f}\int_V\left(W\frac{\partial s}{\partial x_1} - \sigma_{ij}\frac{\partial u_i}{\partial x_1}\frac{\partial s}{\partial x_j}\right)dV\,. \tag{2.17}$$

To make a computable expression of Eq.(2.17), some numerical implementation needs to be defined.

2.2 Numerical Implementation

The 20-node isoparametric brick-shaped elements are frequently used in the three-dimensional finite element analysis of linear elastic crack problems. The typical finite element mesh around the crack front is a fan-type mesh, as shown in Figure 2.3. The shaded area indicates a domain over which the equivalent domain integral is calculated. All elements in and beyond this domain are 20-node elements. The wedge-shaped elements attached on the crack front, however, contain only 15 nodes for each element.

The J-integral is the sum of the domain integral contributed by each element in the designated domain, e.g., the shaded area in Figure 2.3. That is,

$$(J)_{\text{domain}} = \sum_{i=1}^{n_e} (J)_i \,, \tag{2.18}$$

where $(J)_i$ is the volume integral over the i-th element, and n_e is the number of elements enclosed in the domain.

In finite element modeling, the displacements are expressed by shape functions and nodal displacements:

$$u_k = \sum_{j=1}^{20} N_j (u_k)_j \,, \qquad k = 1, 2, 3 \tag{2.19}$$

where $N_j = N_j(\xi, \eta, \zeta)$ is the element shape function for a three-dimensional solid element, and ξ, η, ζ are the element's local coordinates that range between ±1. $(u_k)_j$ is the displacement component at the j-th node where j is the local node number within an element. Then for the volume integral of a single element, Eq.(2.17) can be written as

$$(J_1)_i = -\frac{1}{f} \int_{-1}^{1} \int_{-1}^{1} \int_{-1}^{1} \left(W \frac{\partial s}{\partial x_1} - \sigma_{jk} \frac{\partial u_j}{\partial x_1} \frac{\partial s}{\partial x_k} \right) \det[\mathbf{J}] d\xi d\eta d\zeta \,. \tag{2.20}$$

For an element with 2×2×2 Gaussian integration points, Eq.(2.20) can be modified in the form of numerical integration as

$$(J_1)_i = -\frac{1}{f}\left[\sum_{m=1}^{2}\sum_{n=1}^{2}\sum_{p=1}^{2}\left(W\frac{\partial s}{\partial x_1} - \mathbf{u}_{x_1}'^{\mathrm{T}}\boldsymbol{\sigma}\mathbf{s}'\right)w_m w_n w_p \det[\mathbf{J}]\right]_i . \tag{2.21}$$

In Eq.(2.21), W is the stress-work density, $\mathbf{u}_{x_1}'^{\mathrm{T}}$ is the vector of displacement derivatives, σ is the stress tensor, $\mathbf{s}'$ is the derivatives of the s-function, and det[**J**] denotes the determinant of the Jacobian matrix. w_m, w_n, and w_p are integration weights, and they all have the values of unity for 2×2×2 reduced integration [31].

Eq.(2.21) is the equation to be used for computation; therefore, the numerical implementation of each item in this equation needs to be explicitly expressed, as shown in the following sections. Once all items in Eq.(2.21) can be readily calculated, the J-integral over the domain can be evaluated from Eq.(2.18).

2.2.1 The Jacobian Matrix

The Jacobian matrix is defined by

$$\mathbf{J} = \begin{bmatrix} \frac{\partial x_1}{\partial \xi} & \frac{\partial x_2}{\partial \xi} & \frac{\partial x_3}{\partial \xi} \\ \frac{\partial x_1}{\partial \eta} & \frac{\partial x_2}{\partial \eta} & \frac{\partial x_3}{\partial \eta} \\ \frac{\partial x_1}{\partial \zeta} & \frac{\partial x_2}{\partial \zeta} & \frac{\partial x_3}{\partial \zeta} \end{bmatrix} . \tag{2.22}$$

Each component of the matrix, according to the finite element theory, is defined as

$$\frac{\partial x_k}{\partial \xi} = \sum_{j=1}^{20}\frac{\partial N_j}{\partial \xi}(x_k)_j , \qquad k = 1, 2, 3 \tag{2.23a}$$

$$\frac{\partial x_k}{\partial \eta} = \sum_{j=1}^{20}\frac{\partial N_j}{\partial \eta}(x_k)_j , \qquad k = 1, 2, 3 \tag{2.23b}$$

$$\frac{\partial x_k}{\partial \zeta} = \sum_{j=1}^{20}\frac{\partial N_j}{\partial \zeta}(x_k)_j , \qquad k = 1, 2, 3 \tag{2.23c}$$

where $(x_k)_j$ is the local coordinate component at the j-th node within an element.

2.2.2 The Stress Tensor and Stress-Work Density

The stress tensor σ of a linear elastic material is a 3×3 symmetric matrix shown as

$$\boldsymbol{\sigma} = \begin{bmatrix} \sigma_{11} & \sigma_{12} & \sigma_{13} \\ \sigma_{12} & \sigma_{22} & \sigma_{23} \\ \sigma_{13} & \sigma_{23} & \sigma_{33} \end{bmatrix}. \tag{2.24}$$

The stress-work density of the linear elastic material is $(\sigma_{ij}\varepsilon_{ij})/2$, or

$$W = \frac{1}{2}(\sigma_{11}\varepsilon_{11} + \sigma_{22}\varepsilon_{22} + \sigma_{33}\varepsilon_{33}) + \sigma_{12}\varepsilon_{12} + \sigma_{23}\varepsilon_{23} + \sigma_{13}\varepsilon_{13}. \tag{2.25}$$

Note that σ_{ij} and ε_{ij} are the stress and strain components from the finite element solutions output on the integration points.

2.2.3 The Derivatives of the *s*-Function

s' is the vector containing derivatives of the *s*-function with respect to the local coordinate system and is expressed as

$$\mathbf{s}' = \begin{bmatrix} \frac{\partial s}{\partial x_1} & \frac{\partial s}{\partial x_2} & \frac{\partial s}{\partial x_3} \end{bmatrix}^{\mathrm{T}}. \tag{2.26}$$

To evaluate Eq.(2.26), the *s*-function must be defined first. Since the *s*-function is arbitrary and satisfies Eq.(2.5), it can be conveniently defined by the sums of the element shape functions as

$$s(\xi,\eta,\zeta) = \sum_{j=1}^{20} N_j s_j. \tag{2.27}$$

For the 20-node brick-shaped element shown in Figure 2.4, the *s*-function is completely defined by specifying $s^{(10)} = s^{(14)} = 1$ and zero on all other nodes in order to satisfy Eq.(2.5). This definition yields a quadratic *s*-function over a single element. With the definition, Eq.(2.7) also can be evaluated and hence $f = (2/3)\Delta$ where Δ is the length of the domain segment [30].

It is clear that the s-function is a function of the element coordinate system (ξ, η, ζ), rather than the crack front coordinate system (x_1, x_2, x_3). Thus **s'** should be expressed in terms of (ξ, η, ζ) before it can be evaluated. This can be done by the chain rule, as shown in the following equation:

$$\mathbf{s}' = \begin{Bmatrix} \dfrac{\partial s}{\partial x_1} \\ \dfrac{\partial s}{\partial x_2} \\ \dfrac{\partial s}{\partial x_3} \end{Bmatrix} = \begin{Bmatrix} \dfrac{\partial s}{\partial \xi}\dfrac{\partial \xi}{\partial x_1} + \dfrac{\partial s}{\partial \eta}\dfrac{\partial \eta}{\partial x_1} + \dfrac{\partial s}{\partial \zeta}\dfrac{\partial \zeta}{\partial x_1} \\ \dfrac{\partial s}{\partial \xi}\dfrac{\partial \xi}{\partial x_2} + \dfrac{\partial s}{\partial \eta}\dfrac{\partial \eta}{\partial x_2} + \dfrac{\partial s}{\partial \zeta}\dfrac{\partial \zeta}{\partial x_2} \\ \dfrac{\partial s}{\partial \xi}\dfrac{\partial \xi}{\partial x_3} + \dfrac{\partial s}{\partial \eta}\dfrac{\partial \eta}{\partial x_3} + \dfrac{\partial s}{\partial \zeta}\dfrac{\partial \zeta}{\partial x_3} \end{Bmatrix} = \mathbf{J}^{-1} \begin{Bmatrix} \dfrac{\partial s}{\partial \xi} \\ \dfrac{\partial s}{\partial \eta} \\ \dfrac{\partial s}{\partial \zeta} \end{Bmatrix}. \tag{2.28}$$

$\mathbf{J}^{-1}$ is the inverse Jacobian matrix containing the following components:

$$\mathbf{J}^{-1} = \begin{bmatrix} \dfrac{\partial \xi}{\partial x_1} & \dfrac{\partial \eta}{\partial x_1} & \dfrac{\partial \zeta}{\partial x_1} \\ \dfrac{\partial \xi}{\partial x_2} & \dfrac{\partial \eta}{\partial x_2} & \dfrac{\partial \zeta}{\partial x_2} \\ \dfrac{\partial \xi}{\partial x_3} & \dfrac{\partial \eta}{\partial x_3} & \dfrac{\partial \zeta}{\partial x_3} \end{bmatrix}. \tag{2.29}$$

The derivatives of the s-function with respect to the element coordinate system, i.e. $\dfrac{\partial s}{\partial \xi}$, $\dfrac{\partial s}{\partial \eta}$ and $\dfrac{\partial s}{\partial \zeta}$ in Eq.(2.28), can be evaluated in the same manner as Eq.(2.23).

2.2.4 The Derivatives of the Displacements

$\mathbf{u}'^{\mathrm{T}}_{x_1}$ is the vector of displacement derivatives and can be expressed as

$$\mathbf{u}'^{\mathrm{T}}_{x_1} = \begin{bmatrix} \dfrac{\partial u_1}{\partial x_1} & \dfrac{\partial u_2}{\partial x_1} & \dfrac{\partial u_3}{\partial x_1} \end{bmatrix}. \tag{2.30}$$

The components in Eq.(2.30) are the derivatives of the displacements with respect to the local coordinate system. Similar to the derivatives of the s-function, they should be evaluated in terms of the element coordinate system (ξ, η, ζ). With the use of the chain rule on Eq.(2.19), each component of Eq.(2.30) can be obtained by

$$\frac{\partial u_k}{\partial x_1} = \sum_{j=1}^{20} \left(\frac{\partial N_j}{\partial \xi} \frac{\partial \xi}{\partial x_1} + \frac{\partial N_j}{\partial \eta} \frac{\partial \eta}{\partial x_1} + \frac{\partial N_j}{\partial \zeta} \frac{\partial \zeta}{\partial x_1} \right) (u_k)_j \,. \qquad k = 1, 2, 3 \qquad (2.31)$$

In Eq.(2.31), $\frac{\partial \xi}{\partial x_1}$, $\frac{\partial \eta}{\partial x_1}$ and $\frac{\partial \zeta}{\partial x_1}$ are the components of the first row of the inverse Jacobian matrix of Eq.(2.29); $\frac{\partial N_j}{\partial \xi}$, $\frac{\partial N_j}{\partial \eta}$ and $\frac{\partial N_j}{\partial \zeta}$ are the derivatives of the shape functions that can be readily computed.

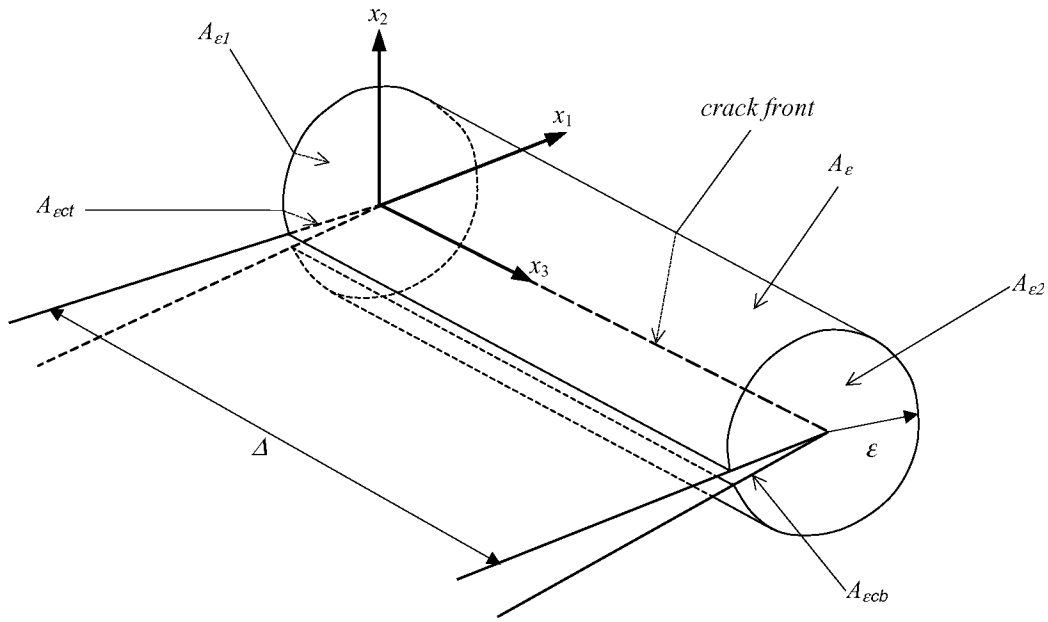

Figure 2.1 A small cylindrical volume around a segment of crack front, with the local coordinate system shown.

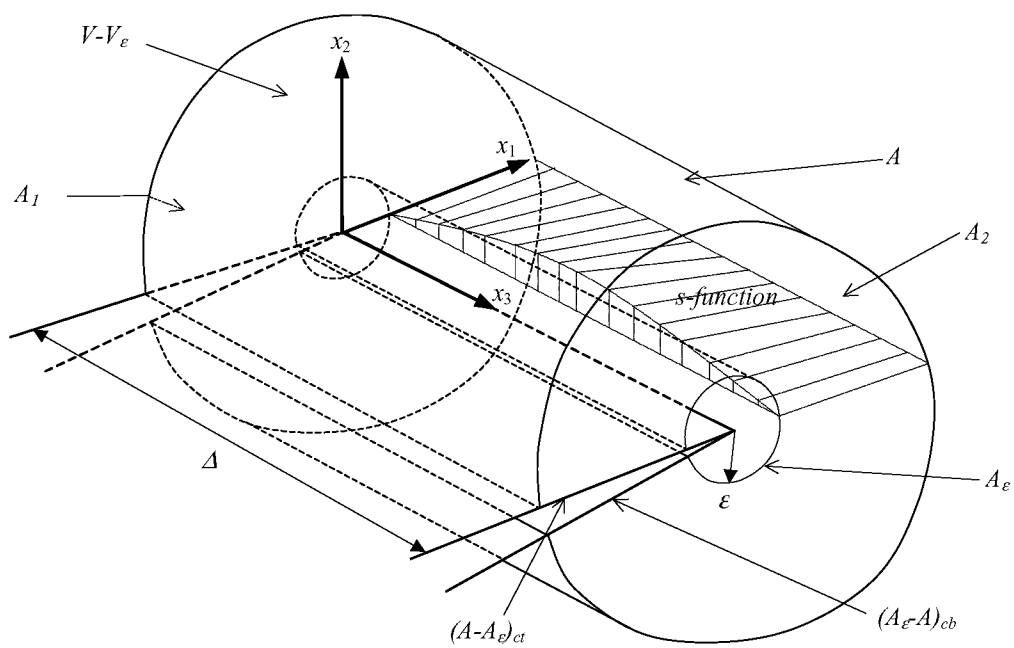

Figure 2.2 A domain enclosing a segment of crack front.

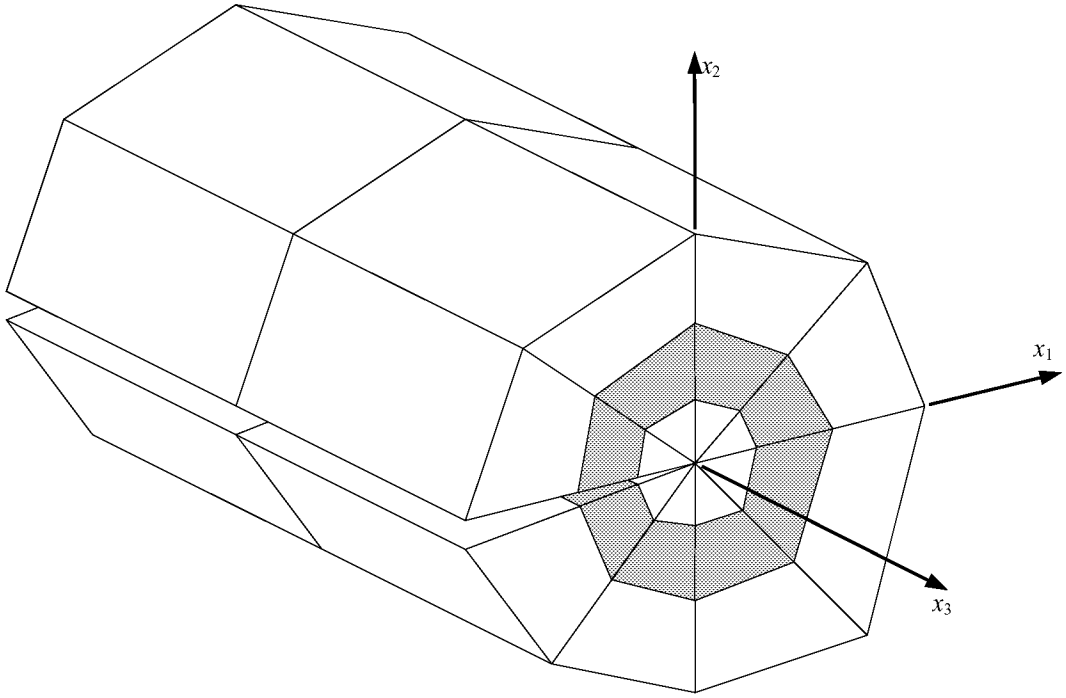

Figure 2.3 The schematic finite element mesh near a segment of the crack front.

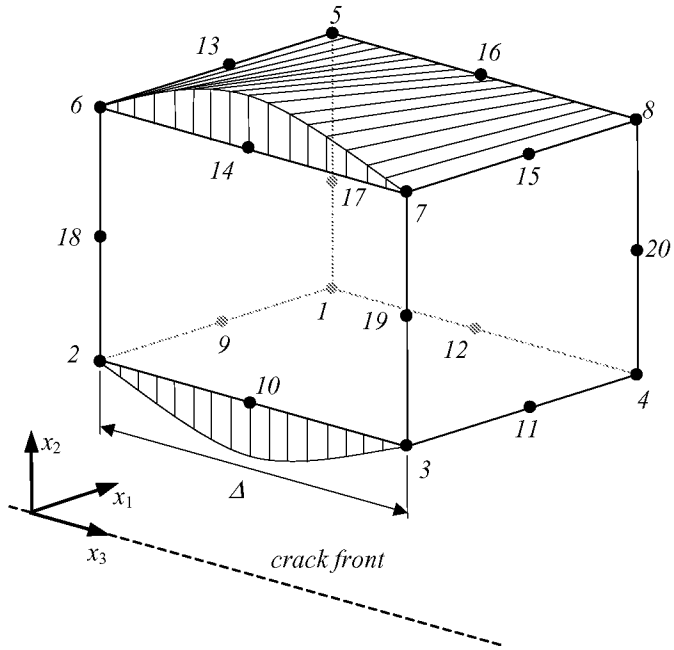

Figure 2.4 A 20-node element with the associated s-functions.

3 Interaction Integral

The interaction integral is necessary for extracting the elastic T-stress from an existing finite element solution. It is based upon the formulation of the EDI method as well as a superimposed auxiliary stress field. Kfouri [32] gave the auxiliary stress field that is the analytical solution corresponding to a point force applied to a crack tip and parallel to the crack surface under plane strain in isotropic solids. For a three-dimensional crack, the point force becomes a uniform line load that is applied along the crack front, as shown in Figure 3.1(a). This stress field is a function of r, the distance from the crack front, and θ, the angle from x_1 axis toward x_2 axis; but it is independent of the crack front location x_3.

Nakamura and Parks [28] applied the auxiliary stress field with the interaction integral and successfully calculated the T-stress distribution along the three-dimensional crack front. The auxiliary stress field, however, is valid only for isotropic materials. For anisotropic materials, the corresponding auxiliary fields have been derived using Stroh formalism [34].

Similar to Eq.(2.17) of the equivalent domain integral, the interaction integral for mode-I loading in a given domain may be expressed as

$$I_1 = \frac{1}{f}\int_V \left[-\sigma_{ij}\varepsilon_{ij}^{\mathrm{a}} \frac{\partial s}{\partial x_1} + \left(\sigma_{ij}\frac{\partial u_i^{\mathrm{a}}}{\partial x_1} + \sigma_{ij}^{\mathrm{a}}\frac{\partial u_i}{\partial x_1} \right)\frac{\partial s}{\partial x_j} \right] dV \,, \qquad i,j = 1,2,3 \tag{3.1}$$

where σ_{ij}^{a}, $\varepsilon_{ij}^{\mathrm{a}}$, and u_i^{a} are the components of the auxiliary stress, strain, and displacement fields, respectively. For the purpose of numerical integration of each individual element in a domain, Eq.(3.1) can be written similarly to Eq.(2.21) as

$$(I_1)_i = \frac{1}{f}\left\{ \sum_{m=1}^{2}\sum_{n=1}^{2}\sum_{p=1}^{2} \left[-\sigma_{jk}\varepsilon_{jk}^{\mathrm{a}} \frac{\partial s}{\partial x_1} + \left((\mathbf{u}^{\mathrm{a}})_{x_1}'^{\mathrm{T}}\boldsymbol{\sigma} + \mathbf{u}_{x_1}'^{\mathrm{T}}\boldsymbol{\sigma}^{\mathrm{a}} \right)\mathbf{s}' \right] w_m w_n w_p \det[\mathbf{J}] \right\}_i . \tag{3.2}$$

In Eq.(3.2), $\boldsymbol{\sigma}^{\mathrm{a}}$ and $\mathbf{u}^{\mathrm{a}}$ denote the stress tensor and displacement vector of the auxiliary

fields, respectively. $\varepsilon_{jk}^{\mathrm{a}}$ are components of the auxiliary strain tensor. These entities are expressed in terms of the components of the associated tensor or vector as follows:

$$\boldsymbol{\sigma}^{\mathrm{a}} = \begin{bmatrix} \sigma_{11}^{\mathrm{a}} & \sigma_{12}^{\mathrm{a}} & \sigma_{13}^{\mathrm{a}} \\ \sigma_{12}^{\mathrm{a}} & \sigma_{22}^{\mathrm{a}} & \sigma_{23}^{\mathrm{a}} \\ \sigma_{13}^{\mathrm{a}} & \sigma_{23}^{\mathrm{a}} & \sigma_{33}^{\mathrm{a}} \end{bmatrix}; \tag{3.3}$$

$$\sigma_{jk}\varepsilon_{jk}^{\mathrm{a}} = \sigma_{11}\varepsilon_{11}^{\mathrm{a}} + \sigma_{22}\varepsilon_{22}^{\mathrm{a}} + \sigma_{33}\varepsilon_{33}^{\mathrm{a}} + 2\left(\sigma_{12}\varepsilon_{12}^{\mathrm{a}} + \sigma_{23}\varepsilon_{23}^{\mathrm{a}} + \sigma_{13}\varepsilon_{13}^{\mathrm{a}}\right); \tag{3.4}$$

$$(\mathbf{u}^{\mathrm{a}})_{x_1}'^{\mathrm{T}} = \begin{bmatrix} \dfrac{\partial u_1^{\mathrm{a}}}{\partial x_1} & \dfrac{\partial u_2^{\mathrm{a}}}{\partial x_1} & \dfrac{\partial u_3^{\mathrm{a}}}{\partial x_1} \end{bmatrix}. \tag{3.5}$$

Quantities of Eq.(3.3) and Eq.(3.4) can be obtained by straightforward substitution of auxiliary stress and strain fields. Components in Eq.(3.5) can be computed similarly to Eq.(2.31) as

$$\frac{\partial u_k^{\mathrm{a}}}{\partial x_1} = \sum_{j=1}^{20}\left(\frac{\partial N_j}{\partial \xi}\frac{\partial \xi}{\partial x_1} + \frac{\partial N_j}{\partial \eta}\frac{\partial \eta}{\partial x_1} + \frac{\partial N_j}{\partial \zeta}\frac{\partial \zeta}{\partial x_1}\right)\left(u_k^{\mathrm{a}}\right)_j, \qquad k = 1, 2, 3 \tag{3.6}$$

where u_k^{a} are components of the auxiliary displacement vector. All of the other items not associated with the auxiliary fields are calculated exactly in the same way as the equivalent domain integral is.

Since the auxiliary strain and displacement fields are derived from the auxiliary stress field which is a function of r and θ, both are functions of r and θ as well. All terms in Eq.(3.2), however, should be evaluated with respect to the local coordinates (x_1, x_2, x_3). Therefore, the auxiliary field calculation must be done by converting the Cartesian coordinates of nodes or integration points to the polar coordinates before substituting them into the auxiliary field formulation. The computation of the auxiliary displacement field is straightforward because it needs only substitution of all 20 nodes' coordinates within an element. The auxiliary stresses and strains will need the coordinates of the 8 integration points. The location of these integration points with respect to the element coordinate system is illustrated in Figure 3.2.

Let us recall the Williams expansion of Eq.(1.4) which can be generalized to three-dimensional problems. It is assumed that the asymptotic expansion of the stress field near the crack front location under general loading conditions can be expressed as

$$\sigma_{ij} = \sum_{n=1(\mathrm{I})}^{3(\mathrm{III})} \frac{k_n}{\sqrt{2\pi r}} f_{ij}^{(n)}(\theta) + T_{ij} + o(1), \qquad i,j = 1, 2, 3 \tag{3.7}$$

where k_{I}, k_{II}, and k_{III} are local stress intensity factors, $f_{ij}^{(n)}(\theta)$ are angular distributions for the crack-tip field given by the two-dimensional deformation of anisotropic elasticity theory, and $o(1)$ represents other higher order terms. T_{ij} are the non-singular T-stresses, which have three distinct components, namely

$$[T_{ij}] = \begin{bmatrix} T_{11} & 0 & T_{13} \\ 0 & 0 & 0 \\ T_{13} & 0 & T_{33} \end{bmatrix}. \tag{3.8}$$

T_{11} is obviously the stress component acting parallel to the crack plane [24] and can be determined by the interaction integral with an imposed uniform line load f_1 as shown in Figure 3.1(a). Similarly T_{13} can be determined by using a different set of auxiliary fields. Instead of the line load perpendicular to the crack front and the x_2-x_3 plane, a constant force f_3 in x_3-direction and through the full length of crack front should be imposed. This configuration, as shown in Figure 3.1(b), will yield an auxiliary stress field necessary to extract T_{13}. T_{33} is a combination of T_{11} and T_{13} and can be readily obtained after the other two T-stresses are determined (see Chapter 4).

In the following sections, the derivations of both types of auxiliary fields are presented in order to determine all of the T-stress components.

3.1 Auxiliary Fields for T_{11}

In this dissertation, we will be concerned with the composite plate structures, which usually have at least one plane of symmetry in materials. The convention of orientation for a composite plate is that the plate is on the x_1-x_2 plane while the x_3 is the

direction out of plane [34]. Since most composite plates have at least one symmetry plane at x_3=0, we will limit the derivation under this restriction. This kind of material is called the monoclinic material with the plane of symmetry at x_3=0, or simply the monoclinic material about x_3=0.

The generalized Hooke's law states the stress-strain relation in contracted notation as

$$\boldsymbol{\sigma}^c = \mathbf{C}\boldsymbol{\varepsilon}^c, \tag{3.9}$$

where $\boldsymbol{\sigma}^c = [\sigma_1 \;\; \sigma_2 \;\; \sigma_3 \;\; \sigma_4 \;\; \sigma_5 \;\; \sigma_6]^T = [\sigma_{11} \;\; \sigma_{22} \;\; \sigma_{33} \;\; \sigma_{23} \;\; \sigma_{13} \;\; \sigma_{12}]^T$ (3.10)

and $\boldsymbol{\varepsilon}^c = [\varepsilon_1 \;\; \varepsilon_2 \;\; \varepsilon_3 \;\; \varepsilon_4 \;\; \varepsilon_5 \;\; \varepsilon_6]^T = [\varepsilon_{11} \;\; \varepsilon_{22} \;\; \varepsilon_{33} \;\; 2\varepsilon_{23} \;\; 2\varepsilon_{13} \;\; 2\varepsilon_{12}]^T$. (3.11)

C is a 6×6 matrix, and is called the stiffness matrix in which the components C_{ij} are material properties. A monoclinic material about x_3=0 has the following form of the stiffness matrix:

$$\mathbf{C} = \begin{bmatrix} C_{11} & C_{12} & C_{13} & 0 & 0 & C_{16} \\ C_{12} & C_{22} & C_{23} & 0 & 0 & C_{26} \\ C_{13} & C_{23} & C_{33} & 0 & 0 & C_{36} \\ 0 & 0 & 0 & C_{44} & C_{45} & 0 \\ 0 & 0 & 0 & C_{45} & C_{55} & 0 \\ C_{16} & C_{26} & C_{36} & 0 & 0 & C_{66} \end{bmatrix}. \tag{3.12}$$

The inverse of the stress-strain relation defines the compliance matrix **s**, as

$$\boldsymbol{\varepsilon}^c = \mathbf{s}\boldsymbol{\sigma}^c, \tag{3.13}$$

where **s** is the inverse of **C**. Thus the compliance matrix of a monoclinic material about x_3=0 has the form of

$$\mathbf{s} = \mathbf{C}^{-1} = \begin{bmatrix} s_{11} & s_{12} & s_{13} & 0 & 0 & s_{16} \\ s_{12} & s_{22} & s_{23} & 0 & 0 & s_{26} \\ s_{13} & s_{23} & s_{33} & 0 & 0 & s_{36} \\ 0 & 0 & 0 & s_{44} & s_{45} & 0 \\ 0 & 0 & 0 & s_{45} & s_{55} & 0 \\ s_{16} & s_{26} & s_{36} & 0 & 0 & s_{66} \end{bmatrix}. \tag{3.14}$$

As stated earlier, the auxiliary fields for T_{11} are independent of x_3. This implies it is under the condition of two-dimensional deformation for which ε_3=0. By ignoring the

equation for σ_3 in Eq.(3.9), the stress-strain relation of the monoclinic material can be written as

$$[\sigma_1 \;\; \sigma_2 \;\; \sigma_6 \;\; \sigma_4 \;\; \sigma_5]^{\mathrm{T}} = \mathbf{C}^0 [\varepsilon_1 \;\; \varepsilon_2 \;\; \varepsilon_6 \;\; \varepsilon_4 \;\; \varepsilon_5]^{\mathrm{T}}, \tag{3.15}$$

where $\mathbf{C}^0$ is the reduced stiffness matrix, shown as

$$\mathbf{C}^0 = \begin{bmatrix} C_{11} & C_{12} & C_{16} & 0 & 0 \\ C_{12} & C_{22} & C_{26} & 0 & 0 \\ C_{16} & C_{26} & C_{66} & 0 & 0 \\ 0 & 0 & 0 & C_{44} & C_{45} \\ 0 & 0 & 0 & C_{45} & C_{55} \end{bmatrix}. \tag{3.16}$$

The inverse of Eq.(3.16) gives the definition of the reduced compliance matrix $\mathbf{s}^0$, as

$$\mathbf{s}^0 = \left(\mathbf{C}^0\right)^{-1} = \begin{bmatrix} s'_{11} & s'_{12} & s'_{16} & 0 & 0 \\ s'_{12} & s'_{22} & s'_{26} & 0 & 0 \\ s'_{16} & s'_{26} & s'_{66} & 0 & 0 \\ 0 & 0 & 0 & s'_{44} & s'_{45} \\ 0 & 0 & 0 & s'_{45} & s'_{55} \end{bmatrix}. \tag{3.17}$$

The components of $\mathbf{s}^0$ can be also obtained by solving for σ_3 in the third equation of Eq.(3.13) that will yield

$$\sigma_3 = \sigma_{33} = -\frac{1}{s_{33}} \sum_{\beta=1}^{6} s_{3\beta}\sigma_\beta \,. \qquad \beta \neq 3 \tag{3.18}$$

Substituting Eq.(3.18) into the other five equations of Eq.(3.13) will have

$$s'_{ij} = s_{ij} - \frac{s_{i3}s_{3j}}{s_{33}}. \qquad i, j = 1, 2, 4, 5, 6 \tag{3.19}$$

According to Stroh formalism for two-dimensional deformations of an anisotropic elastic body [35], the characteristic equations have the reduced compliance as coefficients:

$$s'_{11}\mu^4 - 2s'_{16}\mu^3 + (2s'_{12} + s'_{66})\mu^2 - 2s'_{26}\mu + s'_{22} = 0\,; \tag{3.20a}$$

$$s'_{55}\mu^2 - 2s'_{45}\mu + s'_{44} = 0\,. \tag{3.20b}$$

The solutions to Eq.(3.20) are the eigenvalues of elastic constants, μ_α ($\alpha = 1, 2, 3$), where μ_1, μ_2, $\overline{\mu}_1$, and $\overline{\mu}_2$ are roots of Eq.(3.20a), and μ_3, $\overline{\mu}_3$ are roots of Eq.(3.20b). μ_α are

complex numbers, and $\overline{\mu}_\alpha$ are the conjugates of μ_α.

Under the uniform line load f_1 shown in Figure 3.1(a), the auxiliary stresses are inversely proportion to r, or $\sigma_{ij}^{\mathrm{a}} \propto r^{-1}$. In Stroh formalism, the real form solution for the displacement $\mathbf{u}^{\mathrm{a}}$ and the stress function ϕ^{a} due to the point forces can be written as

$$2\mathbf{u}^{\mathrm{a}} = -\left[\frac{\ln r}{\pi}\mathbf{I} + \mathbf{S}(\theta)\right]\mathbf{L}^{-1}\mathbf{f}\,, \tag{3.21a}$$

$$2\phi^{\mathrm{a}} = \mathbf{L}(\theta)\mathbf{L}^{-1}\mathbf{f}\,, \tag{3.21b}$$

where $\mathbf{S}$ and $\mathbf{L}$ are Barnette-Lothe tensors, $\mathbf{S}(\theta)$ and $\mathbf{L}(\theta)$ are their associate tensors, $\mathbf{f}$ is the vector of the line load per unit thickness, and $\mathbf{I}$ is the 3×3 identity matrix. These items are defined as follows:

$$\mathbf{f} = [f_1 \quad 0 \quad 0]^{\mathrm{T}}; \tag{3.22}$$

$$\mathbf{S}(\theta) = \frac{2}{\pi}\mathrm{Re}\left\{\mathbf{A}\left\langle \ln(\cos\theta + \mu_\alpha \sin\theta)\right\rangle \mathbf{B}^{\mathrm{T}}\right\}; \tag{3.23a}$$

$$\mathbf{L}(\theta) = -\frac{2}{\pi}\mathrm{Re}\left\{\mathbf{B}\left\langle \ln(\cos\theta + \mu_\alpha \sin\theta)\right\rangle \mathbf{B}^{\mathrm{T}}\right\}; \tag{3.23b}$$

$$\mathbf{L}^{-1} = s'_{11}\begin{bmatrix} z_1 & z_2 & 0 \\ z_2 & e & 0 \\ 0 & 0 & (ms'_{11})^{-1} \end{bmatrix}. \tag{3.24}$$

The definitions of the terms in Eq.(3.23) and Eq.(3.24) are given as follows.

For the purpose of simplicity, let $\varsigma_\alpha = \cos\theta + \mu_\alpha \sin\theta$. In Eq.(3.23), $\langle\ \rangle$ implies a diagonal matrix, thus

$$\left\langle \ln(\cos\theta + \mu_\alpha \sin\theta)\right\rangle = \begin{bmatrix} \ln\varsigma_1 & 0 & 0 \\ 0 & \ln\varsigma_2 & 0 \\ 0 & 0 & \ln\varsigma_3 \end{bmatrix}. \tag{3.25}$$

$\mathbf{A}$ and $\mathbf{B}$ are 3×3 complex matrices containing Stroh eigenvectors and are defined as

$$\mathbf{A} = \begin{bmatrix} k_1 p_1 & k_2 p_2 & 0 \\ k_1 q_1 & k_2 q_2 & 0 \\ 0 & 0 & k_3(s'_{45} - s'_{44}/\mu_3) \end{bmatrix} \text{ and} \tag{3.26a}$$

$$\mathbf{B} = \begin{bmatrix} -k_1\mu_1 & -k_2\mu_2 & 0 \\ k_1 & k_2 & 0 \\ 0 & 0 & -k_3 \end{bmatrix}, \tag{3.26b}$$

where p_1, p_2, q_1, q_2 can be obtained from

$$p_\alpha = s'_{11}\mu_\alpha^2 - s'_{16}\mu_\alpha + s'_{12} \text{ and } q_\alpha = s'_{12}\mu_\alpha - s'_{26} + s'_{22}/\mu_\alpha . \qquad \alpha = 1, 2 \tag{3.27}$$

k_1, k_2, k_3 are normalization factors satisfying the following relations:

$$2k_1^2(q_1 - \mu_1 p_1) = 1;\ 2k_2^2(q_2 - \mu_2 p_2) = 1;\ 2k_3^2(s'_{44}/\mu_3 - s'_{45}) = 1. \tag{3.28}$$

The components of $\mathbf{L}^{-1}$ in Eq.(3.24) are defined by the following relations:

$$\mu_1 + \mu_2 = y_1 + z_1 i; \tag{3.29a}$$

$$\mu_1\mu_2 = y_2 + z_2 i; \tag{3.29b}$$

$$e = y_1 z_2 - y_2 z_1; \tag{3.29c}$$

$$m = \left(s'_{44}s'_{55} - s'_{45}s'_{45}\right)^{-1/2}. \tag{3.29d}$$

Upon substitution of Eq.(3.22) through Eq.(3.24), the stress function of Eq.(3.21b) can be obtained as

$$\phi^{\mathrm{a}} = -\frac{f_1 s'_{11}}{\pi}\mathrm{Re}\begin{Bmatrix} \phi_1 \\ \phi_2 \\ 0 \end{Bmatrix}, \tag{3.30}$$

where $\phi_1 = z_1\left(k_1^2\mu_1^2 \ln\varsigma_1 + k_2^2\mu_2^2 \ln\varsigma_2\right) - z_2\left(k_1^2\mu_1 \ln\varsigma_1 + k_2^2\mu_2 \ln\varsigma_2\right)$ (3.31a)

and $\phi_2 = -z_1\left(k_1^2\mu_1 \ln\varsigma_1 + k_2^2\mu_2 \ln\varsigma_2\right) + z_2\left(k_1^2 \ln\varsigma_1 + k_2^2 \ln\varsigma_2\right)$. (3.31b)

To determine the auxiliary stress field from the stress function, let $\mathbf{t}_r$ be the traction vector on a cylindrical surface of r = *constant* which can be obtained as [33]

$$\mathbf{t}_r = -\frac{1}{r}\frac{\partial\phi}{\partial\theta}, \tag{3.32}$$

$$\text{or } \mathbf{t}_r = \frac{f_1 s'_{11}}{\pi r} \operatorname{Re}\begin{Bmatrix} t_{r_1} \\ t_{r_2} \\ 0 \end{Bmatrix}, \tag{3.33}$$

where $t_{r_1} = z_1\left(k_1^2\mu_1^2\Omega_1 + k_2^2\mu_2^2\Omega_2\right) - z_2\left(k_1^2\mu_1\Omega_1 + k_2^2\mu_2\Omega_2\right)$ (3.34a)

and $t_{r_2} = -z_1\left(k_1^2\mu_1\Omega_1 + k_2^2\mu_2\Omega_2\right) + z_2\left(k_1^2\Omega_1 + k_2^2\Omega_2\right)$. (3.34b)

In Eq.(3.34) Ω_α is defined as

$$\Omega_\alpha(\theta) = \frac{\partial}{\partial\theta}\ln\varsigma_\alpha = \frac{-\sin\theta + \mu_\alpha\cos\theta}{\cos\theta + \mu_\alpha\sin\theta}. \qquad \alpha = 1, 2, 3 \tag{3.35}$$

Then the stresses in the cylindrical coordinate system are

$$\sigma_{rr} = \begin{bmatrix}\cos\theta & \sin\theta & 0\end{bmatrix}\mathbf{t}_r; \tag{3.36a}$$

$$\sigma_{r3} = \begin{bmatrix}0 & 0 & 1\end{bmatrix}\mathbf{t}_r; \tag{3.36b}$$

$$\sigma_{\theta\theta} = \sigma_{r\theta} = \sigma_{\theta 3} = 0. \tag{3.36c}$$

σ_{r3} is found to be equal to zero after substituting Eq.(3.33) into Eq.(3.36b). Substitution of Eq.(3.33) into Eq.(3.36a) also gives σ_{rr}, which is a function of r and θ, as

$$\sigma_{rr} = \frac{f_1 s'_{11}}{\pi r}\operatorname{Re}\left\{t_{r_1}\cos\theta + t_{r_2}\sin\theta\right\}. \tag{3.37}$$

It should be noted that the auxiliary fields in the calculation of the interaction integral of Eq.(3.1) are all in the Cartesian coordinate system. Hence the auxiliary stresses σ_{ij}^{a} must be obtained by applying coordinate transformation on Eq.(3.36). The results, which will be able to be implemented into the numerical computing procedure, are given as follows:

$$\sigma_{11}^{\mathrm{a}} = \frac{f_1 s'_{11}\cos^2\theta}{\pi r}\operatorname{Re}\left\{t_{r_1}\cos\theta + t_{r_2}\sin\theta\right\}; \tag{3.38a}$$

$$\sigma_{22}^{\mathrm{a}} = \frac{f_1 s'_{11}\sin^2\theta}{\pi r}\operatorname{Re}\left\{t_{r_1}\cos\theta + t_{r_2}\sin\theta\right\}; \tag{3.38b}$$

$$\sigma_{12}^{\mathrm{a}} = \frac{f_1 s'_{11}\sin\theta\cos\theta}{\pi r}\operatorname{Re}\left\{t_{r_1}\cos\theta + t_{r_2}\sin\theta\right\}; \tag{3.38c}$$

$$\sigma_{13}^{\mathrm{a}} = \sigma_{23}^{\mathrm{a}} = 0. \tag{3.38d}$$

σ_{33}^{a} can be obtained by substitution of Eq.(3.38) into Eq.(3.18), which yields

$$\sigma_{33}^{\mathrm{a}} = -\frac{f_1 s_{11}' \left(s_{13}\cos^2\theta + s_{23}\sin^2\theta\right)}{\pi r s_{33}} \mathrm{Re}\left\{t_{r_1}\cos\theta + t_{r_2}\sin\theta\right\}. \tag{3.38e}$$

Once the auxiliary stress field is available, the auxiliary strain field can be readily obtained from the inverse of the stress-strain relation of Eq.(3.13).

The auxiliary displacement field is readily available from Eq.(3.21a) which, after a series of substitution of Eq.(3.22) through Eq.(3.24), will yield $u_3^{\mathrm{a}} = 0$ and non-zero items of u_1^{a} and u_2^{a} as

$$\begin{Bmatrix} u_1^{\mathrm{a}} \\ u_2^{\mathrm{a}} \end{Bmatrix} = -\frac{f_1 s_{11}'}{2\pi}\left(\begin{Bmatrix} z_1 \\ z_2 \end{Bmatrix}\ln r + 2\,\mathrm{Re}\begin{Bmatrix} z_1 S_{11} + z_2 S_{12} \\ z_1 S_{21} + z_2 S_{22} \end{Bmatrix}\right), \tag{3.39}$$

where S_{11}, S_{21}, S_{12}, and S_{22} are components of $\mathbf{S}(\theta)$ and are defined as

$$S_{11} = -k_1^2\mu_1 p_1 \ln\varsigma_1 - k_2^2\mu_2 p_2 \ln\varsigma_2\,; \tag{3.40a}$$

$$S_{12} = k_1^2 p_1 \ln\varsigma_1 + k_2^2 p_2 \ln\varsigma_2\,; \tag{3.40b}$$

$$S_{21} = -k_1^2\mu_1 q_1 \ln\varsigma_1 - k_2^2\mu_2 q_2 \ln\varsigma_2\,; \tag{3.40c}$$

$$S_{22} = k_1^2 q_1 \ln\varsigma_1 + k_2^2 q_2 \ln\varsigma_2\,. \tag{3.40d}$$

Without loss of generality, the magnitude of the line load may be chosen as f_1=1 as **f** is arbitrary. This assumption, as well as the information on material properties and nodal coordinates, will enable the calculation of the auxiliary fields necessary for the evaluation of the interaction integral, which in turn will determine T_{11}.

The auxiliary stress field for T_{11} in an isotropic material was given by Nakamura and Parks [28] as

$$\sigma_{11}^{\mathrm{a}} = -\frac{f_1}{\pi r}\cos^3\theta\,; \tag{3.41a}$$

$$\sigma_{22}^{\mathrm{a}} = -\frac{f_1}{\pi r}\cos\theta\sin^2\theta\,; \tag{3.41b}$$

$$\sigma_{12}^{\mathrm{a}} = -\frac{f_1}{\pi r}\cos^2\theta\sin\theta\,; \tag{3.41c}$$

$$\sigma_{33}^{\mathrm{a}} = -\frac{f_1}{\pi r}\nu\cos\theta\,; \tag{3.41d}$$

$$\sigma_{13}^{\mathrm{a}} = \sigma_{23}^{\mathrm{a}} = 0\,. \tag{3.41e}$$

It can be shown from strain-displacement relations that the auxiliary displacement field is

$$u_1^{\mathrm{a}} = -\frac{(1-\nu^2)f_1}{\pi E}\left[\ln r + \frac{\sin^2\theta}{2(1-\nu)}\right]; \tag{3.42a}$$

$$u_2^{\mathrm{a}} = -\frac{(1+\nu)f_1}{2\pi E}\left[(1-2\nu)\theta - \sin\theta\cos\theta\right]; \tag{3.42b}$$

$$u_3^{\mathrm{a}} = 0\,. \tag{3.42c}$$

3.2 Auxiliary Fields for T_{13}

The approach to determine the auxiliary fields for T_{13} is similar to that of T_{11}, except the line load f_1 is replaced by a constant force f_3 in the x_3-direction, as shown in Figure 3.1(b). This configuration will change the line load vector **f** in Eq.(3.22) as

$$\mathbf{f} = [0 \;\; 0 \;\; f_3]^{\mathrm{T}}\,, \tag{3.43}$$

which will yield a different stress function as

$$\phi^{\mathrm{a}} = -\frac{f_3}{\pi m}\mathrm{Re}\begin{Bmatrix} 0 \\ 0 \\ k_3^2\ln\varsigma_3 \end{Bmatrix}. \tag{3.44}$$

By applying a similar derivation following Eq.(3.32) and Eq.(3.36), the auxiliary stresses in the polar coordinate system can be obtained as

$$\sigma_{r3} = \frac{f_3}{\pi m r}\mathrm{Re}\{k_3^2\Omega_3\}, \tag{3.45a}$$

$$\sigma_{\theta\theta} = \sigma_{r\theta} = \sigma_{\theta 3} = \sigma_{rr} = 0\,. \tag{3.45b}$$

Note that Ω_3 is obtained through the definition of Eq.(3.35).

The transformation of stresses from r-θ plane to x_1-x_2 plane gives the results that

σ_{11}^{a}, σ_{12}^{a}, and σ_{22}^{a} all are equal to zero because $\sigma_{\theta\theta} = \sigma_{rr} = \sigma_{r\theta} = 0$. The transformation of σ_{r3}, and $\sigma_{\theta 3}$ is conducted by the following relation [36]:

$$\begin{Bmatrix} \sigma_{13} \\ \sigma_{23} \end{Bmatrix} = \begin{bmatrix} \cos\theta & -\sin\theta \\ \sin\theta & \cos\theta \end{bmatrix} \begin{Bmatrix} \sigma_{r3} \\ \sigma_{\theta 3} \end{Bmatrix}. \tag{3.46}$$

This operation yields the non-zero auxiliary stress components

$$\sigma_{13}^{a} = \frac{f_3 \cos\theta}{\pi m r} \mathrm{Re}\{k_3^2 \Omega_3\}, \tag{3.47a}$$

$$\sigma_{23}^{a} = \frac{f_3 \sin\theta}{\pi m r} \mathrm{Re}\{k_3^2 \Omega_3\}. \tag{3.47b}$$

Then σ_{33}^{a} can be obtained by the use of Eq.(3.18) that also shows $\sigma_{33}^{a} = 0$. This operation assumes a monoclinic material about x_3=0 by using its compliance components shown in Eq.(3.14).

The auxiliary strain field is also readily obtained from the inverse of the stress-strain relation of Eq.(3.13). And the auxiliary displacement field is available from Eq.(3.21a) as well. But with a different **f**, both u_1^{a} and u_2^{a} will be equal to zero while only u_3^{a} is the non-zero displacement as

$$u_3^{a} = -\frac{f_3}{2\pi m}\left(\ln r + \mathrm{Re}\{\ln \varsigma_3\}\right). \tag{3.48}$$

The magnitude of the constant force may also be chosen as f_3=1 because **f** is arbitrary. Hence the auxiliary fields can be calculated, and therefore the T_{13} for a monoclinic material about x_3=0 will be determined.

For an isotropic material, the auxiliary fields may be obtained by applying the material properties on the stiffness matrix of Eq.(3.12). A similar derivation will yield

$$\sigma_{13}^{a} = -\frac{f_3 \cos\theta}{2\pi r}, \tag{3.49a}$$

$$\sigma_{23}^{a} = -\frac{f_3 \sin\theta}{2\pi r}, \tag{3.49b}$$

$$\sigma_{11}^{\mathrm{a}} = \sigma_{22}^{\mathrm{a}} = \sigma_{33}^{\mathrm{a}} = \sigma_{12}^{\mathrm{a}} = 0\,; \tag{3.49c}$$

$$u_3^{\mathrm{a}} = -\frac{f_3(1+\nu)}{\pi E}\ln r\,. \tag{3.50}$$

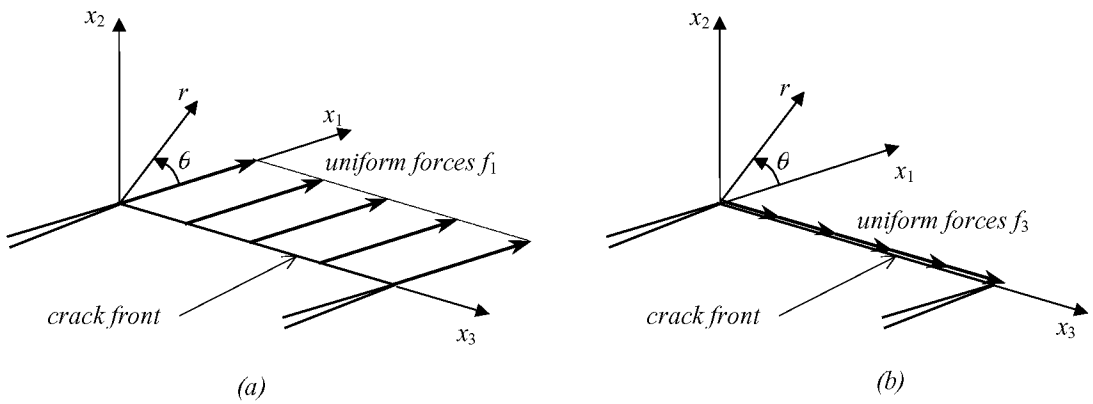

Figure 3.1 Auxiliary line load on a three-dimensional crack: (a) uniform forces f_1 normal to crack front; (b) uniform forces f_3 parallel to crack front.

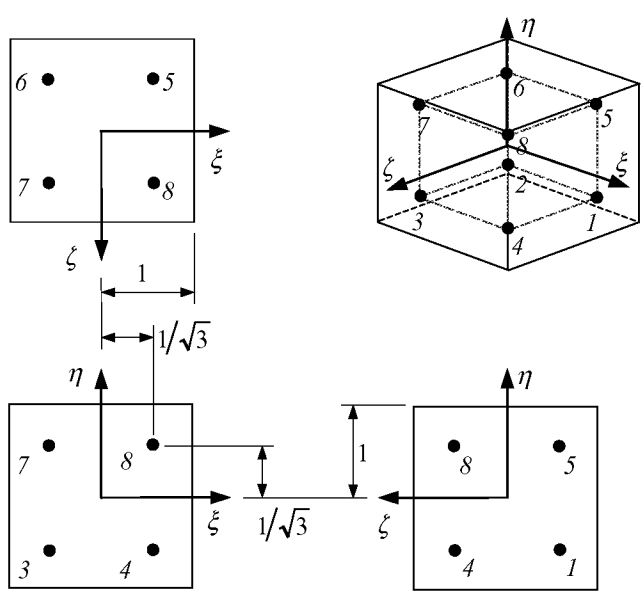

Figure 3.2 Locations of the integration points inside an element.

4 Stress Intensity Factor and *T*-Stress

The formulations regarding the equivalent domain integral and the interaction integral are implemented into a FORTRAN computer program, which uses the finite element solutions computed from another ANSYS program as the input. Once the equivalent domain integral and the interaction integral are evaluated, the stress intensity factor and *T*-stresses can be determined. In the following sections, formulation to determine both parameters will be shown in terms of those integral quantities and appropriate material properties. These formulations can be easily implemented into the FORTRAN program as well. The full contents of the ANSYS and FORTRAN programs are provided in the Appendices.

4.1 Stress Intensity Factor

For an anisotropic cracked solid, the energy release rate G is related to the stress intensity factor through [29,33,37]

$$G = \frac{1}{2}\mathbf{k}^{\mathrm{T}}\mathbf{L}^{-1}\mathbf{k}\,, \tag{4.1}$$

where $\mathbf{k}^{\mathrm{T}} = [k_{\mathrm{II}} \quad k_{\mathrm{I}} \quad k_{\mathrm{III}}]$ are stress intensity factors and $\mathbf{L}^{-1}$ is the inverse of one of the Barnett-Lothe tensors as shown in Eq.(3.24). In elastic materials, the energy release rate G is equal to the value of J-integral. For a pure mode-I crack in an elastic material, $k_{\mathrm{II}} = k_{\mathrm{III}} = 0$, and Eq.(4.1) will reduce to

$$J_1(x_3) = \frac{s'_{11}e}{2}k_{\mathrm{I}}^2(x_3)\,, \tag{4.2}$$

where x_3 is the crack front location defined in Section 2.1, and $J_1(x_3)$ is value of the equivalent domain integral, as defined in Eq.(2.17), on this location. Therefore the local stress intensity factor $k_{\mathrm{I}}(x_3)$ can be determined as

$$k_{\mathrm{I}}(x_3) = \sqrt{\frac{2J_1(x_3)}{s'_{11}e}}\,. \tag{4.3}$$

For an isotropic material, $\mathbf{L}^{-1}$ has the form of

$$\mathbf{L}^{-1} = \frac{2(1-\nu^2)}{E}\begin{bmatrix} 1 & 0 & 0 \\ 0 & 1 & 0 \\ 0 & 0 & \dfrac{1}{1-\nu} \end{bmatrix}. \tag{4.4}$$

The Eq.(4.3) will become

$$k_1(x_3) = \sqrt{\frac{EJ_1(x_3)}{1-\nu^2}}, \tag{4.5}$$

which is the plane strain condition as shown in Eq.(1.3).

4.2 *T*-Stress

The *T*-stress, in general, includes three components, namely T_{11}, T_{13} and T_{33}, as shown in Eq.(3.8). T_{11} and T_{13} should be determined from the evaluation of interaction integrals, while T_{33} can be readily obtained after T_{11} and T_{13} are computed.

Let $I^{(1)}$ and $I^{(2)}$ be the values of interaction integral of Eq.(3.1) when the superposed uniform load is f_1 and f_3, respectively. For an anisotropic material, it can be shown that the following relation between *T*-Stress and interaction integral exists [37]:

$$\begin{bmatrix} s'_{11} & s'_{15} \\ s'_{15} & s'_{55} \end{bmatrix}\begin{Bmatrix} T_{11} \\ T_{13} \end{Bmatrix} = \begin{Bmatrix} \dfrac{I^{(1)}(x_3)}{f_1} - \dfrac{s_{13}}{s_{33}}\varepsilon_{33}(x_3) \\ \dfrac{I^{(2)}(x_3)}{f_3} \end{Bmatrix}, \tag{4.6}$$

where $\varepsilon_{33}(x_3)$ is the crack front extension strain at a given crack front location x_3. $I^{(1)}(x_3)$ and $I^{(2)}(x_3)$ are the interaction integrals on the domain at x_3 due to f_1 and f_3, respectively. Then T_{11} and T_{13} at the same crack front location may be expressed as

$$\begin{Bmatrix} T_{11}(x_3) \\ T_{13}(x_3) \end{Bmatrix} = \begin{bmatrix} s'_{11} & s'_{15} \\ s'_{15} & s'_{55} \end{bmatrix}^{-1}\begin{Bmatrix} \dfrac{I^{(1)}(x_3)}{f_1} - \dfrac{s_{13}}{s_{33}}\varepsilon_{33}(x_3) \\ \dfrac{I^{(2)}(x_3)}{f_3} \end{Bmatrix}. \tag{4.7}$$

The extension strain $\varepsilon_{33}(x_3)$ can be determined independently from finite element results.

For a monoclinic material about x_3=0, $s'_{15} = 0$. Since f_1 and f_3 are arbitrary, they may be chosen as $f_1 = f_3 = 1$ without loss of generality. Therefore for this kind of material, at any given crack front location x_3, T_{11} and T_{13} can be determined solely by $I^{(1)}$ and $I^{(2)}$, respectively. Eq.(4.7) then can be de-coupled as

$$T_{11}(x_3) = \frac{1}{s'_{11}}\left[I^{(1)}(x_3) - \frac{s_{13}}{s_{33}}\varepsilon_{33}(x_3)\right]; \tag{4.8a}$$

$$T_{13}(x_3) = \frac{I^{(2)}(x_3)}{s'_{55}}. \tag{4.8b}$$

In modeling three-dimensional cracks along a given location x_3, the T_{33} component is also induced by the extension strain $\varepsilon_{33}(x_3)$ along the crack front. Thus T_{33} can be evaluated as [37]

$$T_{33}(x_3) = \frac{1}{s_{33}}\left[\varepsilon_{33}(x_3) - (s_{13}T_{11} + s_{35}T_{13})\right]. \tag{4.8c}$$

For isotropic materials,

$$s_{13} = -\frac{\nu}{E},\ s_{33} = \frac{1}{E},\ s_{35} = 0;\ s'_{11} = \frac{1-\nu^2}{E},\ s'_{55} = \frac{2(1+\nu)}{E}. \tag{4.9}$$

Then Eq.(4.8) reduces to

$$T_{11}(x_3) = \frac{E}{1-\nu^2}\left[I^{(1)}(x_3) + \nu\varepsilon_{33}(x_3)\right]; \tag{4.10a}$$

$$T_{13}(x_3) = \frac{E}{2(1+\nu)}I^{(2)}(x_3); \tag{4.10b}$$

$$T_{33}(x_3) = E\varepsilon_{33}(x_3) + \nu T_{11}(x_3). \tag{4.10c}$$

Note that Eq.(4.10a) and Eq.(4.10c) have been derived by Nakamura and Parks [28].

5 Models

5.1 Plates

Due to loading and geometry symmetry, one-eighth of a through-thickness center-cracked plate is modeled by finite elements. The entire plate, shown in Figure 5.1, has a total length of $2l = 80\,\text{in.}$, a total width of $2w = 40\,\text{in.}$, and a total thickness of $2t = 0.33\,\text{in.}$ The origin of the global Cartesian coordinate system is located at the center of the plate. The X-axis is parallel to the crack flank surfaces and the Y-axis is orthogonal to X and to the crack flank. The Z-axis is normal to the X-Y plane. A uniform displacement u_∞ equivalent to a strain value of 0.1% is prescribed on the far ends at $Y = \pm l$. For the finite element model, symmetric boundary conditions are imposed on the planes of $X = 0$, $Y = 0$ ($a \le X \le w$), and $Z = 0$. The displacement loading is also applied on the surface at $Y = l$. A local coordinate system is defined on the crack front at the centerline of thickness. The x_1-axis is perpendicular to the crack front and coincident with the global X-axis. The x_2-axis is also normal to the crack front but parallel to the global Y-axis, and the x_3-axis lies on the crack front and is parallel to global Z-axis as well, as shown in Figure 5.2.

The finite element model is generated and solved by ANSYS, a general-purpose finite element code. A typical mesh of the finite element model is shown in Figure 5.3. It includes large brick-shaped elements far away from the crack front and small fan-shaped elements near the crack front. The elements attached on the crack front are 15-node wedge-shaped elements. The radial size of these elements, e_0, is always equal to or less than 1% of the characteristic length l_c, defined as $l_c = \min[a, w-a, t]$, i.e. $e_0 \le 0.01 \times l_c$, as shown in Figure 5.4. Other than these wedge-shaped elements, the crack front region consists of 12 rings, each of which contains 12 elements. The width of each ring (equivalent to the radial element size) increases as the ring moves farther away from the

crack tip. The largest radial element size at Ring #12 is 26 times the smallest one at Ring #1, and its outer radius is kept at 100 times of e_0, as shown in Figure 5.5. The half thickness is divided into 20 element layers, in which are 5 small layers near the free surface, 8 large layers near the centerline, and 7 mid-size layers in between. The three element sizes of each of these layers, in terms of the half thickness t, are $0.03t$, $0.05t$, and $0.0625t$, respectively. Figure 5.6 shows the mesh refinement and element sizes near the crack front and through the thickness. The overall mesh contains 5640 elements and 25183 nodes with 75549 degrees of freedom. This mesh result showed appropriate convergence on the calculation of the fracture parameters.

5.2 Stiffened Panels

A stiffened panel based on the dimensions of the plate mentioned in Section 5.1 has five stiffeners attached longitudinally on one side of the plate. This structure is designed by Boeing for the all-composite wing skin in a commercial aircraft [29]. A center crack of length $2a$ cuts through the central stiffener and the panel. Figure 5.7 shows the configuration of the panel as well as the detail dimensions of the stiffener. Due to the presence of stiffeners and geometry symmetry, one-fourth of the entire panel is modeled by finite elements, as shown in Figure 5.8. Both of the global and local Cartesian coordinate systems are defined in the same way they are defined in a plate. Hence the symmetric boundary conditions are imposed on the planes of $X = 0$ and $Y = 0$ ($a \le X \le w$). To prevent a free-body motion in Z-direction, a constraint in the Z-direction is also imposed on the node at $(0, 0, -t)$, i.e. the point at the center of the panel's back side. Here t is defined as one half of the panel thickness that is not including the stiffener portion. A uniform displacement u_∞ equivalent to a strain value of 0.1% is prescribed on the far end at $Y = l$.

Since the crack is not expected to propagate across the “second stiffeners”, which are the stiffeners next to the central one, the crack front will only extend to near the edge of the second stiffeners. Under this assumption, the definition of the crack aspect ratio

will be different from what is defined in unstiffened plates. Instead of a/w, the crack aspect ratio in stiffened panels is defined as a'/w'. Here a' is the crack length calculated from the edge of the central stiffener to the crack front, and w' is the distance between edges of two adjacent stiffeners. Figure 5.9 shows an enlarged region along the crack surface with the designation of a, a', and w'.

The mesh pattern on the cracked panel portion of the finite element model is similar to that of the entire plate described in Section 5.1. The characteristic length l_c, however, is defined as $l_c = \min[a', w' - a', 2t]$. The radial size, e_0, of those 15-node wedge-shaped elements attached on the crack front is set to be equal to 0.4% of the characteristic length, i.e. $e_0 = 0.004 l_c$. On the part of the finite element model containing uncracked panel and 3 stiffeners, the mesh is controlled to be as coarse as possible in order to reduce the overall number of elements. The full thickness of the panel, $2t$, is divided into 30 element layers, in which are two symmetric parts that includes 15 layers each. For each half thickness, 5 large layers are near the centerline, 5 small layers are near the free surface, and 5 mid-size layers are in between. The three element sizes of each category of these layers, in terms of the half thickness t and from large to small, are $0.04t$, $0.07t$, and $0.09t$, respectively. Figure 5.10 shows the mesh refinement and element sizes near the crack front and through the thickness. The overall mesh contains 10539 elements and 46780 nodes with 140340 degrees of freedom.

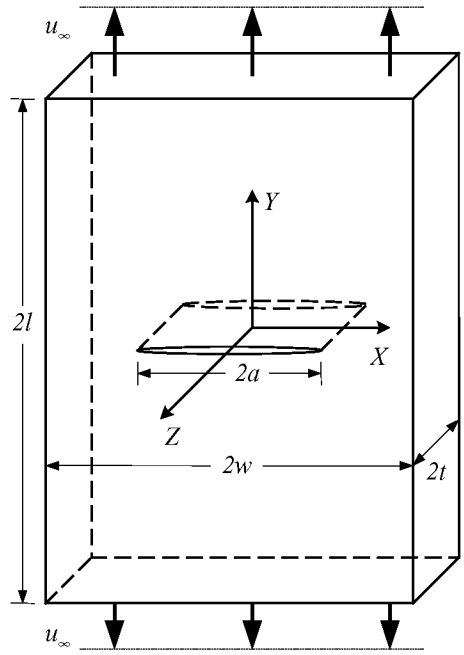

Figure 5.1 A through-thickness center-cracked plate subjected to a uniform far-field displacement.

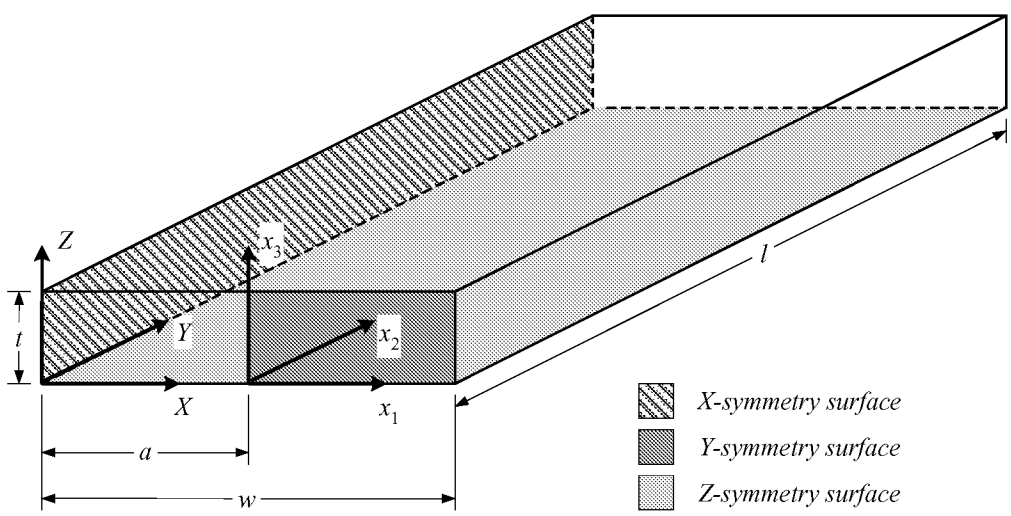

Figure 5.2 One-eighth of the plate to be generated as a finite element model.

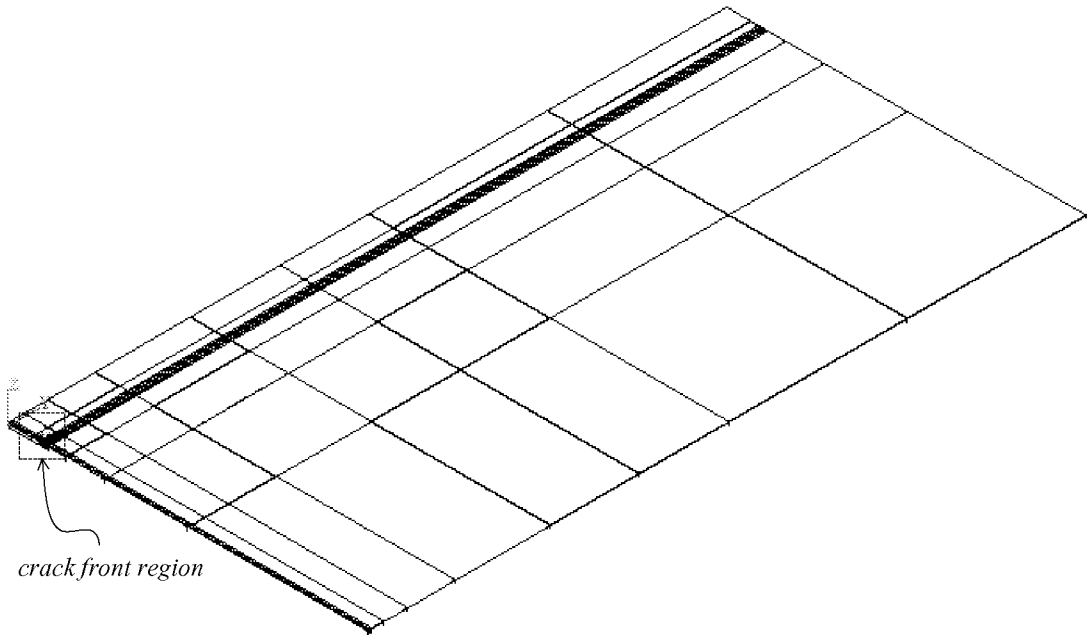

Figure 5.3 Finite element mesh of a one-eighth center-cracked plate (a/w=0.1).

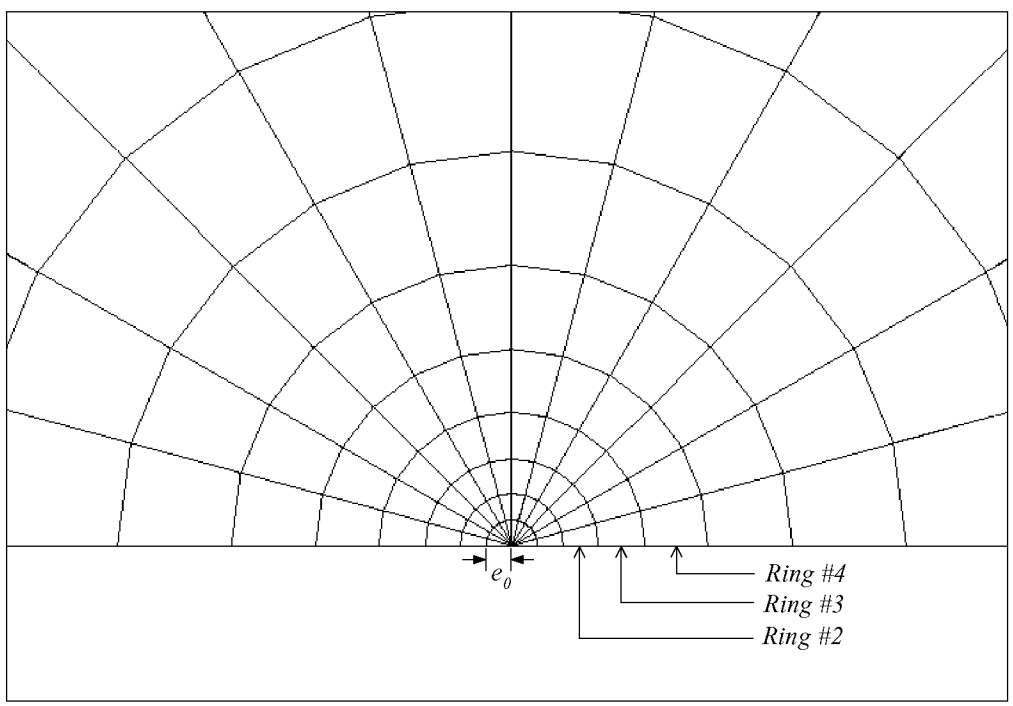

Figure 5.4 Mesh refinement near crack front region.

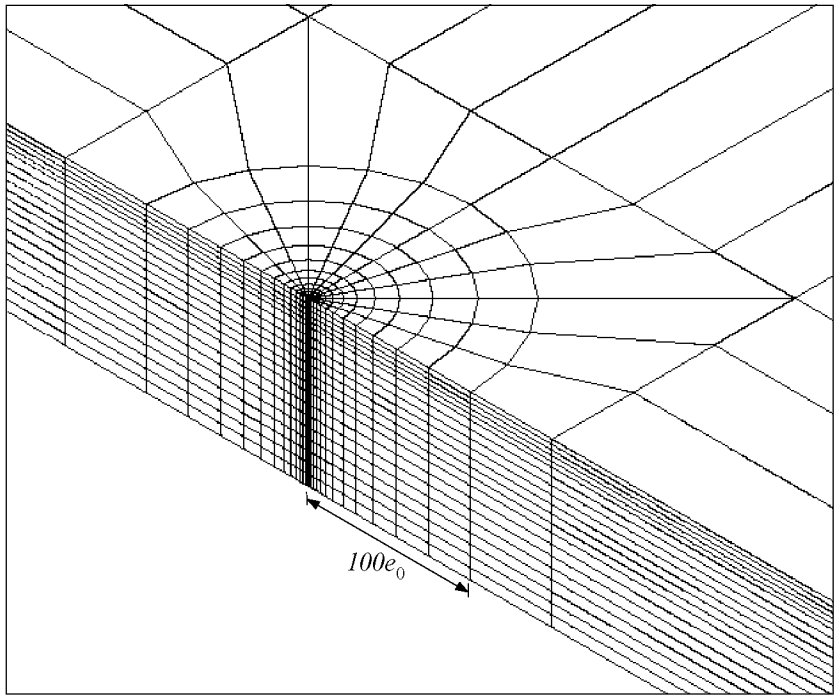

Figure 5.5 Radius of the outer surface of Ring #12 equals to $100e_0$.

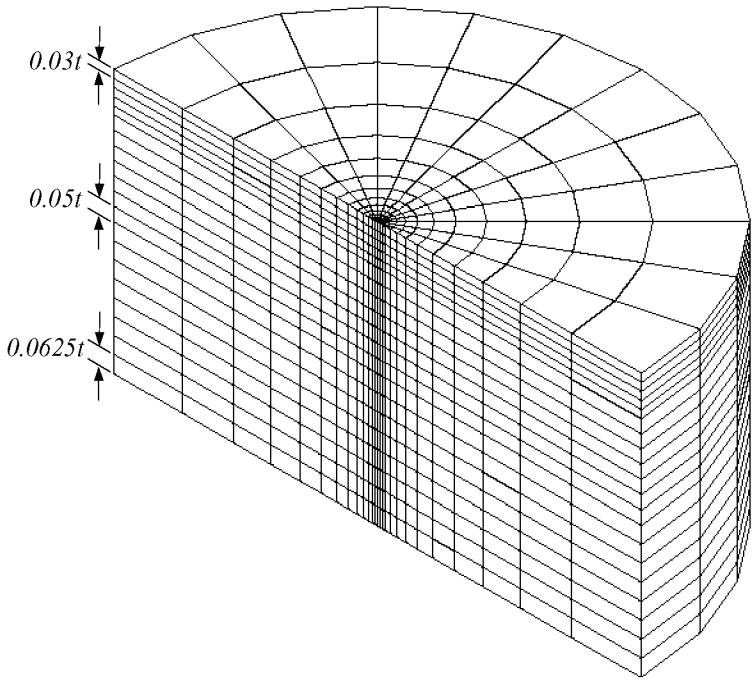

Figure 5.6 Sizes of element layers in terms of the half thickness t.

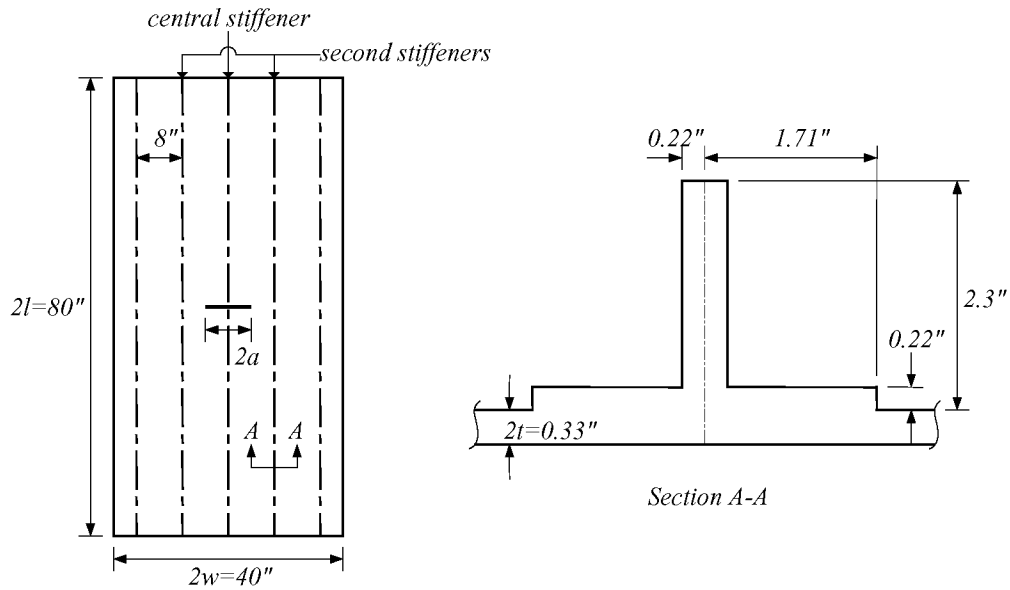

Figure 5.7 Configuration and dimensions of a center-cracked panel with stiffeners.

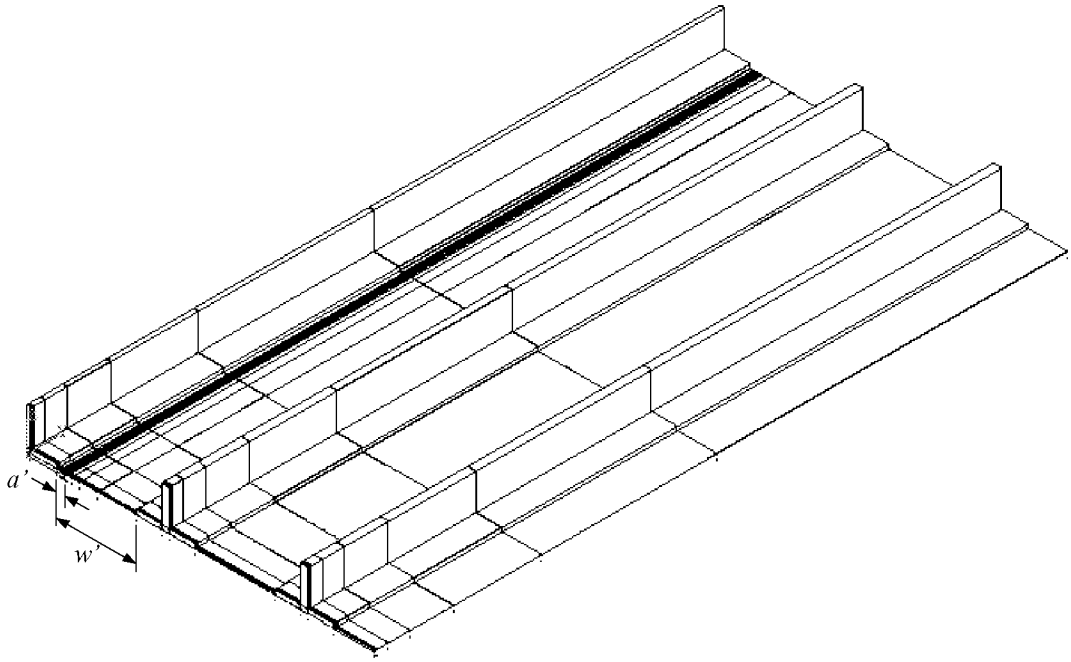

Figure 5.8 The finite element model of a one-fourth center-cracked stiffened panel (a'/w'=0.1).

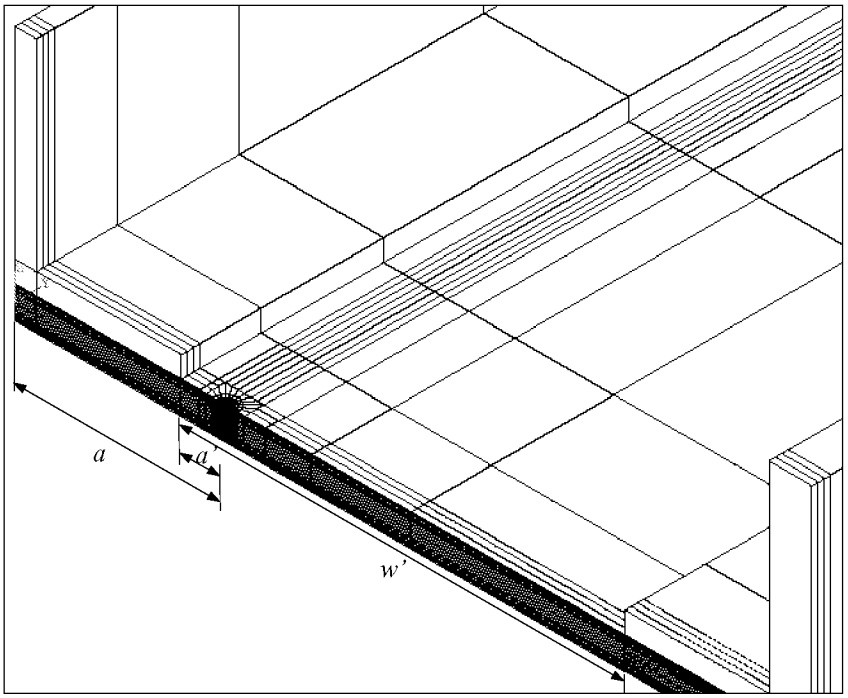

Figure 5.9 Enlarged finite element mesh showing definition of the crack aspect ratio a'/w' (a'/w'=0.1).

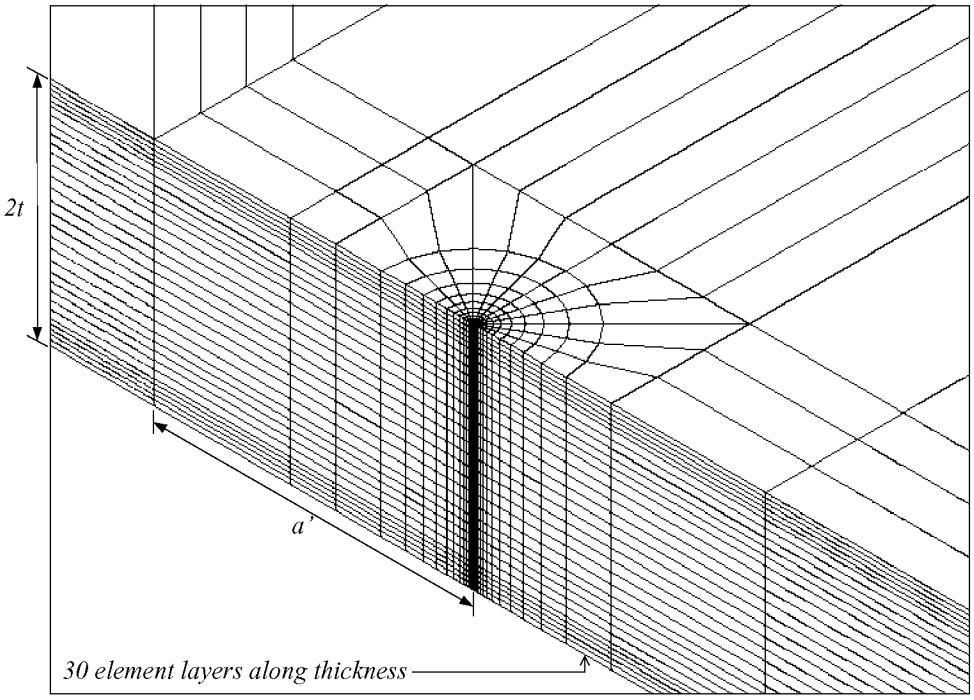

Figure 5.10 Mesh refinements near the crack front of the stiffened panel (a'/w'=0.1).

6 Results

For the purpose of comparison, the stress intensity factors and T-stresses are normalized as dimensionless numbers. The normalized stress intensity factor has the form of $\overline{K}_{\mathrm{I}} = K_{\mathrm{I}} / \left(\sigma_{\infty}\sqrt{\pi a}\right)$, while the two normalized T-stresses are defined as $\overline{T}_{11} = T_{11}/\sigma_{\infty}$ and $\overline{T}_{13} = T_{13}/\sigma_{\infty}$, respectively. Here σ_{∞} is the average stress, computed from the total nodal force, F due to the far-field displacement u_{∞}, on the plane of $Y = l$ (see Figure 5.1) divided by the cross-sectional area of the plate. For a cracked plate, $\sigma_{\infty} = F/(wt)$, where w is the half width and t is the half thickness. The thickness of the plate is also normalized because the variations of the stress intensity factor and the T-stresses over the thickness are to be investigated. The normalized thickness of an element is defined as $\bar{t} = x_3/t$, which indicates the normalized x_3 coordinate at the centroid of the element.

To determine the distribution of the stress intensity factor and the T-stresses over the thickness of a particular model, these parameters are first calculated from each of the three adjacent rings of elements very close to the crack front (Rings #2, #3, and #4 as shown in Figure 5.4) by the equivalent domain integral and interaction integral. Then an average value is carried out over three domains.

6.1 Isotropic Plates

A family of isotropic plates with different crack lengths and different thicknesses is examined. The material properties of Young's modulus $E = 10$ Msi and Poisson's ratio $\nu = 0.3$ are used in the modeling. To compare the fracture parameters for different variables, the stress intensity factor K_{I} and T_{11} stress are retrieved from the element layer attached to the centerline of the thickness. As shown in Figure 5.6, this layer has a thickness of $0.0625t$, and the x_3 coordinate of the centroid is located at $0.03125t$. Hence $\overline{K}_{\mathrm{I}}$ and $\overline{T}_{11}$ of different models will be retrieved and plotted at normalized thickness

$\bar{t} = 0.03125$. The T_{13} stress is retrieved from the element layer approximately at the quarter thickness of a plate, or at the thickness between 0.50*t* and 0.55*t*, i.e., Layer #9 as shown in Figure 5.6, and therefore $\bar{t} = 0.525$ for this element.

6.1.1 Crack Length

First we will consider a plate of thickness $2t = 0.33$ in. ($t/w = 0.00825$) with various crack aspect ratios $a/w = 0.1 \sim 0.9$. To compare the effects of the thickness on fracture parameters for the same crack aspect ratios, the results from another set of plates with thickness of $2t = 10.24$ in. ($t/w = 0.256$) are presented as well.

Figure 6.1 shows the distribution of the normalized stress intensity factors $\overline{K}_{\mathrm{I}}$ over half of the thickness for different crack aspect ratios. The distribution of the stress intensity factor is symmetric with respect to x_3=0. $\overline{K}_{\mathrm{I}}$ is fairly constant over half of the thickness, except in the region near the free surface (approximately from $\bar{t} \geq 0.8$ for $a/w = 0.1$ down to $\bar{t} \geq 0.6$ for $a/w = 0.9$), where the stress intensity factor slightly decreases. Note that there exists a weaker corner singularity near the free surface. The normalized stress intensity factors at the center of thickness are retrieved and plotted against the *a/w* ratios in Figure 6.2. The results for $t = 0.165$ in. show that $\overline{K}_{\mathrm{I}}$ rises dramatically from 1.06 at the small crack of $a/w = 0.1$ to 2.72 as the *a/w* ratio reaches 0.9. Results from the other set of plates with thickness of $t = 5.12$ in. ($t/w = 0.256$) are also shown in the same figure, in which the normalized stress intensity factor increases from 1.00 to 2.64 as the *a/w* ratios goes from 0.1 to 0.9. It is slightly smaller than that of the thinner plate.

The 2-D plane strain analytical solution of $\overline{K}_{\mathrm{I}}$, also shown in Figure 6.2, has the following form in terms of the crack aspect ratio *a/w* [38]:

$$\overline{K}_{\mathrm{I}}(\frac{a}{w}) = \sqrt{\sec\left(\frac{\pi}{2}(\frac{a}{w})\right)}\left[1 - 0.025(\frac{a}{w})^2 + 0.06(\frac{a}{w})^4\right]. \tag{6.1}$$

When the normalized stress intensity factor obtained from 3-D analysis is compared with the 2-D solution, i.e. Eq.(6.1), deviation within 4% on the average from the 2-D solution is found for the thicker plate; more than 5% for the thinner plate.

Figure 6.3 shows the distribution of the normalized T_{11} stresses over half of the thickness in the thinner plate ($t = 0.165\,\text{in.}$) for different crack aspect ratios. The T_{11} stress distribution is symmetric with respect to x_3=0. For all *a/w* ratios, the variation of $\overline{T}_{11}$ over half of the thickness is relatively small except in the region near the free surface (approximately $\bar{t} \geq 0.85$), where the corner singularity would cause the T_{11} stress to diverge. For most curves ($a/w < 0.7$), the near-constant part of $\overline{T}_{11}$ stays near –1.0, which is the theoretical 2-D solution. In Figure 6.4 the curve of the thinner plate ($t/w = 0.00825$) confirms this trend as the magnitude of the normalized T_{11} stresses stays between –0.8 and –1.0 before the crack aspect ratio reaches 0.7. Beyond that the normalized T_{11} stress increases (in magnitude) rapidly to –3.77 as the *a/w* ratio reaches 0.9. The other curve representing the thicker plate shows a similar trend, but the magnitude of $\overline{T}_{11}$ at the center increases from –1.02 at the smallest crack, $a/w = 0.1$, to -4.87 at the largest crack, $a/w = 0.9$.

The 2-D solution of $\overline{T}_{11}$, also shown in Figure 6.4, can be obtained from the stress biaxiality ratio *B* and normalized stress intensity factors $\overline{K}_{\mathrm{I}}$:

$$\overline{T}_{11} = B\overline{K}_{\mathrm{I}}, \tag{6.2}$$

where *B* is a function of the crack aspect ratio *a/w* [39]:

$$B(\frac{a}{w}) = -\left[1 + 0.085(\frac{a}{w})\right]. \tag{6.3}$$

Results from the thicker plate are closer to the 2-D solution than those of the thinner plate, although the closeness is only maintained until *a/w* is near 0.7. This indicates that, at a small crack, $\overline{T}_{11}$ of the thicker plate is closer to the plane strain condition than that of the thinner plate.

In Figure 6.5, the distribution of the normalized T_{13} stresses over half of the thickness of the thinner plate for different *a/w* ratios does not have a constant portion shown in the distribution of $\overline{K}_{\mathrm{I}}$ and $\overline{T}_{11}$. Note that the distribution is anti-symmetric with respect to x_3=0. Instead, the magnitude of the normalized T_{13} stresses rises monotonically from zero at the center of thickness to a much larger value near the free surface, and ultimately back to zero to satisfy the stress-free condition at the free surface. The larger the crack length is, the more sharply the $\overline{T}_{13}$ stress results. As the normalized T_{13} stresses at $\bar{t} = 0.5$ are retrieved for all *a/w* ratios, as shown in Figure 6.6, it is observed for the thinner plate that the magnitude of the normalized T_{13} stresses increases from approximately –0.35 for $a/w = 0.1$ to –2.6 for $a/w = 0.9$. For the case of the thicker plate, the trend persists. The overall variation of $\overline{T}_{13}$, however, is much smaller than that of the thinner plate. The absolute value of the normalized T_{13} stresses, which goes from approximately –0.07 for $a/w = 0.1$ up to near –0.6 for $a/w = 0.9$, is relatively smaller. Note that $\overline{T}_{13} = 0$ for the 2-D solution.

6.1.2 Plate Thickness

Another set of plates with different thicknesses is analyzed. The crack aspect ratio of these plates is kept at $a/w = 0.1$. The finite element mesh of each model is also kept the same; i.e., the overall number of elements is unchanged for each finite element model. Only the dimensions of the elements are slightly changed due to thickness change. The thickness ranges from a thinner plate of $2t = 0.33$ in. ($t/w = 0.00825$) to a very thick plate of $2t = 20.48$ in. ($t/w = 0.512$).

Figure 6.7 shows the variation of normalized stress intensity factors over half of the thickness for plates with different *t/w* ratios. It is observed that, for relatively thin plates ($t/w \leq 0.064$), $\overline{K}_{\mathrm{I}}$ tends to decrease as $\bar{t}$ goes away from the center of the plate. In contrast, for relatively thick plates, $\overline{K}_{\mathrm{I}}$ tends to increase in the thickness beyond the

region of $\bar{t} \geq 0.3$. The variation of $\overline{K}_{\mathrm{I}}$ for all *t/w* ratios at the center of thickness is plotted in Figure 6.8. For very thin plates (approximately $t/w \leq 0.03$), the normalized K_{I} almost stays constant near 1.06. As the thickness increases up to $t/w \geq 0.5$, $\overline{K}_{\mathrm{I}}$ gradually decreases to near 1.0, which is the 2-D solution for very small crack length, i.e., $a/w \rightarrow 0$.

The normalized T_{11} stresses over half of the thickness for plates with different *t/w* ratios are plotted in Figure 6.9. The normalized T_{11} stresses are fairly constant in the region of $\bar{t} \leq 0.75$ for all cases. Beyond that, $\overline{T}_{11}$ in a thinner plate deviates much more than it would in a relatively thick plate. These stresses, or the normalized T_{11} stresses at center of the plate thickness, are extracted and plotted against the *t/w* ratios in logarithmic scale in Figure 6.10. The stresses, as shown also in Figure 6.9, increase gradually in magnitude from approximately –0.79 in a very thin plate ($t/w = 0.004$) to –1.01 in a very thick plate ($t/w = 0.512$).

In Figure 6.11, the distribution of the normalized T_{13} stresses over half of the thickness rises in magnitude from zero at $\bar{t} = 0$ to a larger value near the free surface. This trend is the same as that in Figure 6.5. In general the normalized T_{13} stresses decrease in terms of the magnitude as the plate thickness increases. The trend is observed for the normalized T_{13} stresses at $\bar{t} = 0.5$ of each plate in Figure 6.12, in which the magnitude of $\overline{T}_{13}$ decreases from approximately –0.5 for a very thin plate ($t/w = 0.004$) to near –0.02 for a very thick plate ($t/w = 0.512$).

6.2 Orthotropic Plates

The plates of same dimensions are analyzed again with the properties of a composite material. The composite is AS4 carbon warp-knit fabric design by Boeing for the all-composite wing skin in a commercial aircraft [29]. It has the overall orthotropic material properties that are listed in Table 6.1. The orientation of the material coordinates

Table 6.1 Material properties of the orthotropic plate.

$E_X = 5.162$ Msi	$G_{YZ} = 0.64$ Msi	$\nu_{YZ} = 0.22$
$E_Y = 11.773$ Msi	$G_{XZ} = 0.57$ Mpsi	$\nu_{XZ} = 0.29$
$E_Z = 1.53$ Msi	$G_{XY} = 2.479$ Msi	$\nu_{XY} = 0.1758$

is referred to the global coordinate system shown in Figure 5.1.

6.2.1 Crack Length

The distribution of the normalized stress intensity factors $\overline{K}_{\mathrm{I}}$ through half of the thickness for various crack aspect ratios is shown in Figure 6.13. Each curve of the five different *a*/*w* ratios is relatively flat, meaning that $\overline{K}_{\mathrm{I}}$ is almost constant over the thickness. In fact, the amount of fluctuation of $\overline{K}_{\mathrm{I}}$ is less than 3% and occurs only in the region where $\bar{t} \geq 0.85$. In comparison to Figures 6.13 and 6.1, it is observed that $\overline{K}_{\mathrm{I}}$ of the orthotropic material is more constantly distributed than that of the isotropic material. The magnitude for each *a*/*w* ratio for the orthotropic material is also slightly (about 6%) smaller. The normalized stress intensity factors at the center of thickness increases from 1.00 to 2.54 as the *a*/*w* ratio increases from 0.1 to 0.9, as shown in Figure 6.14. Results from the thicker plate ($t/w = 0.256$) are also shown in the same figure, in which $\overline{K}_{\mathrm{I}}$ ranges from 1.00 to about 2.52. Figure 6.14 shows that the two curves are almost identical, indicating that $\overline{K}_{\mathrm{I}}$ is less sensitive to the change of plate thickness in the orthotropic material.

Figure 6.15 shows the distribution of the normalized T_{11} stresses through half of the thickness for various crack lengths in the thin plate ($t = 0.165$ in.). Similar to that of the isotropic material in Figure 6.3, the variation of $\overline{T}_{11}$ is not significant except near the free surface (approximately $\bar{t} \geq 0.85$). For the small crack case ($a/w = 0.1$), the flat part of the $\overline{T}_{11}$ curve stays around –0.660, which is nearly equal to the material anisotropy

ratio in the 2-D solution [29], $-\sqrt{s'_{22}/s'_{11}} = -0.668$. In Figure 6.16, the magnitude of $\overline{T}_{11}$ at the center of the thickness increases gradually from –0.66 to –3.22 as the *a/w* ratio increases from 0.1 to 0.9, for the case of the thinner plate. The curve of the thicker plate ($t/w = 0.256$) is almost identical to that of the thinner plate, as it ranges between –0.67 and –3.24. For the thicker plates in both materials, $\overline{T}_{11}$ in the orthotropic material is about two-third of $\overline{T}_{11}$ in the isotropic material (see also Figure 6.4). The 2-D solutions of both material types are about in the same ratio, i.e., –0.668 and –1.0.

The trend of $\overline{T}_{13}$ distribution over half of the thickness for various crack lengths in Figure 6.17 is similar to that of the isotropic material in Figure 6.5, except the magnitude for the orthotropic material is much smaller than that of the isotropic cases. In Figure 6.18, normalized T_{13} stresses of the thinner plate at quarter thickness ($\bar{t} \approx 0.5$) range from about -3.94×10^{-2} to -2.87×10^{-1} as the *a/w* ratio increases from 0.1 to 0.9. $\overline{T}_{13}$ of the thicker plate ranges approximately between -7.31×10^{-3} and -5.86×10^{-2}. Both curves retain the trend that appeared in Figure 6.6. The magnitude of $\overline{T}_{13}$ for the orthotropic material, however, is one order less than that in the isotropic material.

6.2.2 Plate Thickness

As the crack aspect ratio *a/w* is kept at 0.1, various plate thicknesses are adopted in the finite element model for analysis. The overall mesh configuration and total number of elements are unchanged, although the element size will be slightly changed due to thickness change. The half thickness varies from a very thin plate of 0.04in. ($t/w = 0.002$) to a very thick plate of 10.24in. ($t/w = 0.512$).

The distribution of the normalized stress intensity factors through half of the thickness for plates with various *t/w* ratios is shown in Figure 6.19. The overall variation of $\overline{K}_{\mathrm{I}}$ for each thickness is relatively small (< 3%). A similar trend to the isotropic cases

is that $\overline{K}_{\mathrm{I}}$ tends to decrease in the region of $\bar{t} \geq 0.75$ for thin plates ($t/w \leq 0.064$) and increase in the region of $\bar{t} \geq 0.6$ for thick plates. In the region of $\bar{t} \leq 0.5$, $\overline{K}_{\mathrm{I}}$ of each case stays very close to 1.0, the 2-D solution for very small crack lengths. $\overline{K}_{\mathrm{I}}$ at the center of thickness for all *t/w* ratios is retrieved and plotted in Figure 6.20, in which all normalized stress intensity factors fall between 0.995 and 1.005. The overall difference is within 1%. Therefore, $\overline{K}_{\mathrm{I}}$ is rather stable even if the plate thickness increases more than two orders of magnitude.

Figure 6.21 shows the normalized T_{11} stresses over half of the thickness for various *t/w* ratios. For each plate, $\overline{T}_{11}$ is fairly constant in the region of $\bar{t} \leq 0.75$. In the region near free surface ($\bar{t} \geq 0.85$), however, $\overline{T}_{11}$ tends to diverge as also observed in the isotropic cases (see Figure 6.9). It is observed that approximately at $\bar{t} = 0.8$, all five curves pass through a point where $\overline{T}_{11}$ is near –0.669 that is close to the material anisotropy ratio, –0.668. $\overline{T}_{11}$ at the center of the thickness for all *t/w* ratios is extracted and plotted in Figure 6.22. For the plates of $t/w \geq 0.00825$, $\overline{T}_{11}$ ranges between –0.658 and –0.673, or within $\pm 1.5\%$ of the material anisotropy ratio. As the *t/w* ratio increases beyond 0.016, i.e., plates with moderate to thick thicknesses, $\overline{T}_{11}$ falls within $\pm 1\%$ of the material anisotropy ratio. As the plate becomes thinner ($t/w \leq 0.006$), however, the magnitude of $\overline{T}_{11}$ decreases from near the material anisotropy ratio to about 90% of that at $t/w = 0.002$.

In Figure 6.23, a similar trend to the $\overline{T}_{13}$ distribution of isotropic plates over half of the thickness for various *t/w* ratios is observed. The relative magnitude of $\overline{T}_{13}$ for orthotropic plates is one order less than that in isotropic plates. Figure 6.24 shows $\overline{T}_{13}$ at quarter thickness for all plates. As the plate thickness increases to the very thick case of $t/w = 0.512$, the magnitude of $\overline{T}_{13}$ decreases to near zero. All normalized T_{13} stresses in orthotropic plates are relatively small, compared to those in isotropic plates.

6.3 Stiffened Panels

All stiffened panels have the orthotropic material properties as listed in Table 6.1 and the dimensions as shown in Figure 5.7. Panels with different crack aspect ratios, a'/w', ranging from 0.1 to 0.9 are analyzed. To illustrate the effect of crack aspect ratios on normalized stress intensity factor and the T-stresses, each parameter at the centerline of the thickness will be plotted against a'/w' ratios. The value of a parameter is calculated from the average values over element layers #15 and #16, which are attached on the centerline. The thickness of each layer is $0.09t$. Therefore the centroid is at $-0.045t$ for an element in Layer #15 and $0.045t$ for an element in Layer #16.

The original stiffened panel has a thickness of $2t = 0.33$ in. ($t/w = 0.00825$). To compare the effects of panel thickness on the fracture parameters with the same crack length, the results from another set of thinner panels of $t/w = 0.004$ are presented as well. Note that the stiffener dimensions are fixed for all the normalized studies.

The distribution of the normalized stress intensity factors $\overline{K}_{\mathrm{I}}$ through the entire thickness of the cracked panels is shown in Figure 6.25. For each crack aspect ratio, the distribution of $\overline{K}_{\mathrm{I}}$ appears to be increasing almost linearly from the bottom ($\bar{t} = -1$) to the top ($\bar{t} = 1$) of the panel thickness. The trend clearly shows the bending effect for thinner stiffened panels. The slope of each $\overline{K}_{\mathrm{I}}$ curve decreases as the a'/w' ratio increases. For instance, $\overline{K}_{\mathrm{I}}$ increases from about 0.8 to 1.9 for $a'/w' = 0.1$ but ranges only between 0.96 and 1.06 for $a'/w' = 0.9$. Figure 6.26 shows $\overline{K}_{\mathrm{I}}$ at center of the thickness for panels with various crack aspect ratios. The normalized stress intensity factor of the thicker stiffened panel ($t/w = 0.00825$) decreases from approximately 1.38 to 1.05, as the a'/w' ratio increases from 0.1 to 0.9. The thin stiffened panels ($t/w = 0.004$) generally have larger $\overline{K}_{\mathrm{I}}$, which decreases from 1.67 to 1.05 for a'/w' ratio from 0.1 to 0.9. The difference of two sets of panels, however, becomes smaller as the

crack length increases. Both panels almost have an equal $\overline{K}_{\mathrm{I}}$ of 1.05 at $a'/w' = 0.9$. It indicates that, as the crack length becomes large enough, the panel thickness is irrelevant to the normalized stress intensity factor.

Figure 6.27 shows the distribution of the normalized T_{11} stresses over the thickness of the panel for different a'/w' ratios. The magnitude of $\overline{T}_{11}$ is generally in an increasing trend, although the distribution appears more linearly in larger crack lengths. Overall, the magnitude of $\overline{T}_{11}$ decreases as the crack length increases. This can be observed in Figure 6.28 where the normalized T_{11} stresses are extracted and plotted against different a'/w' ratios. Though all are negative, $\overline{T}_{11}$ of the thicker panel increases from –0.91 at $a'/w' = 0.1$ to –0.52 at $a'/w' = 0.9$, while $\overline{T}_{11}$ of the thinner panel ranges from –1.17 to –0.41. For smaller cracks ($a'/w' \leq 0.7$), the normalized T_{11} stress of the thinner panel is larger (in magnitude) than that of the thicker panel. For larger cracks ($a'/w' \geq 0.8$), however, the trend reverses as the thinner panel has a smaller $\overline{T}_{11}$ (in magnitude).

In Figure 6.29, the distribution of $\overline{T}_{13}$ through the thickness appears in a nearly anti-symmetric manner with respect to the thickness centerline, $\bar{t} = 0$. The shape of each $\overline{T}_{13}$ curve is similar enough that it seems all curves are shifting within a range approximately equal to 0.5. The overall variation of $\overline{T}_{13}$ for all a'/w' ratios ranges between –0.1 and –1.5. $\overline{T}_{13}$ at center of the thickness for each crack length of both sets of panels is retrieved and plotted in Figure 6.30. Both curves form part of a parabola, respectively. For the thicker panels ($t/w = 0.00825$), $\overline{T}_{13}$ decreases from –0.93 at $a'/w' = 0.1$ to –0.95 at $a'/w' = 0.3$ near the lowest point of the curve, then increases to about –0.58 at $a'/w' = 0.9$. For the thinner panels, the normalized T_{13} stress swings from –1.86 at $a'/w' = 0.1$ to –1.22 at $a'/w' = 0.9$. In between the lowest point is near $a'/w' = 0.4$ where $\overline{T}_{13}$ is approximately –2.16. Figure 6.30 shows the thinner panel has larger $\overline{T}_{13}$ (in

magnitude) for different crack lengths. And the maximum amplitude of $\overline{T}_{13}$ for a panel of fixed thickness occurs at a moderate crack aspect ratio.

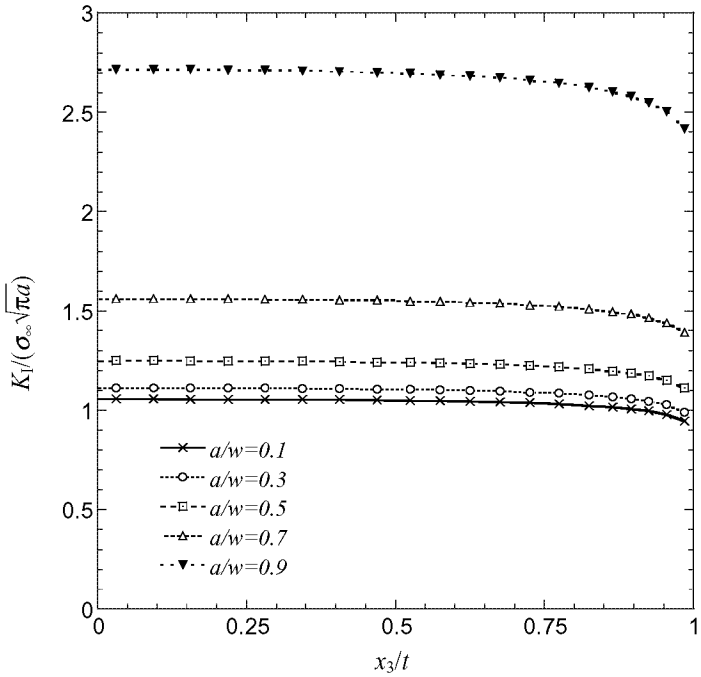

Figure 6.1 Normalized stress intensity factors through half of the thickness for isotropic plates of t=0.165 in. (t/w=0.00825) with various a/w ratios.2

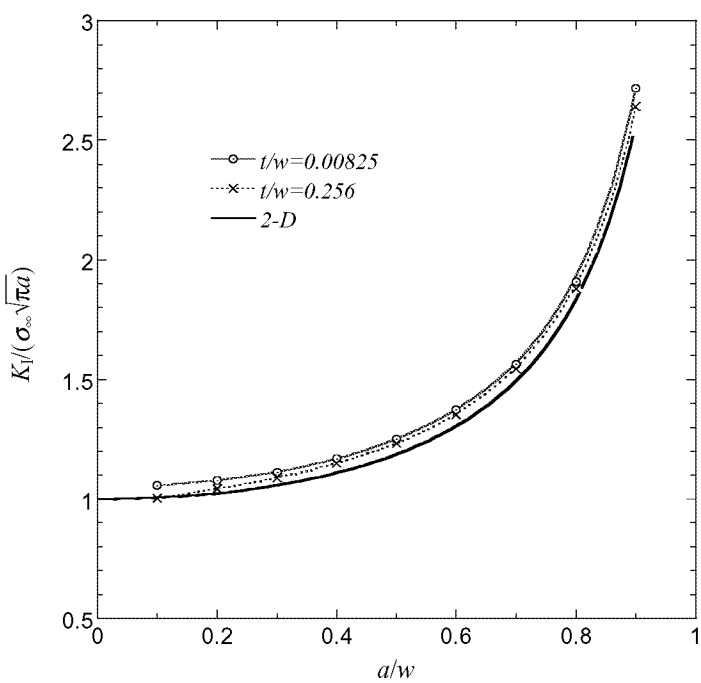

Figure 6.2 Normalized stress intensity factors at center of the thickness ($x_3/t=0$) for isotropic plates with two different thicknesses.

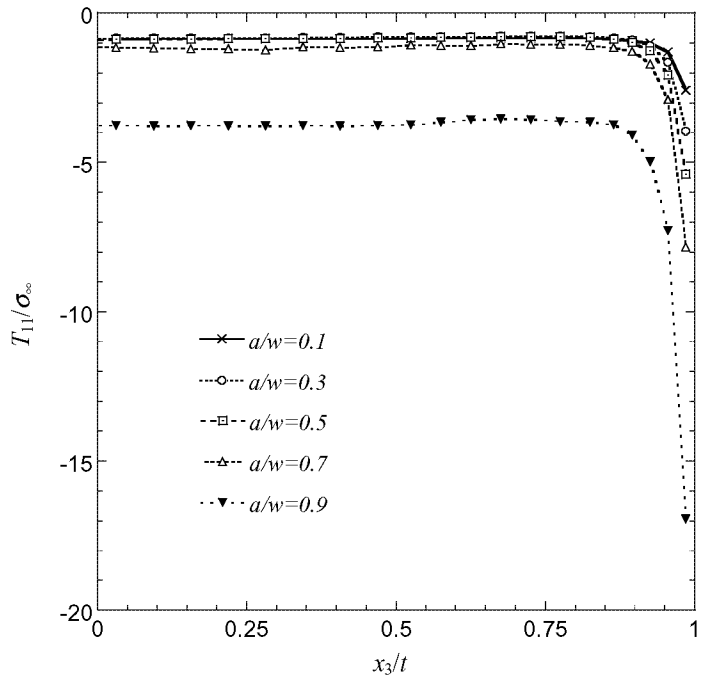

Figure 6.3 Normalized T_{11} stresses through half of the thickness for isotropic plates of t=0.165 in. (t/w=0.00825) with various a/w ratios.

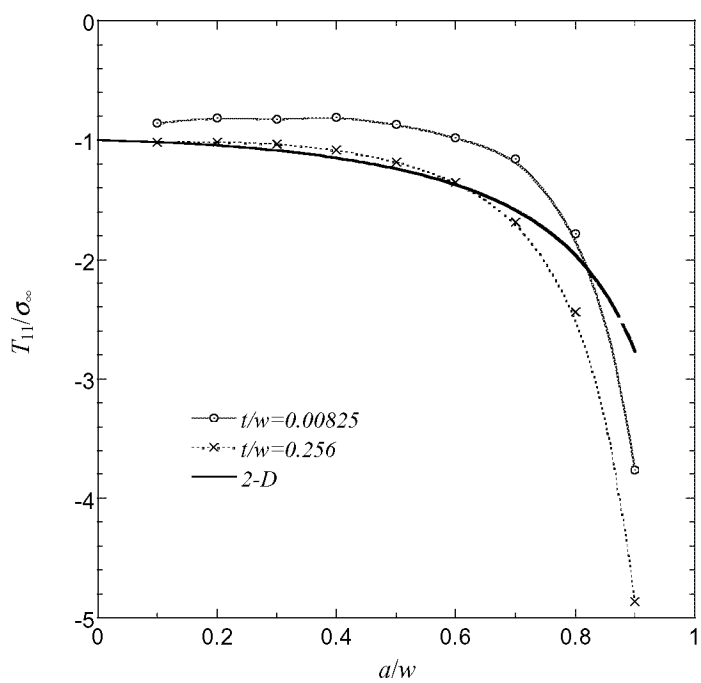

Figure 6.4 Normalized T_{11} stresses at center of the thickness ($x_3/t=0$) for isotropic plates with two different thicknesses.

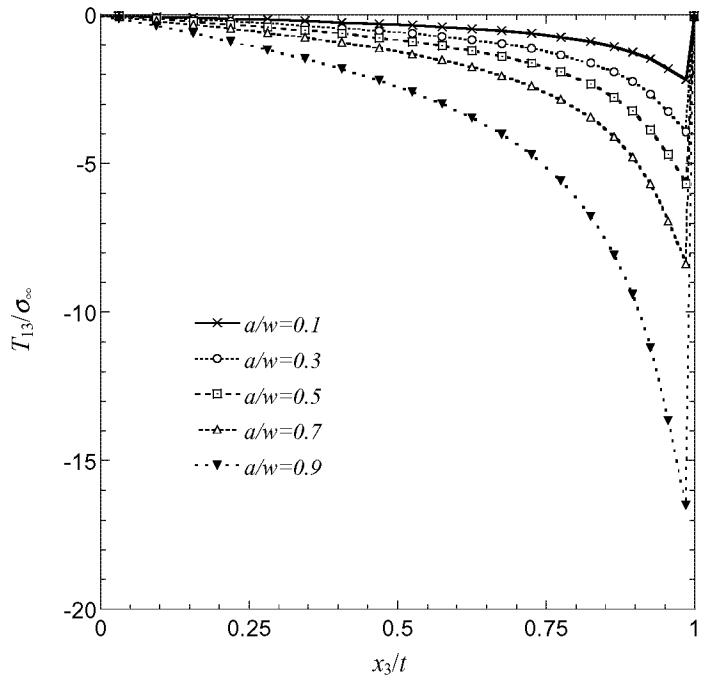

Figure 6.5 Normalized T_{13} stresses through half of the thickness for isotropic plates of t=0.165 in. (t/w=0.00825) with various a/w ratios.

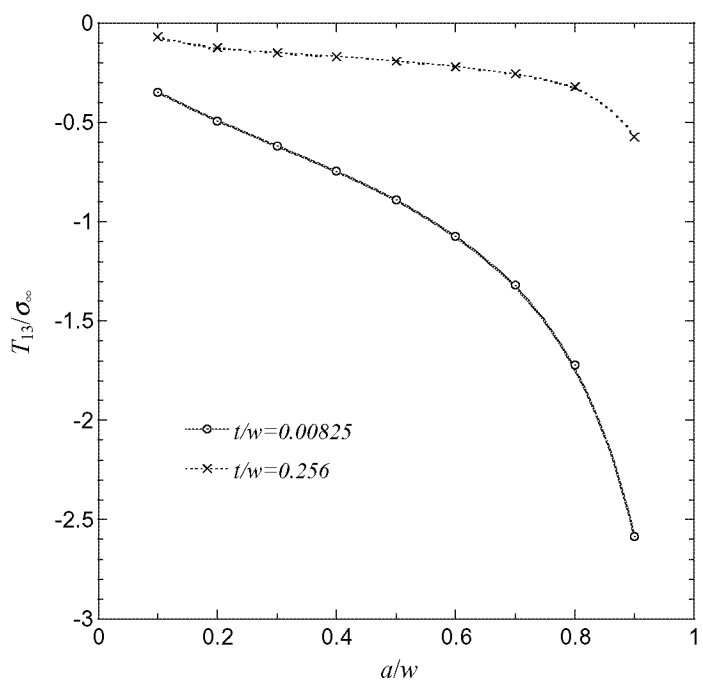

Figure 6.6 Normalized T_{13} stresses at quarter of the thickness (x_3/t=0.5) for isotropic plates with two different thicknesses.

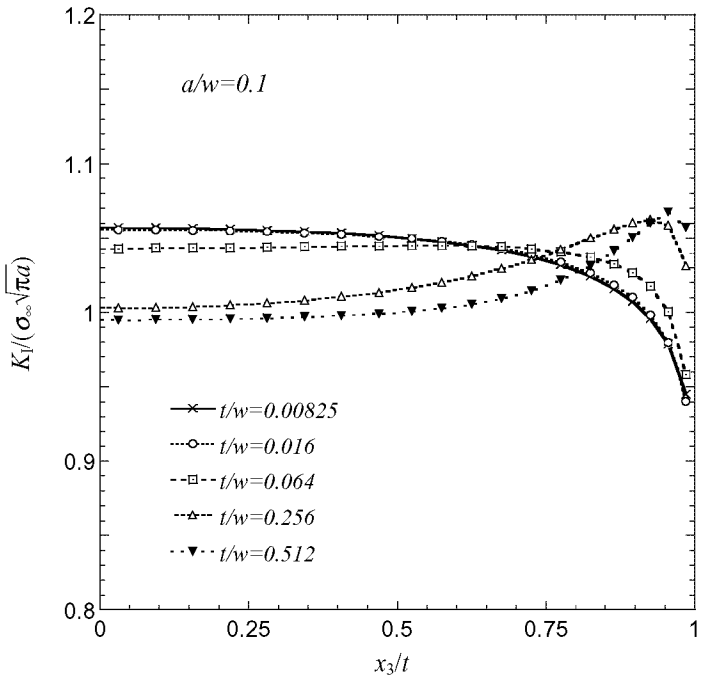

Figure 6.7 Normalized stress intensity factors through half of the thickness for isotropic plates of a/w=0.1 with various t/w ratios.

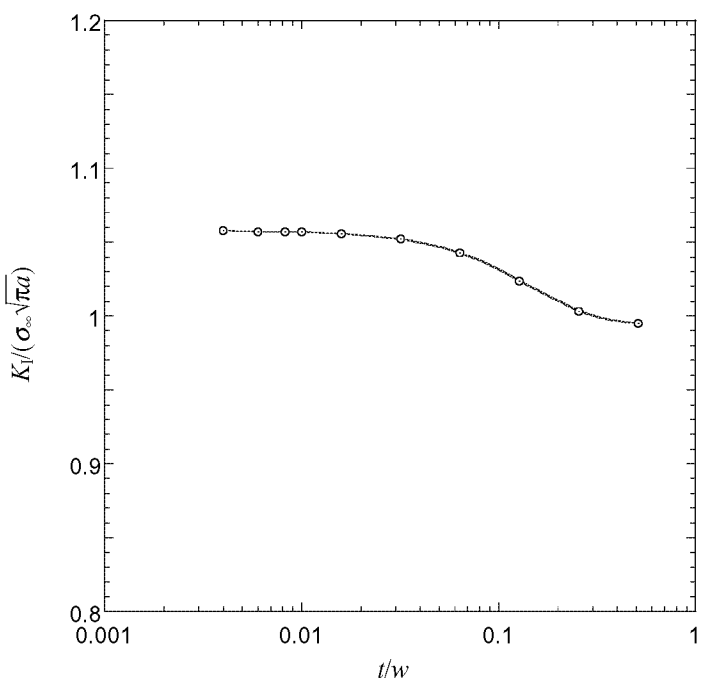

Figure 6.8 Normalized stress intensity factors at center of the thickness ($x_3/t=0$) for isotropic plates of a/w=0.1.

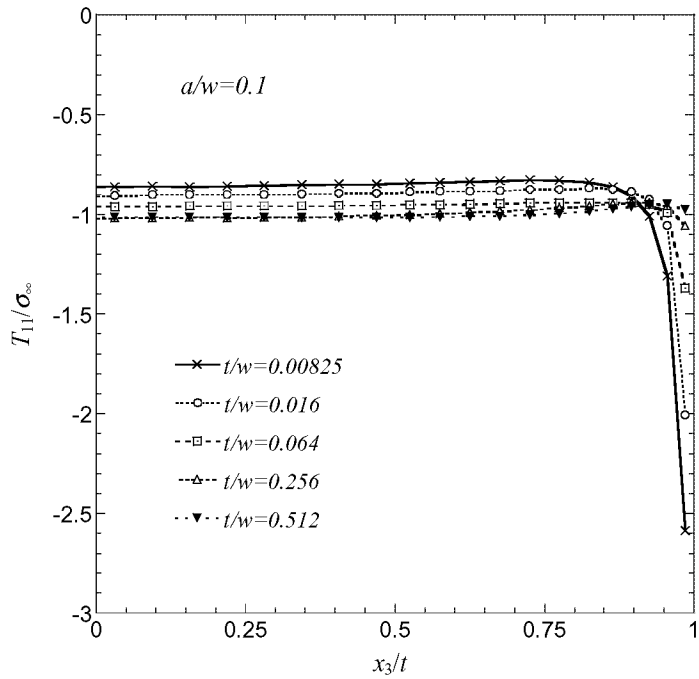

Figure 6.9 Normalized T_{11} stresses through half of the thickness for isotropic plates of a/w=0.1 with various t/w ratios.

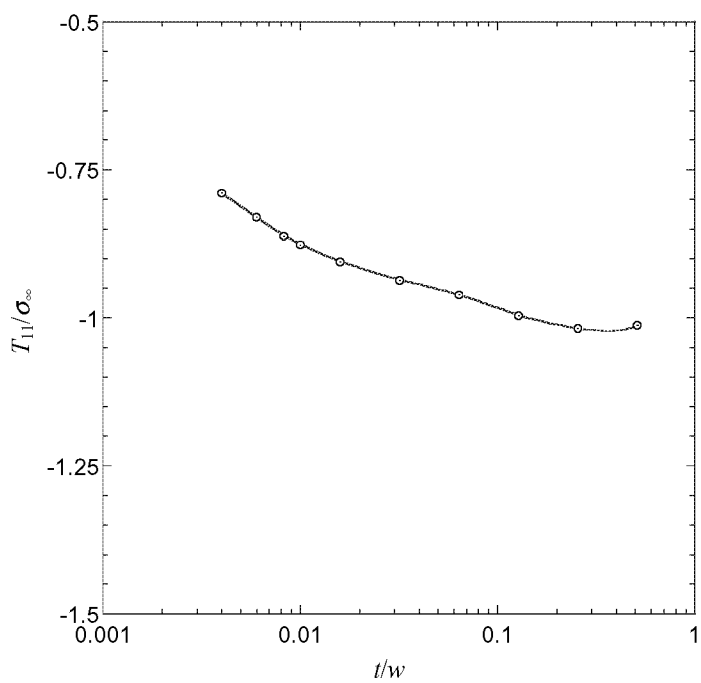

Figure 6.10 Normalized T_{11} stresses at center of the thickness ($x_3/t=0$) for isotropic plates of a/w=0.1.

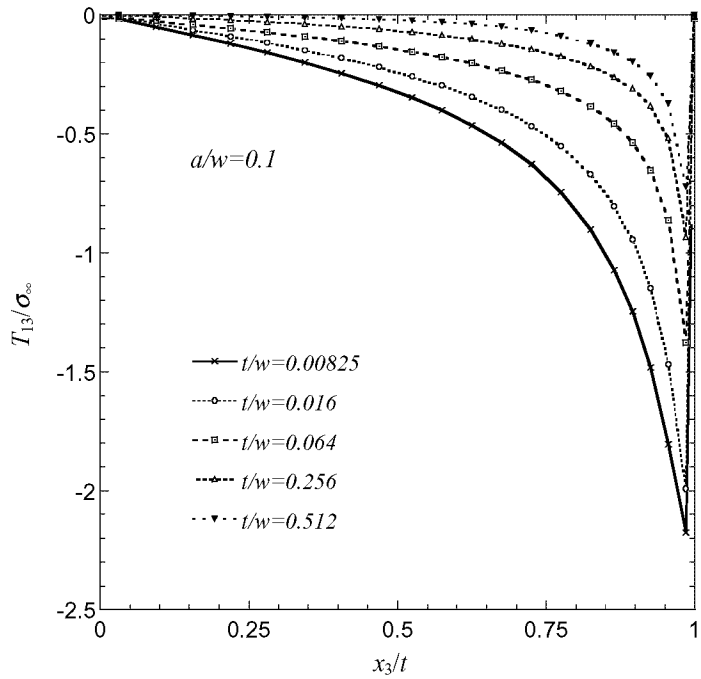

Figure 6.11 Normalized T_{13} stresses through half of the thickness for isotropic plates of a/w=0.1 with various t/w ratios.

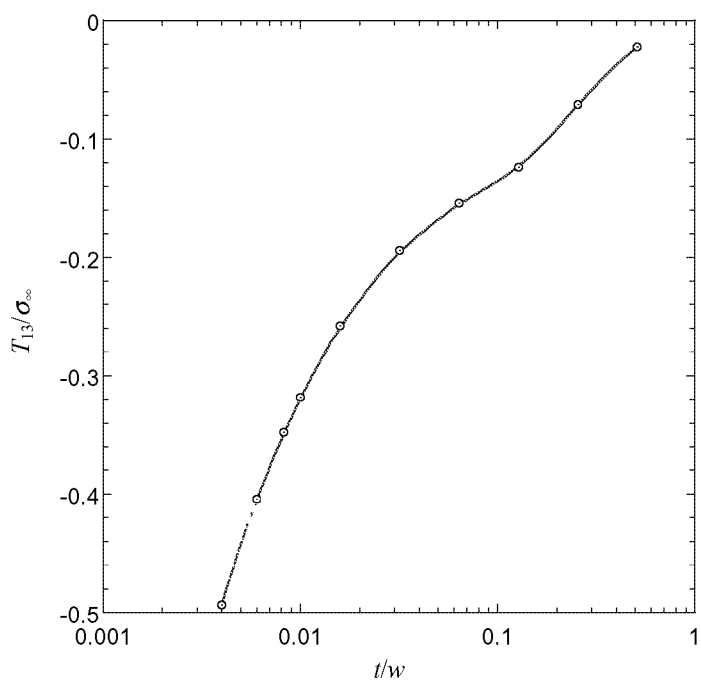

Figure 6.12 Normalized T_{13} stresses at quarter of the thickness (x_3/t=0.5) for isotropic plates of a/w=0.1.

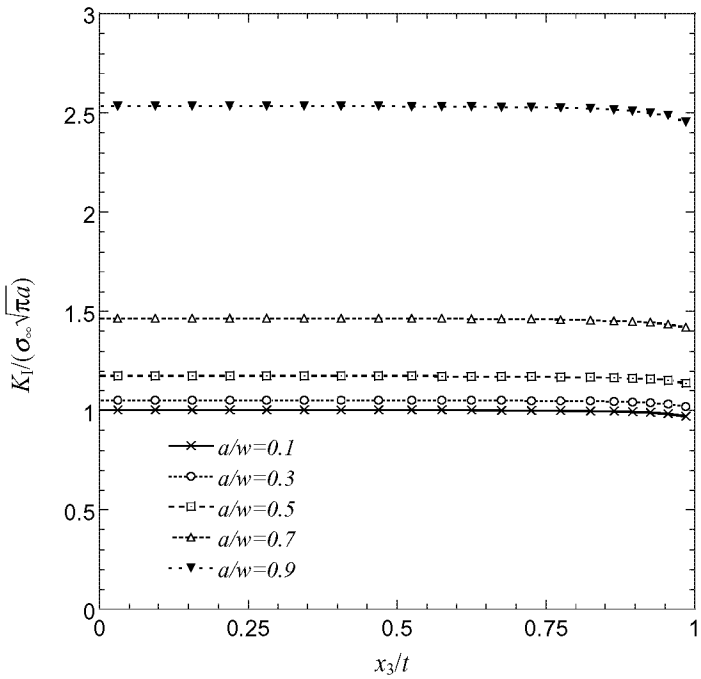

Figure 6.13 Normalized stress intensity factors through half of the thickness for orthotropic plates of t=0.165 in. (t/w=0.00825) with various a/w ratios.

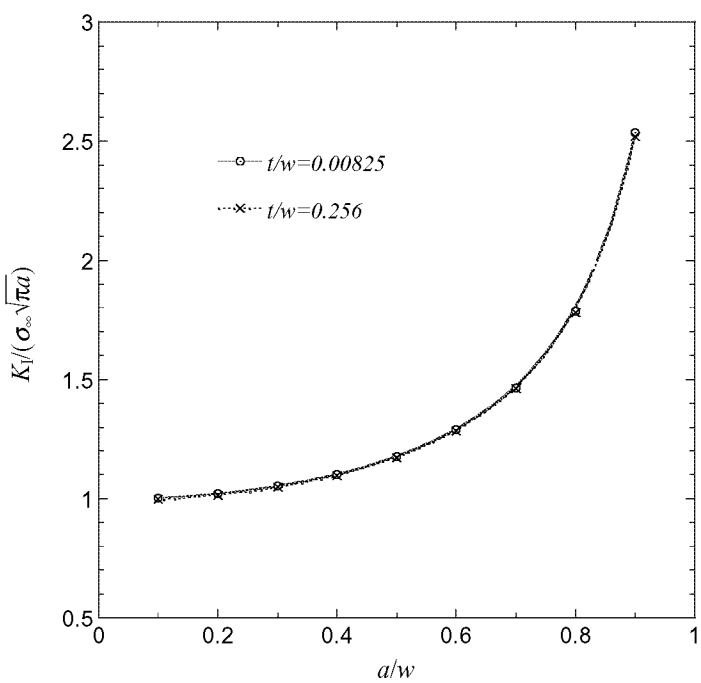

Figure 6.14 Normalized stress intensity factors at center of the thickness ($x_3/t=0$) for orthotropic plates with two different thicknesses.

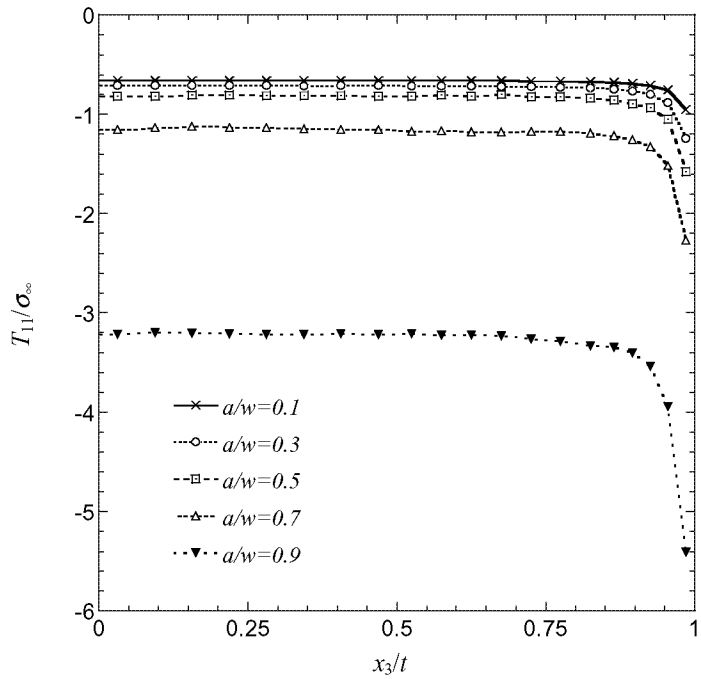

Figure 6.15 Normalized T_{11} stresses through half of the thickness for orthotropic plates of t=0.165 in. (t/w=0.00825) with various a/w ratios.

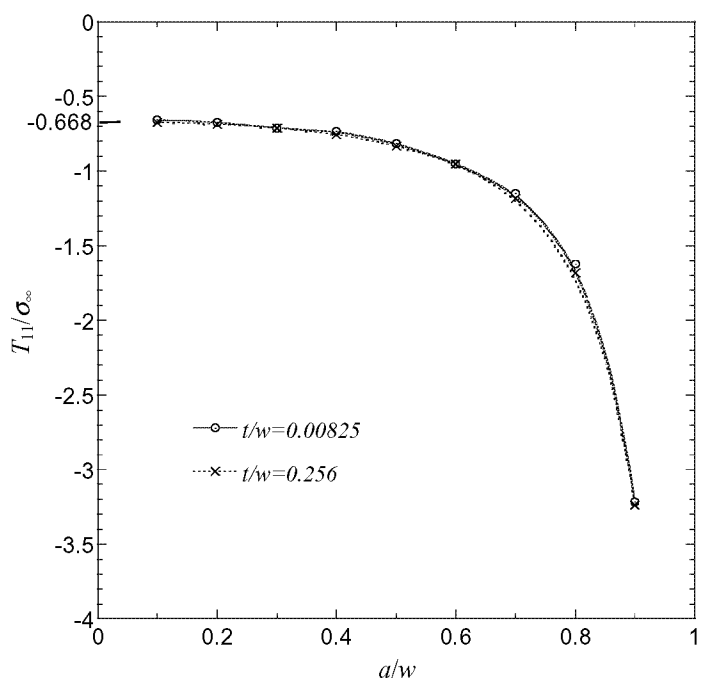

Figure 6.16 Normalized T_{11} stresses at center of the thickness (x_3/t=0) for orthotropic plates with two different thicknesses.

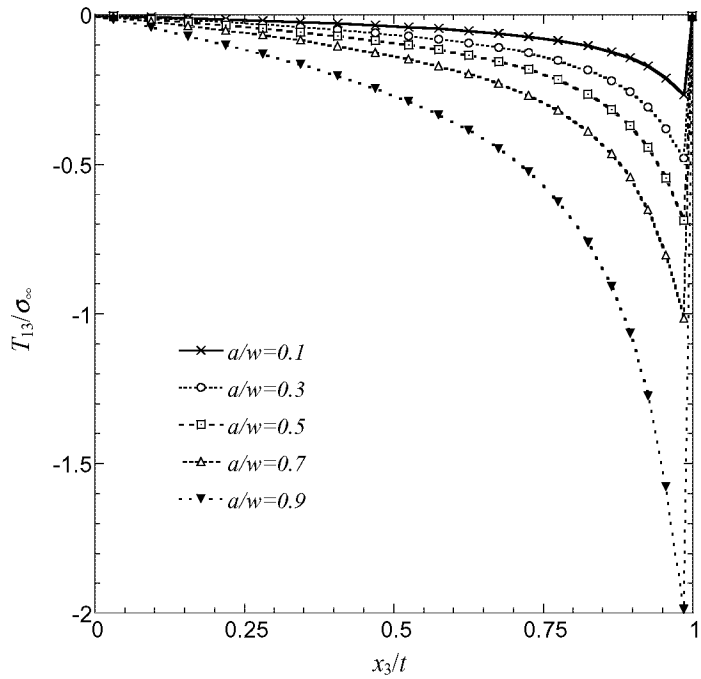

Figure 6.17 Normalized T_{13} stresses through half of the thickness for orthotropic plates of t=0.165 in. (t/w=0.00825) with various a/w ratios.

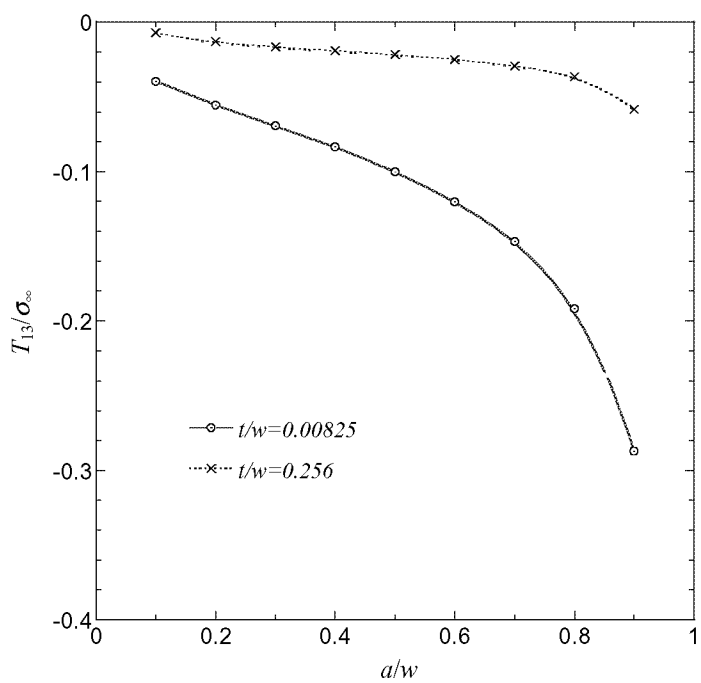

Figure 6.18 Normalized T_{13} stresses at quarter of the thickness (x_3/t=0.5) for orthotropic plates with two different thicknesses.

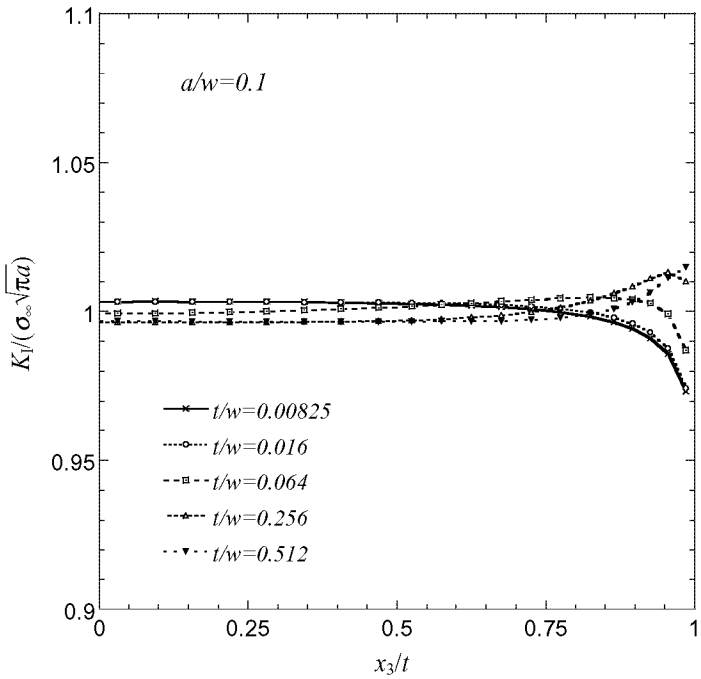

Figure 6.19 Normalized stress intensity factors through half of the thickness for orthotropic plates of a/w=0.1 with various t/w ratios.

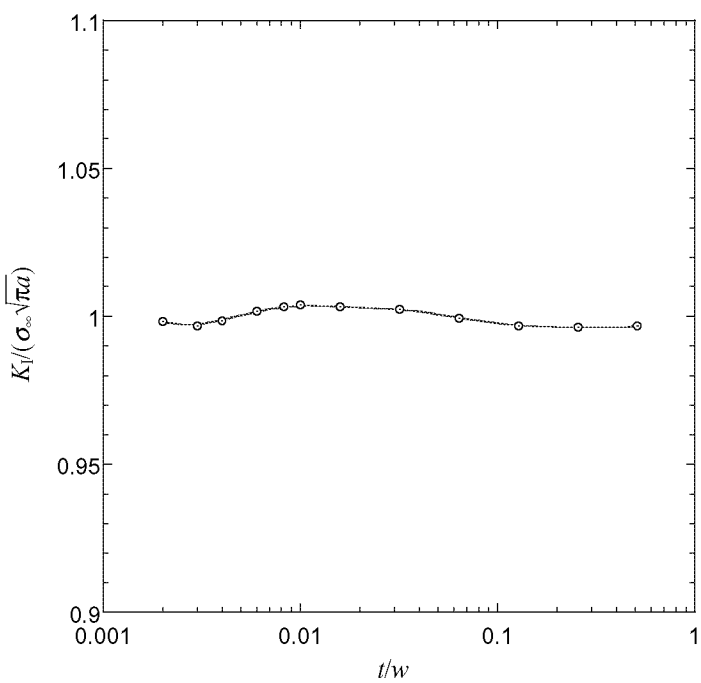

Figure 6.20 Normalized stress intensity factors at center of the thickness ($x_3/t=0$) for orthotropic plates of a/w=0.1.

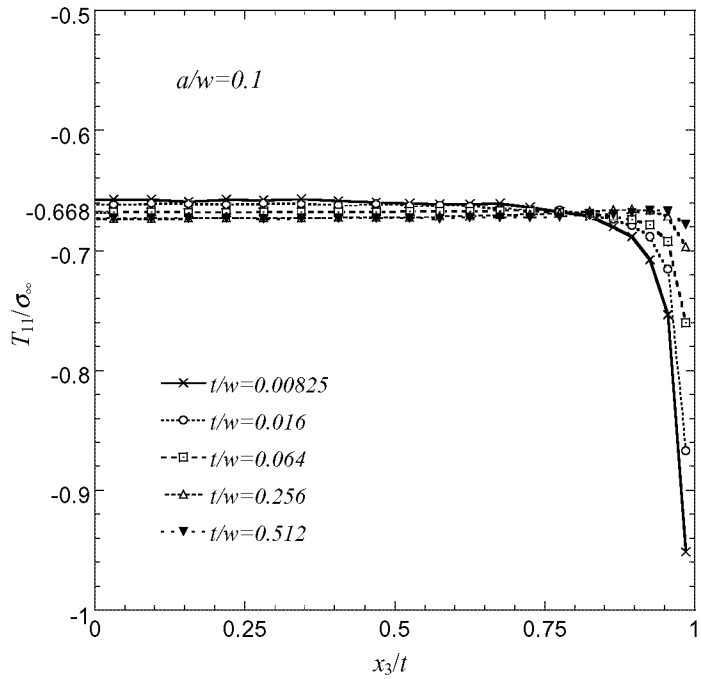

Figure. 6.21 Normalized T_{11} stresses through half of the thickness for orthotropic plates of a/w=0.1 with various t/w ratios.

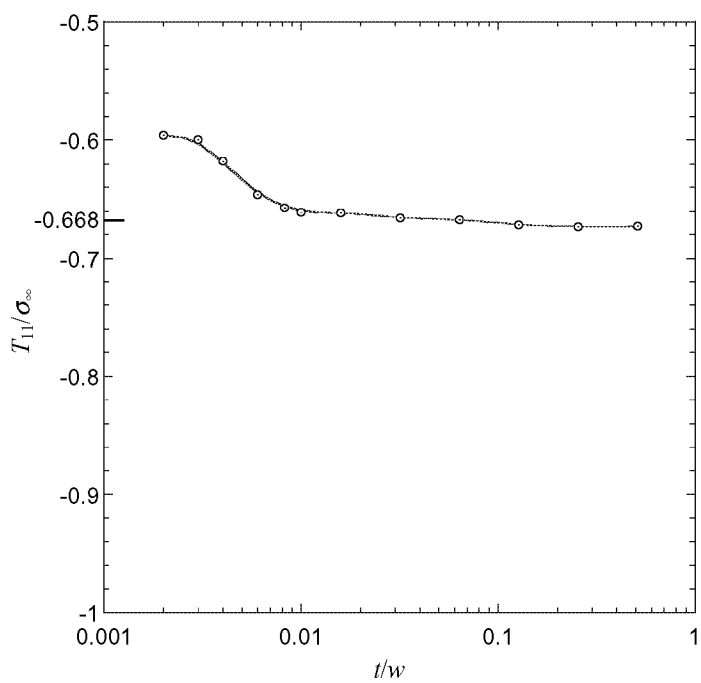

Figure 6.22 Normalized T_{11} stresses at center of the thickness ($x_3/t=0$) for orthotropic plates of a/w=0.1.

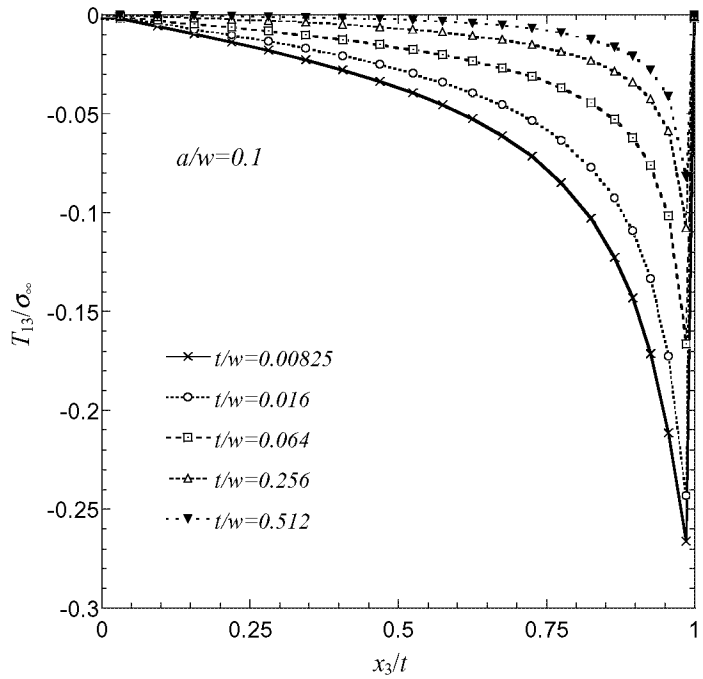

Figure 6.23 Normalized T_{13} stresses through half of the thickness for orthotropic plates of a/w=0.1 with various t/w ratios.

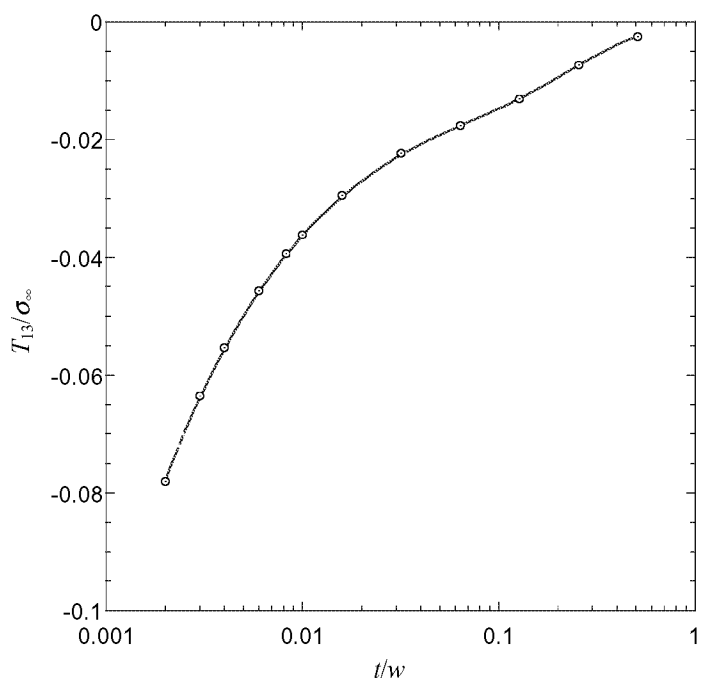

Figure 6.24 Normalized T_{13} stresses at quarter of the thickness (x_3/t=0.5) for orthotropic plates of a/w=0.1.

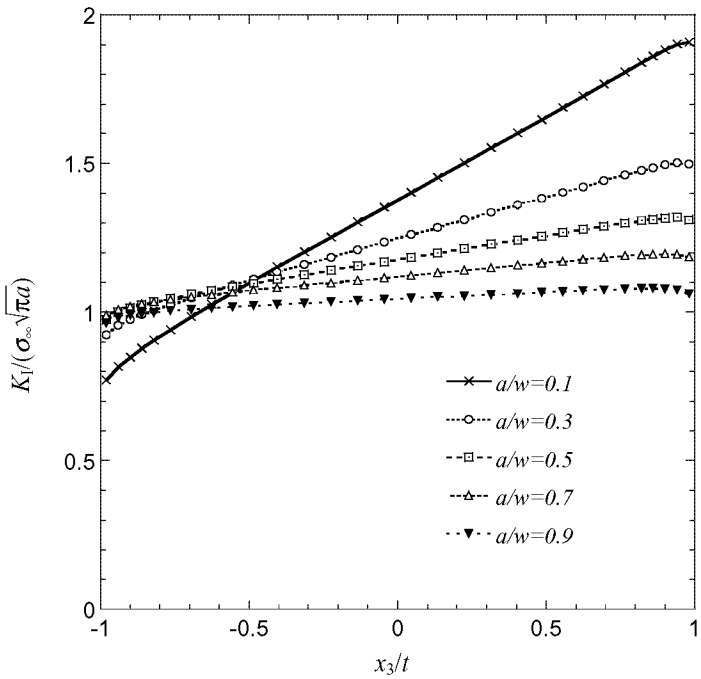

Figure 6.25 Normalized stress intensity factors through the thickness for orthotropic stiffened panels of t=0.165 in. (t/w=0.00825) with various a'/w' ratios.

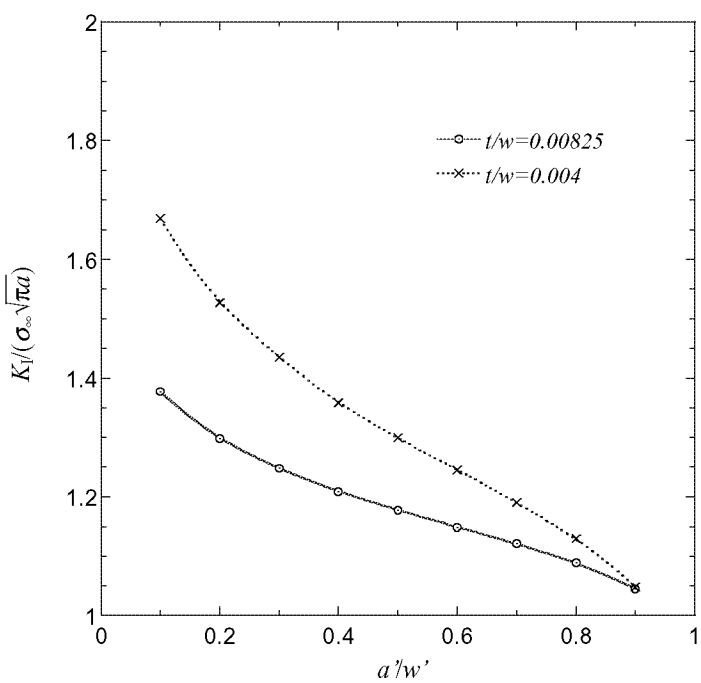

Figure 6.26 Normalized stress intensity factors at center of the thickness ($x_3/t=0$) for orthotropic stiffened panels with various a'/w' ratios for two thicknesses.

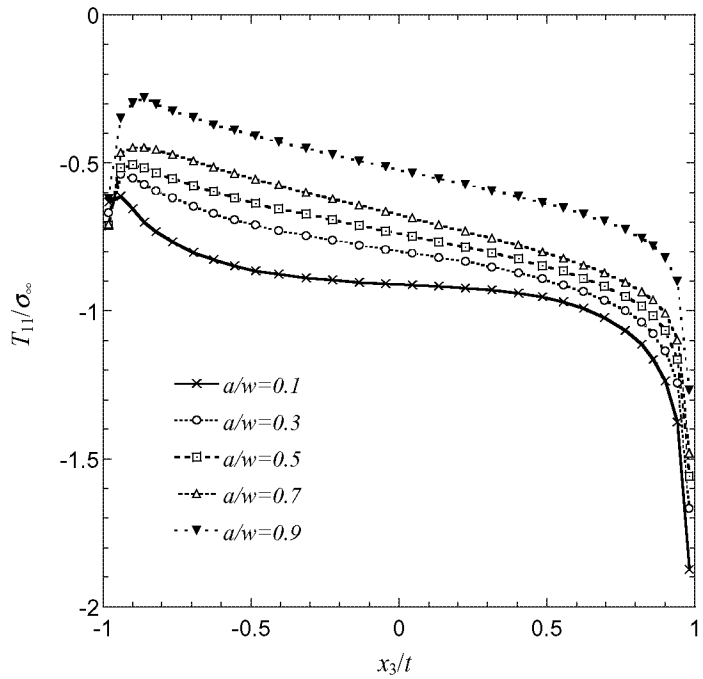

Figure 6.27 Normalized T_{11} stresses through the thickness for orthotropic stiffened panels of t=0.165 in. (t/w=0.00825) with various a'/w' ratios.

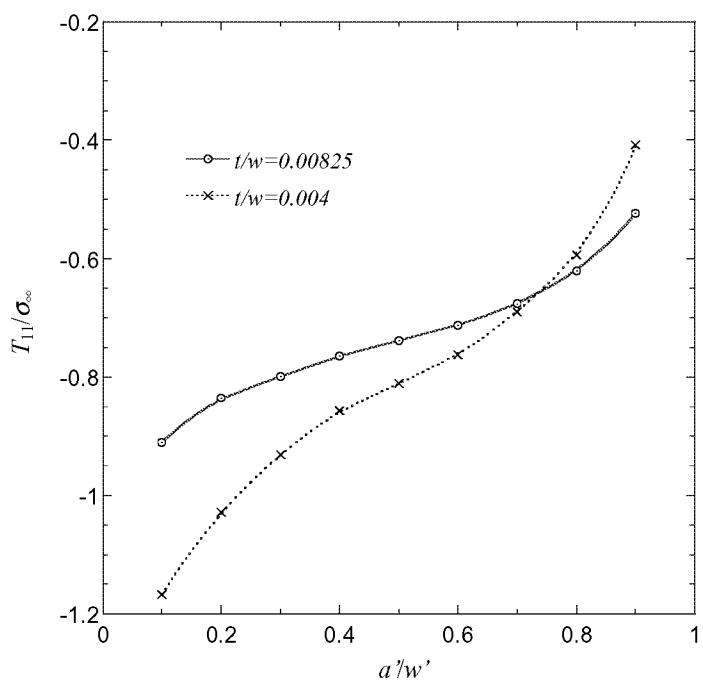

Figure 6.28 Normalized T_{11} stresses at center of the thickness ($x_3/t=0$) for orthotropic stiffened panels with various a'/w' ratios for two thicknesses.

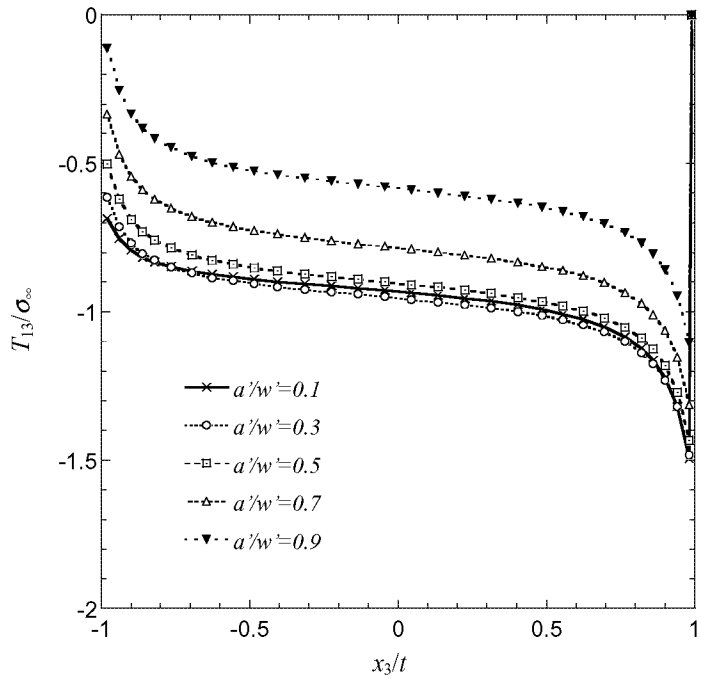

Figure 6.29 Normalized T_{13} stresses through the thickness for orthotropic stiffened panels of t=0.165 in. (t/w=0.00825) with various a'/w' ratios.

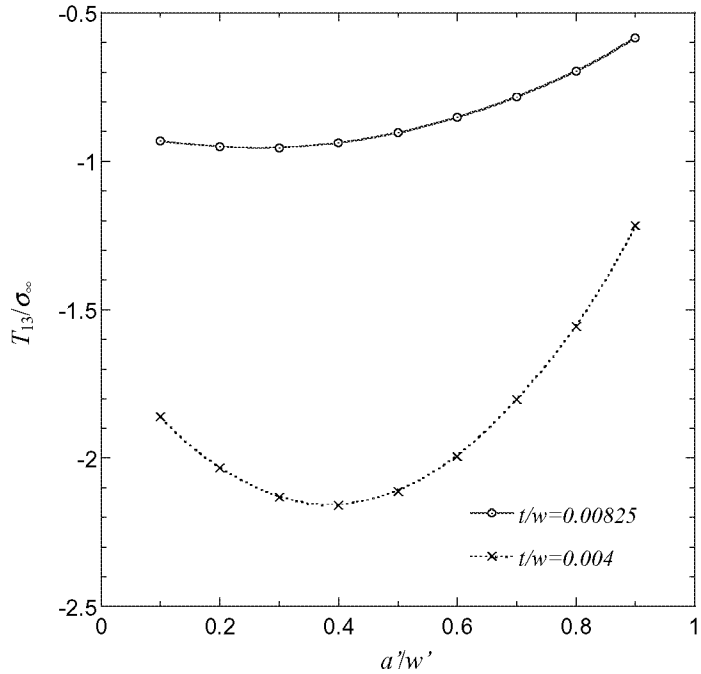

Figure 6.30 Normalized T_{13} stresses at center of the thickness ($x_3/t=0$) for orthotropic stiffened panels with various a'/w' ratios for two thicknesses.

7 Summary and Conclusions

The equivalent domain integral method is used to determine the point-wise stress intensity factor, or the distribution of it along a three-dimensional crack front. This method is modified from J-integral with the use of a weighting function, i.e., the s-function. In the practice of numerical computation, the finite element shape function is applied as the s-function.

In addition to the stress intensity factor, a second fracture parameter, namely the T-stress, is determined in order to better characterize the fracture behavior. The components of T-stress can be obtained by the evaluation of the interaction integral. The interaction integral is derived from the equivalent domain integral method with the concept of an auxiliary field. The auxiliary field is the solution corresponding to uniform force acting on the crack front. The Stroh formalism is used to derive the auxiliary stress and displacement fields associated with different T-stress components, such as T_{11} and T_{13}, in the monoclinic material with the plane of symmetry at x_3=0.

The finite element models are made on two sets of through-thickness center-cracked plates with isotropic and orthotropic material properties, respectively. Similar finite element meshes are generated on another set of orthotropic composite panels with stiffeners. All of these structures are under the mode-I uniform displacement loading.

For plates, the stress intensity factor will increase as the crack length increases in plates with the same dimension. The effect of material properties on the stress intensity factors at the center of the plate is not significant and all of the stress intensity factors are close to the corresponding 2-D solutions, especially for relatively thick plates. For plates of different thicknesses with the same crack length, the stress intensity factor for isotropic plates decreases as the thickness increases while for orthotropic plates the trend is relatively insensitive. For panels with stiffeners, however, the stress intensity factor decreases as the crack length in the panel increases. Similar to the unstiffened plates, a

thinner stiffened panel has a larger stress intensity factor for a given crack length. The exception occurs for the case of relatively larger crack lengths, e.g., $a'/w' = 0.9$, where two sets of thin panels of different thicknesses have nearly identical values of stress intensity factor.

The T_{11} stresses in all cases of center-cracked plates and panels are compressive. Based on the stress field near the crack tip prior to fracture initiation from a couple tests [29], the crack may not have tendency to turn. This is in contradiction to the experimental observation that the crack did turn near the stiffener. A possible reason may be due to other interacting failure modes, such as delamination and disbond with stitched interface, that caused the turning. Among plates, the magnitude of T_{11} increases when the crack length increases, regardless of the material properties or plate thickness. The thickness effect in plates with a small length of crack is more profound for isotropic ones, in which the T_{11} stress increases (in magnitude) as the thickness increases. Although in general the orthotropic plates have the same trend, the changes of T_{11} are relatively small for thicker plates. The trends observed in plates are reversed in stiffened panels, where T_{11} decreases (in magnitude) when a crack length in a panel increases. At small crack lengths, T_{11} in a thin panel also has a larger magnitude then T_{11} in a thick panel.

The T_{13} stress in plates of both materials increases (in magnitude) when the crack length increases, but a larger magnitude is found in isotropic plates. T_{13}, however, decreases in magnitude as the plate thickness increases. For very thick plates, where the plane strain condition dominates near the middle of plate thickness, T_{13} approaches zero. This is also true in two-dimensional analysis, in which T_{11} is the only effective T-stress component. In stiffened panels, the magnitude of T_{13} is generally smaller for large cracks. The largest magnitude of T_{13}, however, is not found in panels with a smallest crack, but with a somewhat larger crack.

This research may be extended in the future according to the following aspects.

(1) The loading condition may be extended from uniaxial tension to others, such as pure bending or biaxial loading. The change of the loading conditions, however, may incur

mixed-mode effects. If the asymptotic stress field near the crack front includes mixed modes, the mode-II and mode-III effects must be taken into account for the equivalent domain integral formulation. The calculation of the stress intensity factors will also require the consideration of the auxiliary fields [21].

(2) The effects of mixed mode may come from the existence of a kinked crack [40]. However, a fracture plate with the kinked crack requires an even larger finite element model to simulate because it usually is not considered as a symmetric geometry.

(3) Since the stress intensity factors and the *T*-stresses are related to the material properties, a composite material may be designed such that a certain level of the desired parameters can be obtained.

References

[1] A. A. Griffith, The phenomena of rupture and flow in solids. *Philosophical Transactions of the Royal Society of London, Series A*, **221**, pp.163-198, 1920.

[2] G. R. Irwin, Onset of fast crack propagation in high strength steel and aluminum alloys. *Segamore Research Conference Proceedings*, **2**, pp.289-305, 1956.

[3] H. M. Westergaard, Bearing pressures and cracks. *ASME Journal of Applied Mechanics*, **6**, pp.49-53, 1939.

[4] G. R. Irwin, Analysis of stresses and strains near the end of a crack traversing a plate. *ASME Journal of Applied Mechanics*, **24**, pp.361-364, 1957.

[5] J. R. Rice, A path independent integral and the approximate analysis of strain concentration by notches and cracks. *ASME Journal of Applied Mechanics*, **35**, pp.379-386, 1968.

[6] D. M. Parks, The virtual crack extension method for nonlinear material behavior. *Computer Methods in Applied Mechanics and Engineering*, **12**, pp.353-364, 1977.

[7] H. G. deLorenzi, On the energy release rate and the J-integral for 3-D crack configuration. *International Journal of Fracture*, **19**, pp.183-193, 1982.

[8] H. G. deLorenzi, Energy release rate calculations by the finite element method. *Engineering Fracture Mechanics*, **21**, No.1, pp.129-143, 1985.

[9] F. Z. Li, C. F. Shih and A. Needleman, A comparison of methods for calculating energy release rates. *Engineering Fracture Mechanics*, **21**, No.2, pp.405-421, 1985.

[10] C. F. Shih, B. Moran and T. Nakamura, Energy release rate along a three-dimensional crack front in a thermally stressed body. *International Journal of Fracture*, **30**, pp.79-102, 1986.

[11] T. Nakamura, C. F. Shih and L. B. Freund, Analysis of a dynamically loaded three-point-bend ductile fracture specimen. *Engineering Fracture Mechanics*, **25**, No.3, pp.323-339, 1986.

[12] G. P. Nikishkov and S. N. Atluri, An equivalent domain integral method for computing crack-tip integral parameters in non-elastic, thermo-mechanical fracture. *Engineering Fracture Mechanics*, **26**, No.6, pp.851-867, 1987.

[13] G. P. Nikishkov and S. N. Atluri, Calculation of fracture mechanics parameters for an arbitrary three-dimensional crack, by the 'equivalent domain integral' method. *International Journal for Numerical Methods in Engineering*, **24**, pp.1801-1821, 1987.

[14] I. S. Raju and K. N. Shivakumar, An equivalent domain integral method in the two-dimensional analysis of mixed mode crack problems. *Engineering Fracture Mechanics*, **37**, No.4, pp.707-725, 1990.

[15] K. N. Shivakumar and I. S. Raju, An equivalent domain integral method for three-dimensional mixed-mode fracture problems. *Engineering Fracture Mechanics*, **42**, No.6, pp.935-959, 1992.

[16] K. S. Woo, C. H. Hong and Y. S. Shin, An extended equivalent domain integral method for mixed mode fracture problems by the *p*-version of FEM. *International Journal for Numerical Methods in Engineering*, **42**, pp.857-884, 1998.

[17] T. Nakamura and D. M. Parks, Three-dimensional stress field near the crack front of a thin elastic plate. *ASME Journal of Applied Mechanics*, **55**, pp.805-813, 1988.

[18] C. F. Shih and R. J. Asaro, Elastic-plastic analysis of cracks on bimaterial interfaces: part I — small scale yielding. *ASME Journal of Applied Mechanics*, **55**, pp.299-315, 1988.

[19] C. F. Shih, B. Moran and T. Nakamura, Crack tip integrals and domain integral representations for three-dimensional crack problems. *Analytical, Numerical, and Experimental Aspects of Three-Dimensional Fracture Processes*, **ASME AMD-Vol. 91**, edited by A. J. Rosakis, K. Ravi-Chandar and Y. Rajapakse, pp.125-139, 1988.

[20] T. Nakamura, C. F. Shih and L. B. Freund, Three-dimensional transient analysis of a dynamically loaded three-point-bend ductile fracture specimen. *Nonlinear Fracture Mechanics: Vol. I — Time-Dependent Fracture*, **ASTM STP 995**, edited by A. Saxena, J. D. Landes and J. L. Bassani, pp.217-241, 1989.

[21] T. Nakamura and D. M. Parks, Antisymmetrical 3-D stress field near the crack front of a thin elastic plate. *International Journal of Solids and Structures*, **25**, No.12, pp.1411-1426, 1989.

[22] M. L. Williams, On the stress distribution at the base of a stationary crack. *ASME Journal of Applied Mechanics*, **24**, pp.109-114, 1957.

[23] S. G. Larsson and A. J. Carlsson, Influence of non-singular stress terms and specimen geometry on small-scale yielding at crack tips in elastic-plastic materials. *Journal of the Mechanics and Physics of Solids*, **21**, pp.263-277, 1973.

[24] J. R. Rice, Limitations to the small scale yielding approximation for crack tip plasticity. *Journal of the Mechanics and Physics of Solids*, **22**, pp.17-26, 1974.

[25] A. H. Sherry, C. C. France and M. R. Goldthorpe, Compendium of T-stress solutions for two and three dimensional cracked geometries. *Fatigue and Fracture of Engineering Materials and Structures*, **18**, No.1, pp.141-155, 1995.

[26] B. S. Henry and A. R. Luxmoore, Three-dimensional evaluation of the T-stress in centre cracked plates. *International Journal of Fracture*, 7**0**, pp.35-50, 1995.

[27] B. Yang and K. Ravi-Chandar, Evaluation of elastic T-stress by the stress difference method. *Engineering Fracture Mechanics*, **64**, No.5, pp.589-605, 1999.

[28] T. Nakamura and D. M. Parks, Determination of elastic T-stress along three-dimensional crack fronts using an interaction integral. *International Journal of Solids and Structures*, **29**, No.13, pp.1597-1611, 1992.

[29] F. G. Yuan and S. Yang, Fracture behavior of stitched warp-knit fabric composites. Accepted by *International Journal of Fracture*, 2000.

[30] G. P. Nikishkov, Some numerical methods of fracture mechanics based on domain invariant integrals. *Fracture*, edited by G. P. Cherepanov, Krieger Publishing Company, Malabar, FL, U.S.A. pp.542-556, 1998.

[31] K. -J. Bathe, *Finite Element Procedures in Engineering Analysis*, Prentice-Hall Inc., Englewood Cliffs, NJ, U.S.A., 1982.

[32] A. P. Kfouri, Some evaluations of the elastic T-term using Eshelby's method. *International Journal of Fracture*, **30**, pp.301-315, 1986.

[33] F. G. Yuan, Determination of stress coefficient terms in cracked solids for monoclinic materials with plane symmetry at x_3=0. *NASA Contractor Report*, NASA/CR-1998-208729, 1998.

[34] R. M. Jones, *Mechanics of Composite Materials*, Scripta Book Company, Washington, DC, U.S.A., 1975.

[35] T. C. T. Ting, *Anisotropic Elasticity: Theory and Applications*, Oxford University Press, Inc., New York, NY, U.S.A., 1996.

[36] S. G. Lekhnitskii, *Theory of Elasticity of an Anisotropic Body*, Mir Publishers, Moscow, Russia, 1981.

[37] S. Yang and F. G. Yuan, Determination and representation of the stress coefficient terms by path-independent integrals in anisotropic cracked solids. *International Journal of Fracture*, **101**, pp.291-319, 2000.

[38] T. L. Anderson, *Fracture Mechanics: Fundamentals and Applications*, Second Edition. CRC Press, Boca Raton, Florida, U.S.A., 1995.

[39] P. S. Leevers and J. C. Radon, Inherent stress biaxiality in various fracture specimen geometries. *International Journal of Fracture*, **19**, pp.311-325, 1982.

[40] S. Yang and F. G. Yuan, Kinked crack in anisotropic bodies. *International Journal of Solids and Structures*, **37**, pp. 6635-6682, 2000.

Appendices

A. ANSYS Program

The following ANSYS program is to generate a finite element model of one-fourth of a stiffened panel with a center crack. The structural dimensions are described in Chapter 5, and the material properties are listed in Table 6.1. The program will output plain text files which includes data of displacements, strains, stresses, nodal coordinates, and other parameters to be used later in a FORTRAN program. This program is tested on ANSYS/ResearchFS, the product combination of ANSYS Revision 5.5.1 licensed to the North Carolina Supercomputing Center. This program can be modified to generate a finite element model for the simpler center-cracked plate.

ANSYS commands are not case-sensitive, i.e., a command in uppercase is identical to a command in lowercase. For the purpose of clarity, however, all commands and associated arguments are listed with uppercase characters, except the user-defined parameters that use lowercase characters.

```
/BATCH
/UNITS,BIN                ! British system of units using inches
! ================ BEGINNING of Parameters Definition =================
! Material Properties
*DIM,mat,ARRAY,3,3,1                ! array to store material properties
mat(1,1) = 5.162e6,11.773e6,1.530e6          ! Ex,Ey,Ez
mat(1,2) = 0.22,0.29,5.162/11.773*0.401      ! NUyz,NUxz,NUxy
mat(1,3) = 0.640e6,0.570e6,2.479e6           ! Gyz,Gxz,Gxy

! Parameters for Loading Conditions
appstn = 0.001            ! applied far-field uniform strain

! Geometric Parameters
*DIM,cir,ARRAY,5,1,1      ! array of dimensions of the fan-type area
aow = 0.1                 ! a/w ratio
plz = 0.33                ! full length of the panel in Z-direction (thickness)
plx = 20                  ! 1/2 length of the panel in X-direction (w)
ply = 40                  ! 1/2 length of the panel in Y-direction (l)
tst = 0.22                ! 1/2 thickness of the stiffener
hst = 2.3                 ! height of the stiffener
wst = 1.6+tst/2           ! 1/2 width of the stiffener (a0)
ws1 = wst-tst             ! 1/2 width of the base of the stiffener
dxc = 8                   ! distance between the center of 2 stiffeners
dxe = dxc-2*wst           ! distance between the edge of 2 stiffeners
dsp = ply*appstn          ! applied far-field displacement
clp = aow*dxe             ! crack length in panel portion (a')
ckl = wst+clp             ! 1/2 crack length (a=a0+a')
ctf = dxe-clp             ! panel length in front of crack tip

! Parameters for Mesh Control
*DIM,neci,ARRAY,3,1,1     ! mesh-control parameters over the fan
*DIM,srrl,ARRAY,3,1,1     ! spacing ratios for radial lines
*DIM,zkpn,ARRAY,4,1,1     ! keypoint numbers at Z-direction interfaces
*DIM,zntk,ARRAY,6,1,1     ! normalized thicknesses for different spacing
*DIM,nezi,ARRAY,6,1,1     ! number of elements in each region
neci(1) = 1,12,1
srrl(1) = 1,26,1
zntk(1) = 0.20,0.35,0.45,0.45,0.35,0.20
nezi(1) = 5,5,5,5,5,5
narc = 6                  ! number of arcs for a 90-degree span
angc = 90/narc            ! arc angle per element
nezz = nezi(1)+nezi(2)+nezi(3)      ! number of element layers along 1/2
!                                     thickness
nerr = neci(2)            ! number of elements in r-direction
neyf = 6                  ! number of solid model divisions in
!                           Y-direction of far-field portion
sryf = 32                 ! spacing ratio in Y-direction of far-field portion

! Define spacing ratios in X-direction
*IF,aow,LE,0.3,THEN
 nec1 = 2
 sr1 = 3
 nec2 = 4
 sr2 = 10
*ELSEIF,aow,GE,0.7,THEN
 nec1 = 4
 sr1 = 10
 nec2 = 2
 sr2 = 3
*ELSE                     ! 0.3 < a'/w' < 0.7
```

```
 nec1 = 3
 sr1 = 9
 nec2 = 3
 sr2 = 9
*ENDIF

! Define critical length
*IF,aow,LE,0.5,THEN      ! a'/w' <= 0.5
 *IF,plz,LE,clp,THEN     ! (2t<=a')
  lcr = plz              ! critical length = min[a',w'-a',2t]
 *ELSE                   ! (2t>a')
  lcr = clp              ! critical length = min[a',w'-a',2t]
 *ENDIF
*ELSE                    ! a'/w' > 0.5
 *IF,plz,LE,ctf,THEN     ! (2t<=w'-a')
  lcr = plz              ! critical length = min[a',w'-a',2t]
 *ELSE                   ! (2t>w'-a')
  lcr = ctf              ! critical length = min[a',w'-a',2t]
 *ENDIF
*ENDIF

rac = 0.004*lcr          ! radial size of the smallest element (e0)
cir(1) = 0,rac,100*rac,150*rac
dyf = ply-cir(4)         ! length in Y-direction
tw = (plz/2)/plx         ! t/w ratio
! ~~~~~~~~~~~~~~~~~~~ END of Parameters Definition ~~~~~~~~~~~~~~~~~~~~

/TITLE,1/4 stiffened panel,a'/w'=%aow%,t/w=%tw%,lcr=%lcr%,e0=%rac%; C. Lin

! ================ BEGINNING of Preprocessing Phase =================
/PREP7
ET,1,95,,,,,1            ! element type: SOLID95, the 20-node 3-D structural
!                          element with solution output at integration points
KEYOPT,1,11,1            ! 2x2x2 reduced integration option
ET,2,93                  ! SHELL93, 8-node plate element
MP,EX,1,mat(1,1)         ! assign material properties
MP,EY,1,mat(2,1)
MP,EZ,1,mat(3,1)
MP,PRXY,1,mat(3,2)
MP,PRYZ,1,mat(1,2)
MP,PRXZ,1,mat(2,2)
MP,GXY,1,mat(3,3)
MP,GYZ,1,mat(1,3)
MP,GXZ,1,mat(2,3)

! Solid Model Generation:
! Generate fan-type areas over a span of 90 degrees
LOCAL,14,0,ckl,0,-plz/2  ! local Cartisian c.s. #14 at crack tip
WPCSYS,1,14              ! set working plane at local c.s. #14
*DO,i,1,narc             ! generate the innermost ring, Ring #0
 PCIRC,cir(1),cir(2),(i-1)*angc,i*angc
*ENDDO
PCIRC,cir(2),cir(3),0,90      ! annular area to be mapped meshed later
RECTNG,0,cir(4),0,cir(4)
ARSYM,X,ALL
BTOL,rac/100             ! set Boolean operation tolerance
AOVLAP,ALL               ! create areas on the x-y plane
BTOL,DEFA

! Set line divisions on all circumferencial and radial lines
```

```
LOCAL,15,1,ckl,0,0       ! local cylindrical c.s. #15 at crack tip
LSEL,S,LOC,X,cir(2)
LESIZE,ALL,,,1           ! set divisions on circumferencial lines
*DO,i,1,3
 LSEL,S,LOC,X,(cir(i)+cir(i+1))/2
 LESIZE,ALL,,,neci(i),srrl(i)      ! set divisions on radial lines
*ENDDO

! Concatenate lines around the fan-type area for mapped mesh later
*DO,i,1,2
 LSEL,S,LOC,X,cir(2)
 LSEL,R,LOC,Y,(i-1)*90,i*90
 LCCAT,ALL
 LSEL,S,LOC,X,cir(4)/2*SQRT(5)
 LSEL,R,LOC,Y,(i-1)*90,i*90
 LESIZE,ALL,,,narc/2,1
 LCCAT,ALL
*ENDDO
LSEL,ALL
NUMCMP,ALL               ! compress all numbering

! Mesh areas on X-Y plane
/NERR,3                  ! turn off warning messages
ASEL,S,LOC,X,0,cir(2)
AATT,1,1,2
MSHAPE,1,2D         ! mesh areas containing crack tip with triangle elements
AMESH,ALL                ! areas meshed with SHELL93 elements
ASEL,INVE
AATT,1,1,2
MSHAPE,0,2D              ! mesh other areas with quadrilateral elements
AMESH,ALL                ! areas meshed with SHELL93 elements
LSEL,S,SPACE,,0          ! select concatenated lines to be deleted
LDELE,ALL                ! delete concatenated lines

! Generate the finite element model along full panel thickness
ASEL,ALL
TYPE,1                   ! designate element type as SOLID95
CSYS,0                   ! set active c.s. as global Cartesian
zi = -plz/2
*DO,i,1,6           ! generate SOLID95 elements by extending selected areas
 ESIZE,,nezi(i)
 VEXT,ALL,,,,,zntk(i)*plz/2
 zi = zi+zntk(i)*plz/2   ! Z-coordinate of the areas to be offset
 ASEL,S,LOC,Z,zi
*ENDDO
ASEL,S,TYPE,,2,,,1
ACLEAR,ALL               ! delete all SHELL93 elements

! Construct the other portions of the panel
CSYS,14                  ! switch to the local Cartesian c.s. on the crack tip
NUMSTR,KP,1001
NUMSTR,LINE,2001
KSEL,S,LOC,Z,0
KSEL,R,LOC,Y,0
KSEL,R,LOC,X,-cir(4)
*GET,nkp1,KP,0,NUM,MAX   ! nkp1: keypoint # of this keypoint
KGEN,2,ALL,,,-(clp-cir(4))    ! keypoint #1001
L,nkp1,1001,nec1,sr1     ! line #2001
KSEL,S,LOC,Z,0
KSEL,R,LOC,Y,0
```

```
KSEL,R,LOC,X,cir(4)
*GET,nkp2,KP,0,NUM,MAX   ! nkp2: keypoint # of this keypoint
KGEN,2,ALL,,,dxe-clp-cir(4)   ! keypoint #1002
L,nkp2,1002,nec2,sr2     ! line #2002
NUMSTR,DEFA
ASEL,S,LOC,X,-cir(4)
VDRAG,ALL,,,,,,2001      ! generate cracked portion of the panel
ASEL,S,LOC,X,cir(4)
VDRAG,ALL,,,,,,2002      ! generate uncracked portion of the panel

! Generate the central stiffener
CSYS,0                   ! switch back to global Cartesian c.s.
ASEL,S,LOC,X,wst
ESIZE,,1
VEXT,ALL,,,-ws1
ASEL,S,LOC,X,tst
ESIZE,,1
VEXT,ALL,,,-tst
ASEL,S,LOC,Z,plz/2
ASEL,R,LOC,X,0,wst
ESIZE,,1
VEXT,ALL,,,,,tst
ASEL,S,LOC,Z,plz/2+tst
ASEL,R,LOC,X,0,tst
ESIZE,,1
VEXT,ALL,,,,,hst-tst

! Generate the second stiffener
VSEL,S,LOC,X,tst,wst,,1       ! select volumes on the outer central
!                               stiffener
LOCAL,11,0,dxc/2,0,0     ! set local Cartesian c.s. #11
VSYMM,X,ALL              ! generate volumes on the inner second stiffener
LOCAL,12,0,dxc,0,0       ! set Cartesian c.s. #12 at the center of the
!                          second stiffener
ASEL,S,LOC,X,-tst
ESIZE,,1
VEXT,ALL,,,2*tst         ! create volumes in the base of the second stiffener
ASEL,S,LOC,Z,plz/2+tst
ASEL,R,LOC,X,-tst,tst
ESIZE,,1
VEXT,ALL,,,,,hst-tst     ! generate volumes in the height of the second
!                          stiffener
VSEL,S,LOC,X,-wst,-tst,,1
VGEN,2,ALL,,,wst+tst     ! generate volumes in the outer part of the
!                          second stiffener

! Generate the outmost stiffener
VSEL,S,LOC,X,-wst,wst,,1      ! select all volumes in the second stiffener
LOCAL,13,0,1.5*dxc,0,0   ! set Cartesian c.s. #13
VSYMM,X,ALL              ! generate the entire outmost stiffener

! Generate the uncracked panel and the outmost panel
LOCAL,16,0,2*dxc,0,0     ! set Cartesian c.s. #16
ASEL,S,LOC,X,-wst
ASEL,R,LOC,Z,-plz/2,plz/2
VEXT,ALL,,,-dxe          ! generate the uncracked part of the panel
ASEL,S,LOC,X,wst
ASEL,R,LOC,Z,-plz/2,plz/2
VEXT,ALL,,,dxe/2         ! generate the outmost part of the panel
```

```
ALLSEL,ALL,ALL
NUMMRG,ALL,1e-6
NUMCMP,ALL                ! compress all numbering

! Construct the entire FE model by extending areas along Y-axis
CSYS,0
NUMSTR,KP,1001
NUMSTR,LINE,2001
KSEL,S,LOC,X,0
KSEL,R,LOC,Z,0
KSEL,R,LOC,Y,cir(4)
*GET,nkp3,KP,0,NUM,MAX    ! nkp1: keypoint # of this keypoint
KGEN,2,ALL,,,,dyf         ! keypoint #1001
L,nkp3,1001,neyf,sryf     ! line #2001
ASEL,S,LOC,Y,cir(4)
VDRAG,ALL,,,,,,2001       ! the entire finite element model completed

ALLSEL,ALL,ALL
NUMMRG,ALL,1e-6
NUMCMP,ALL                ! compress all numbering
/VIEW,1,1,1,1             ! set viewing point for plots
/ANGLE,1,-90,XM
/AUTO,1
/TYPE,ALL,2

ASEL,S,LOC,Y,ply
ASUM                      ! calculate the total area on the far-field end
*GET,ayt,AREA,0,AREA
/OUTPUT,par,dat           ! output data in <par.dat> file
*STATUS,ayt               ! "ayt": total area on the far-field end
/OUTPUT
ASEL,ALL
FINISH                    ! finish generation of the finite element model
! ~~~~~~~~~~~~~~~~~~~~~ END of Preprocessing Phase ~~~~~~~~~~~~~~~~~~~~

! ==================== BEGINNING of Solution Phase ====================
/SOLU
ANTYPE,STATIC             ! static analysis
NSEL,S,LOC,X,0
D,ALL,UX,0                ! set X-symmetry boundary conditions
NSEL,R,LOC,Y,0
NSEL,R,LOC,Z,-plz/2
D,ALL,UZ,0                ! set Z-constraints at the center of plate
NSEL,S,LOC,Y,ply
D,ALL,UY,dsp              ! apply the prescribed displacement at far end
NSEL,S,LOC,Y,0
NSEL,R,LOC,X,ckl,plx
D,ALL,UY,0                ! set Y-symmetry boundary conditions
NSEL,ALL
EQSLV,PCG,1e-8            ! use the PCG solver
ERESX,NO                  ! ouput integration point results to the nodes
SAVE
SOLVE
FINISH
! ~~~~~~~~~~~~~~~~~~~~~~~~ END of Solution Phase ~~~~~~~~~~~~~~~~~~~~~~~

! ================= BEGINNING of Postprocessing Phase =================
/POST1
nezt = nezz*2             ! number of element layers along thickness
*DIM,cmring,CHAR,3,1,1
```

```
*DIM,zf,ARRAY,nezt+1,1,1      ! array to store Z-coordinate of every layer
cmring(1) = 'ring2','ring3','ring4'
srr = srrl(2)**(1/(neci(2)-1))     ! spacing ratio between adjacent
!                                    elements in r-direction
esr = (cir(3)-cir(2))*(1-srr)/(1-srr**neci(2))    ! element size in r-direction

zf(1) = -plz/2           ! Z-coordinate at bottom of the first layer
kring = 3                ! number of rings to be recorded
k = 1
*DO,i,1,6           ! i: index for mesh-size region (= dimension of "zntk")
 eszi = zntk(i)*(plz/2)/nezi(i)    ! element size (z) in each region
 *DO,j,1,nezi(i)         ! j: index for the number of element layer
  k = k+1
  zf(k) = zf(k-1)+eszi
 *ENDDO
*ENDDO

SET,1
NSEL,S,LOC,Y,ply         ! select nodes on the far end
FSUM                     ! calculate total nodal force on the far end
*GET,fyt,FSUM,0,ITEM,FY
/OUTPUT,par,dat,,APPEND
*STATUS,fyt              ! "fyt": total nodal force on the far end
*STATUS,nezt             ! number of elements layers along thickness
*STATUS,plx
*STATUS,plz
*STATUS,mat,1,3,1,3
*STATUS,appstn
*STATUS,ckl
*STATUS,narc
*STATUS,kring
*STATUS,nerr
*STATUS,aow
/OUTPUT
NSEL,ALL
CSYS,15                  ! activate local cylindrical c.s. at crack tip
DSYS,15                  ! set display c.s. to #15

! Write stresses, strains, displacements, and nodal coordinates of
! every elements into files
/OUTPUT,sts,dat          ! <sts.dat> file to store stresses
/OUTPUT
/OUTPUT,stn,dat          ! <stn.dat> file to store strains
/OUTPUT
/OUTPUT,dis,dat          ! <dis.dat> file to store displacements
/OUTPUT
/OUTPUT,node,dat         ! <node.dat> file to store node coordinates
/OUTPUT

*DO,k,2,kring+1          ! select from Ring #2 to Ring #(kring+1)
 NSEL,S,LOC,X,rac+esr*(1-srr**(k-1))/(1-srr),rac+esr*(1-srr**k)/(1-srr)
 CM,cmring(k-1),NODE     ! group all nodes in the domain to be integrated
 *DO,i,1,nezt            ! i: index for layer in Z-direction
  NSEL,R,LOC,Z,zf(i),zf(i+1)
  CM,nlayer,NODE
  *DO,j,1,narc*2         ! j: index for element in the same layer
   NSEL,R,LOC,Y,angc*(j-1),angc*j
   ESLN,S,1              ! select an element
   /FORMAT,,E
   /HEADER,OFF,OFF,OFF,OFF,ON,ON
```

```
    /OUTPUT,sts,dat,,APPEND
    *MSG,INFO,k,i,j
    Ring # %I , Segment # %I ,  Element # %I :
    PRESOL,S
    /OUTPUT
    /OUTPUT,stn,dat,,APPEND
    *MSG,INFO,k,i,j
    Ring # %I , Segment # %I ,  Element # %I :
    PRESOL,EPEL
    /OUTPUT
    /HEADER,OFF,OFF,OFF,OFF,OFF,OFF
    /OUTPUT,dis,dat,,APPEND
    *MSG,INFO,k,i,j
    Ring # %I , Segment # %I ,  Element # %I :
    PRNSOL,DOF
    /OUTPUT
    /OUTPUT,node,dat,,APPEND
    *MSG,INFO,k,i,j
    Ring # %I , Segment # %I ,  Element # %I :
    ELIST,ALL,,,0,0
    NLIST,ALL,,,,Z,Y,X
    /OUTPUT
    CMSEL,S,nlayer
   *ENDDO
   CMSEL,S,cmring(k-1)
  *ENDDO
 *ENDDO

 ! Write Strain_33 for every crack-front element.
 /OUTPUT,stn33,dat        ! <stn33.dat> file to store strains e_33
 /OUTPUT
 NSEL,S,LOC,X,0,rac
 CM,fan,NODE              ! group all nodes in the fan-type domain
 /FORMAT,,E
 /HEADER,OFF,OFF,OFF,OFF,ON,ON

 *DO,i,1,nezt             ! i: index for layer in Z-direction
  NSEL,R,LOC,Z,zf(i),zf(i+1)
  CM,nlayer,NODE
  NSEL,R,LOC,X,0          ! select 3 nodes on the crack front
  CM,nfront,NODE
  CMSEL,S,nlayer
  *DO,j,1,narc*2          ! j: index for element in the same layer
   NSEL,R,LOC,Y,angc*(j-1),angc*j
   *IF,j,GT,1,THEN
    CMSEL,A,nfront
   *ENDIF
   ESLN,S,1               ! select an element
   /OUTPUT,stn33,dat,,APPEND
   *MSG,INFO,0,i,j
   Ring # %I , Segment # %I ,  Element # %I :
   PRESOL,EPEL
   /OUTPUT
   CMSEL,S,nlayer
  *ENDDO
  CMSEL,S,fan
 *ENDDO

 /HEADER,DEFA
 NSEL,ALL
```

```
ESEL,ALL
DSYS,0
CSYS,0
FINISH
! ~~~~~~~~~~~~~~~~~~~~ END of Postprocessing Phase ~~~~~~~~~~~~~~~~~~~~

/EXIT
```

B. FORTRAN Program

The following FORTRAN program is used to calculate the stress intensity factor and the *T*-stresses along a three-dimensional crack front in the stiffened panel. The crack is under mode-I loading (either a uniform displacement or a uniform stress) on the far ends of the structure. The material type can be isotropic or orthotropic. The general input of the program is from data files containing stresses, strains, displacements, nodal coordinates and other associated parameters that are generated from a finite element analysis run by ANSYS.

The program is created and tested in the Microsoft Fortran PowerStation 4.0, a commercially available FORTRAN development software for Windows NT and Windows 95 operating systems. Although the Fortran PowerStation 4.0 incorporates all the features of Fortran 90, this program is intentionally written by the FORTRAN 77 syntax. This arrangement would maintain the flexibility that the program can be also run on the platforms that still carry FORTRAN 77. However, the program employs some of the IMSL libraries, the integrated mathematical and statistical functions, which may not be available on every platform with the FORTRAN capability.

```
PROGRAM T_STRESS
C     This program calculates the stress intensity factor K_I and the T-stress
C  components of T11, T13 and T33 of a 3-D crack problem.
C     The capabilities of the program in calculation of the finite element
C  model are 50 element layers along the crack front, 24 elements per 180
C  degrees.

C  Definition of Selected Variables:
C  ADISP(i,j)  Array for the auxiliary displacement field (for T11) within an
C              element. i=1..20. j=1..3.
C  ADISP13(i,j)     Array for the auxiliary displacement field (for T13) within
C                   an element. i=1..20. j=1..3.
C  APPSTN      Far-field strain.
C  APPSTS      Applied far-field stress.
C  ARC         Arc length (in degree) of a single element
C  ASTRN(i,j)  Array for the auxiliary strain field (for T11) within an
C              element. i=1..8. j=1..6.
C  ASTRN13(i,j)     Array for the auxiliary strain field (for T13) within an
C                   element. i=1..8. j=1..6.
C  ASTRS(i,j)  Array for the auxiliary stress field (for T11) within an
C              element. i=1..8. j=1..6.
C  ASTRS13(i,j)     Array for the auxiliary stress field (for T13) within an
C                   element. i=1..8. j=1..6.
C  AYT         Total cross sectional area on the far end.
C  COORD(i,j)  Array for the j-th local cylindrical coordinates of the i-th
C              node of the element. i=1..20.
C  COORDL(i,j)      Array for the j-th local Cartesian coordinates of the i-th
C                   node of the element. i=1..20.
C  CPL(i,j)    Array for the 6x6 compliance matrix.
C  CPLR(i,j)   Array for the 5x5 reduced compliance matrix.
C  CRKL        1/2 crack length.
C  DISP(i,j)   Aarray for the displacements of the i-th node, i=1..20. j=1..3
C              representing UX, UY, and UZ, respectively.
C  EM(i)       Array for 3 Young's moduli.
C  ES          Element thickness, or the length of "delta".
C  EZZ(i)      Array for the average Ezz strains within an element.
C  EZZA(i)     Array for the average Ezz strains of an element layer.
C  EX          Young's modulus of the isotropic material.
C  F           Area under the s-function curve.
C  FF          Magnitude of the uniform force on the crack front.
C  FYT         Total nodal force on the far end.
C  GM(i)       Array for 3 shear moduli.
C  IRING       Number of the element rings to be computed.
C  K2(i)       Array for the square of the Stroh normalization factors.
C  LOAD        Loading ID number. 1=fixed displacement, 2=fixed stress.
C  MAT         Material ID number. 1=anisotropic, 2=isotropic.
C  MIE(i,j)    Array for the global element number at the j-th location of the
C              i-th layer(segment).
C  MNE(i,j,k)  Array for the global node number at the j-th location of the
C              i-th layer(segment). k=1..20 is the local node number.
C  MU(i,j)     Array for the Storh eigenvalues.
C  N180        Number of the elements per 180 degrees.
C  N90         Number of the elements per 90 degrees.
C  NSEG        Number of the element layers(segments) along crack front.
C  PL          Location for the integration points.
C  PLX         1/2 panel width.
C  PLZ         Panel thickness.
C  PR          Poisson's ratio of the isotropic material.
C  PRM(i)      Array for 3 Poisson's ratios.
C  RG(i),SG(i),TG(i)     Arrays for the natural coordinates of Gaussian
```

```
C                        integration points, i=1..8.
C  S11P        The 1-1 component of the reduced compliance, s11'.
C  SIF1(i,j)   Array for the value of the stress intesity factor in the i-th
C              element layer of the j-th ring.
C  SIF1N(i,j)  Array for the value of the normalized stress intesity factor in
C              the i-th element layer of the j-th ring.
C  SIF1NAVG(i,2)    The average normalized stress intensity factor.
C  SINF        Equivalent far-field stress.
C  STRN(i,j)   Array for the FE result of strains within an element. The
C              i-th row stores strain components at the i-th Gaussian
C              integration point, i=1..8. Strain components from 1st to 6th
C              column are [Exx,Eyy,Ezz,Exy,Eyz,Exz], respectively.
C  STRS(i,j)   Array for FE result of stresses within an element. See "STRN"
C              for similar definition.
C  T11(i,j)    Array for the value of the T11 stress in the i-th element layer
C              of the j-th ring.
C  T11N(i,j)   Array for the value of the normalized T11 stress in the i-th
C              element layer of the j-th ring.
C  T13(i,j)    Array for the value of the T13 stress in the i-th element layer
C              of the j-th ring.
C  T13N(i,j)   Array for the value of the normalized T13 stress in the i-th
C              element layer of the j-th ring.
C  T33(i,j)    Array for the value of the T33 stress in the i-th element layer
C              of the j-th ring.
C  T33N(i,j)   Array for the value of the normalized T33 stress in the i-th
C              element layer of the j-th ring.
C  T11NAVG(i,2)     The average normalized T11 stress in the i-th layer.
C  T13NAVG(i,2)     The average normalized T13 stress in the i-th layer.
C  T33NAVG(i,2)     The average normalized T33 stress in the i-th layer.
C  THICK(i,j)  Array for Z-coordinate (j=1 global; j=2 normalized) of the
C              center of the i-th segment, i.e. the "s" corresponding to the
C              local I(s).
C  UMINU       Difference of mu1 and mu2 (Stroh eigenvalues).
C  UPLUS       Sum of mu1 and mu2 (Stroh eigenvalues).
C  UPROD       Product of mu1 and mu2 (Stroh eigenvalues).
C  VEDI(i,j)   Aarray for the value of local I(s) (equivalent domain
C              integral of the i-th segment) in the j-th ring.
C  VII(i,j)    Aarray for the value of local I(s) (interaction integral
C              of the i-th segment) for T11 in the j-th ring.
C  VI2(i,j)    Aarray for the value of local I(s) (interaction integral
C              of the i-th segment) for T13 in the j-th ring.
C  X0J(i,j,k)  Array for the value of the equivalent domain integral of
C              each element. i=1..IRING; j=1..NSEG.
C  X1J(i,j,k)  Array for the value of the interaction integral of each
C              element for T11. i=1..IRING; j=1..NSEG.
C  X2J(i,j,k)  Array for the value of the interaction integral of each
C              element for T13. i=1..IRING; j=1..NSEG.

      IMPLICIT DOUBLE PRECISION (A-H,O-Z)
      COMPLEX(8) MU(3,2),K2,P,Q,UPLUS,UMINU,UPROD
      PARAMETER (FF = 1)
      CHARACTER HEAD*40,RING*7
      DIMENSION RING(6)
      DATA RING /'RING #2','RING #3','RING #4','RING #5','RING #6','RING
     + #7'/
      COMMON PI,PL,HEAD
      COMMON /AUX/ ASTRS(8,6),ASTRN(8,6),ADISP(20,3)
      COMMON /AUX13/ ASTRS13(8,6),ASTRN13(8,6),ADISP13(20,3)
      COMMON /FESOL/ DISP(21,3),STRS(8,6),STRN(8,6)
      COMMON /FEMOD/ MIE(50,24),MNE(50,24,20),COORD(21,3),COORDL(20,3)
```

```
      COMMON /MATL/ CPL(6,6),CPLR(5,5),EX,PR
      COMMON /MUS/ UPLUS,UMINU,UPROD,B,D,K2(3),P(2,2),Q(2,2)
      COMMON /GIP/ RG(8),SG(8),TG(8)
      DIMENSION EM(3),GM(3),PRM(3),CPLN(3)
      DIMENSION VEDI(50,6),VII(50,6),X0J(4,50,24),X1J(4,50,24)
      DIMENSION EZZ(24),EZZA(50),THICK(50,3),SIF1(50,6),T11(50,6)
      DIMENSION SIF1N(50,6),T11N(50,6)
      DIMENSION VI2(50,6),X2J(4,50,24),T13(50,6),T13N(50,6)
      DIMENSION T33(50,6),T33N(50,6)
      DIMENSION SIF1NAVG(50,2),T11NAVG(50,2),T13NAVG(50,2),T33NAVG(50,2)
      OPEN (1,FILE='sts.dat',STATUS='unknown')          ! stress data file
      OPEN (2,FILE='stn.dat',STATUS='unknown')          ! strain data file
      OPEN (3,FILE='dis.dat',STATUS='unknown')          ! displacement data file
      OPEN (4,FILE='node.dat',STATUS='unknown')         ! nodal data file
      OPEN (5,FILE='tsts.out',STATUS='unknown')         ! parameter output file
      OPEN (8,FILE='stn33.dat',STATUS='unknown') ! crack-front strain data file
      OPEN (9,FILE='par.dat',STATUS='unknown')          ! parameter data file
      OPEN (12,FILE='K1N.out',STATUS='unknown')
      OPEN (13,FILE='T11N.out',STATUS='unknown')
      OPEN (24,FILE='T13N.out',STATUS='unknown')
      OPEN (25,FILE='T33N.out',STATUS='unknown')

      PI = ACOS(-1.0)
      PL = 1.0/SQRT(3.0)      ! location for integration points

C...Read parameters:
      READ (9,'(I1,TR4,I1)') MAT,LOAD
      READ (9,'(/////TR11,E16.9)') AYT
      IF (MAT .EQ. 1) WRITE (5,'("Material: Anisotropic")')
      IF (MAT .EQ. 2) WRITE (5,'("Material: Isotropic")')
      IF (LOAD .EQ. 1) WRITE (5,'("Far-field loading: Fixed Displacement
     +")')
      IF (LOAD .EQ. 2) WRITE (5,'("Far-field loading: Fixed Load")')
      READ (9,'(/////TR11,E16.9)') FYT
      IF (LOAD .EQ. 1) WRITE (5,'(A23,1P,E16.9)') 'Total Nodal Force FY
     += ',FYT
      WRITE (5,'(A22,E14.7)') 'Cross-sectional area =',AYT
      READ (9,'(/////TR12,I2)') NSEG
      WRITE (5,'(A17,I3)') 'No. of Segments =',NSEG
      READ (9,'(/////TR11,F11.9)') PLX
      WRITE (5,'(A18,1P,E13.6,A3)') '1/2 Panel width = ',PLX,'in'
      READ (9,'(/////TR11,E16.9)') PLZ
      WRITE (5,'(A23,E13.6,A3)') 'Full Panel Thickness = ',PLZ,'in'
      GOTO (1,6) MAT          ! read mat'l properties based on the mat'l type
1     READ (9,3) (EM(K),K=1,3),(PRM(K),K=1,3),(GM(K),K=1,3)
3     FORMAT (/////9(TR28,E16.9/))
4     FORMAT (3(E14.10,5X)/,3(F11.10,8X)/,3(E14.10,5X))
      WRITE (5,5) (EM(K),K=1,3),(PRM(K),K=1,3),(GM(K),K=1,3)
5     FORMAT ('Ex,Ey,Ez = ',3(1P,E16.9,1X),' psi',/'NUyz,NUxz,NUxy = ',
     +3(0P,F11.9,1X),/'Gyz,Gxz,Gxy = ',3(1P,E16.9,1X),' psi')
      GOTO (7,8) LOAD         ! determine load type
6     READ (9,'(/////TR11,E15.8)') EX
      WRITE (5,'(A21,E15.8,A4)') "Young's Modulus Ex = ",EX,"psi"
      READ (9,'(/////TR12,E15.9)') PR
      WRITE (5,'(A22,F6.4)') "Poisson's Ratio nuxy = ",PR
      GOTO (7,8) LOAD         ! determine load type
7     READ (9,'(/////TR11,E16.9/)') APPSTN
      WRITE (5,'(A18,1P,E13.6)') 'Far-field strain = ',APPSTN
      SINF = ABS(FYT/AYT)     ! equivalent far-field stress
      GOTO 9
```

```
8     READ (9,'(/////TR12,E15.8/)') APPSTS
      WRITE (5,'(A17,1P,E13.6,A4)') 'Far-field load = ',APPSTS,'psi'
      SINF = APPSTS
9     WRITE (5,'(A30,1P,E13.6,A4)') 'Equivalent far-field stress = ',
     +SINF,'psi'
      READ (9,'(////TR12,E13.6)') CRKL
      WRITE (5,'(A18,1P,E13.6,A3)') '1/2 crack length = ',CRKL,'in'
      READ (9,'(/////TR12,I1)') N90
      N180 = N90*2
      ARC = 180/N180          ! arc length (in degree) of a single element
      WRITE (5,'(A30,I2)') 'Elements in 180-degree span = ',N180
      WRITE (5,'(A28,F5.1,A8)') 'Arc length of each element =',ARC,
     +'Degrees'
      READ (9,'(/////TR12,I1)') IRING
      WRITE (5,'(A33,I1)') 'Number of rings to be computed = ',IRING
      GOTO (11,36) MAT

C...Evaluate the full and reduced compliance matrices for the anisotropic
C   material:
11    CALL STRUC(EM,GM,PRM)
      WRITE (5,12) 'Structural Compliance Matrix [S] = ',
     +((CPL(I,J),J=1,6),I=1,6)
12    FORMAT (/A50/,6(6(1P,E13.6,1X)/))
      WRITE (5,13) 'Reduced Structural Compliance Matrix "S_0" = ',
     +((CPLR(I,J),J=1,5),I=1,5)
13    FORMAT (/A46/,5(5(1P,E13.6,1X)/))
      WRITE (5,'(A18,1P,E12.5)') "Sqrt(s22'/s11') = ",
     +SQRT(CPLR(2,2)/CPLR(1,1))
C...Solve for Storh eigenvalues:
      CALL STROH(MU)
      WRITE (5,21) 'Stroh Eigenvalues =',((MU(M,N),N=1,2),M=1,3)
21    FORMAT (/A20/,3(2('(',1P,E13.6,' + ',1P,E13.6,'i )',5X)/))
      WRITE (5,22) 'p: ',(M,(P(M,N),N=1,2),M=1,2)
      WRITE (5,22) 'q: ',(M,(Q(M,N),N=1,2),M=1,2)
22    FORMAT (A3/,2(I1,2X,2('(',1P,E13.6,' + ',1P,E13.6,'i )',5X)/))
      WRITE (5,23) 'k^2: ',(M,K2(M),M=1,3)
23    FORMAT (A5/,3(I1,2X,'(',1P,E13.6,' + ',1P,E13.6,'i )'/))
C...Calculate L_22 value, for later calculation of K_I:
      UPLUS = MU(1,1)+MU(2,1)      ! sum of 2 eigenvalues
      UPROD = MU(1,1)*MU(2,1)      ! product of 2 eigenvalues
      A1 = DREAL(UPLUS)       ! real part of UPLUS
      A2 = DREAL(UPROD)       ! real part of UPROD
      B = DIMAG(UPLUS)        ! imaginary part of UPLUS
      D = DIMAG(UPROD)        ! imaginary part of UPROD
      AB = A1*D-A2*B
      BL22I = CPLR(1,1)*AB    ! L_inverse_22
      CPLN(1) = CPL(1,1)      ! compliance s11
      CPLN(2) = CPL(1,3)      ! compliance s13
      CPLN(3) = CPL(3,3)      ! compliance s33
      BL21 = -D/(CPLR(1,1)*(B*AB-D**2))      ! L21
      BL22 = B/(CPLR(1,1)*(B*AB-D**2))       ! L22
      CPLN(1) = CPL(1,1)      ! compliance s11
      CPLN(2) = CPL(1,3)      ! compliance s13
      CPLN(3) = CPL(3,3)      ! compliance s33
      GOTO 40

C...For isotropic materials:
36    CPLN(1) = 1/EX
      CPLN(2) = -PR/EX
      CPLN(3) = 1/EX
```

```
      BL22 = EX/(2*(1-PR**2))

C...Set Gauss integration point locations within an element:
40    CALL GUASS
      S11P = CPLN(1)-CPLN(2)**2/CPLN(3)      ! s11'

C...Calculate the equivalent domain integral and the interaction integral in
C   every element:
      DO 300 KR = 1,IRING     ! KR: counter for the rings
       DO 200 I = 1,NSEG      ! I: counter for the element layers(segments)
C...Array initialization:
        IF (KR .EQ. 1) THEN   ! initialization for later average calculation
         SIF1NAVG(I,1) = 0
         T11NAVG(I,1) = 0
         T13NAVG(I,1) = 0
         T33NAVG(I,1) = 0
        ENDIF
        VEDI(I,KR) = 0
        VII(I,KR) = 0
        VI2(I,KR) = 0
        IF (KR .EQ. 1) THEN
         EZZA(I) = 0
        ENDIF
        DO 100 J = 1,N180     ! J: counter for the elements in a segment
         CALL FERST(I,J)

C...Set up auxiliary fields:
61       CALL AUXT13(MU,ARC,MAT)        ! auxiliary field for T13
         GOTO (62,63) MAT
62       CALL AUXAN(MU,ARC)   ! auxiliary field for T11 - anisotropic
         GOTO 70
63       CALL AUXI(ARC)       ! auxiliary field for T11 - isotropic

C...Evaluate equivalent domain integral and interaction integral:
70       CALL INTEG(KR,I,J,X0J,X1J,X2J)
         VEDI(I,KR) = VEDI(I,KR)+X0J(KR,I,J) ! equivalent domain integral
         VII(I,KR) = VII(I,KR)+X1J(KR,I,J)   ! interaction integral for T11
         VI2(I,KR) = VI2(I,KR)+X2J(KR,I,J)   ! interaction integral for T13

C...Calculate average Ezz strain in every element on the crack front:
         IF (KR .EQ. 1) THEN
          CALL STRN33(EZZ,J)
          EZZA(I) = EZZA(I)+EZZ(J)
         ENDIF
100     CONTINUE
        IF (KR .EQ. 1) THEN
         EZZA(I) = EZZA(I)/N180         ! average over a layer(segment)
        ENDIF

C...Calculate T-stress and K1 using interaction-integral approach.
        ES = COORDL(5,3)-COORDL(1,3)    ! element thickness
        F = (2./3.)*ES
        THICK(I,1) = (COORDL(1,3)+COORDL(5,3))/2  ! local "s" coordinate
        THICK(I,2) = THICK(I,1)/(PLZ/2)           ! normalized thickness
        THICK(I,3) = COORDL(1,3)/(PLZ/2)          ! local "s" coordinate at
*                                                   bottom of the element
        VEDI(I,KR) = 2*VEDI(I,KR)/F
        VII(I,KR) = 2*VII(I,KR)/F
        VI2(I,KR) = 2*VI2(I,KR)/F
        GOTO (111,112) MAT
```

```
C...For anisotropic materials:
111     SIF1(I,KR) = SQRT(2*VEDI(I,KR)/BL22I)
        T11(I,KR) = 1*(VII(I,KR)-EZZA(I)*CPL(1,3)/CPL(3,3))/CPLR(1,1)
        T13(I,KR) = VI2(I,KR)/CPLR(5,5)
        T33(I,KR) = (EZZA(I)-(CPL(1,3)*T11(I,KR)+CPL(3,5)*T13(I,KR)))/
     +  CPL(3,3)
        GOTO 113
C...For isotropic materials:
112     SIF1(I,KR) = SQRT(VEDI(I,KR)*EX/(1-PR**2))
        T11(I,KR) = 1*(EX/((1-PR**2)*FF))*(VII(I,KR)+FF*PR*EZZA(I))
        T13(I,KR) = (EX/(2*(1+PR)))*VI2(I,KR)
        T33(I,KR) = EX*EZZA(I)+PR*T11(I,KR)

113     SIF1N(I,KR) = SIF1(I,KR)/(SINF*SQRT(PI*CRKL))
        T11N(I,KR) = T11(I,KR)/SINF
        T13N(I,KR) = T13(I,KR)/SINF
        T33N(I,KR) = T33(I,KR)/SINF
        SIF1NAVG(I,1) = SIF1NAVG(I,1)+SIF1N(I,KR)
        T11NAVG(I,1) = T11NAVG(I,1)+T11N(I,KR)
        T13NAVG(I,1) = T13NAVG(I,1)+T13N(I,KR)
        T33NAVG(I,1) = T33NAVG(I,1)+T33N(I,KR)
        IF (KR .EQ. IRING) THEN         ! average over rings
         SIF1NAVG(I,2) = SIF1NAVG(I,1)/IRING
         T11NAVG(I,2) = T11NAVG(I,1)/IRING
         T13NAVG(I,2) = T13NAVG(I,1)/IRING
         T33NAVG(I,2) = T33NAVG(I,1)/IRING
        ENDIF
200    CONTINUE
300   CONTINUE

C...Output calculated T-stresses and K1 data:
      WRITE (12,301) 'SEGMENT','THICKNESS',(RING(K),K=1,IRING),'AVERAGE'
      WRITE (13,301) 'SEGMENT','THICKNESS',(RING(K),K=1,IRING),'AVERAGE'
      WRITE (24,301) 'SEGMENT','THICKNESS',(RING(K),K=1,IRING),'AVERAGE'
      WRITE (25,301) 'SEGMENT','THICKNESS',(RING(K),K=1,IRING),'AVERAGE'
301   FORMAT (A7,1X,A9,4X,4(4X,A7,4X))
302   FORMAT (I4,4X,F9.6,6(2X,1P,E13.6))
      DO 310 I = 1,NSEG
       WRITE (12,302) I,THICK(I,2),(SIF1N(I,K),K=1,IRING),SIF1NAVG(I,2)
       WRITE (13,302) I,THICK(I,2),(T11N(I,K),K=1,IRING),T11NAVG(I,2)
       WRITE (24,302) I,THICK(I,2),(T13N(I,K),K=1,IRING),T13NAVG(I,2)
       WRITE (25,302) I,THICK(I,2),(T33N(I,K),K=1,IRING),T33NAVG(I,2)
310   CONTINUE

999   STOP
      END

      SUBROUTINE STRUC(YOUNG,SHEAR,PSNR)
* * * * * * * * * * * * * * * * * * * * * * * * * * * * * * * * * * * * * *
*      The subroutine computes the full and reduced compliance matrices.      *
*                                                                             *
*  --- Subroutine input: YOUNG,SHEAR,PSNR                                     *
*  --- Subroutine output: CPL,CPLR                                            *
*                                                                             *
*  --- Definition of local variables:                                         *
*  C(i,j)      Array for the stiffness matrix.                                *
*  C0(i,j)     Array for the reduced stiffness matrix.                        *
*  PSNR(i)     Array for 3 Poisson's ratios.                                  *
*  SHEAR(i)    Array for 3 shear moduli.                                      *
```

```
*  YOUNG(i)    Array for 3 Young's moduli.                                  *
* * * * * * * * * * * * * * * * * * * * * * * * * * * * * * * * * * * * * * *
      IMPLICIT DOUBLE PRECISION (A-H,O-Z)
      COMMON /MATL/ CPL(6,6),CPLR(5,5),EX,PR
      DIMENSION YOUNG(3),SHEAR(3),PSNR(3)
      DIMENSION C(6,6),C0(5,5)

C...Construct the 6x6 compliance matrix [S]:
      DO 915 I = 1,3
       CPL(I,I) = 1/YOUNG(I)
       CPL(I+3,I+3) = 1/SHEAR(I)
915   CONTINUE
      CPL(2,1) = -(PSNR(3)/YOUNG(1))
      CPL(1,2) = CPL(2,1)
      CPL(3,1) = -(PSNR(2)/YOUNG(1))
      CPL(1,3) = CPL(3,1)
      CPL(3,2) = -(PSNR(1)/YOUNG(2))
      CPL(2,3) = CPL(3,2)

C...Evaluate the 6x6 stiffness matrix [C], the 5x5 reduced stiffness and the
C   compliance matrices:
      CALL DLINRG(6,CPL,6,C,6)     ! IMSL Library for matrix inversion
      DO 920 I = 1,5
       DO 920 J = 1,5
        IF ((I .NE. 3) .AND. (J .NE. 3)) THEN
         C0(I,J) = C(I,J)
        ELSEIF ((J .EQ. 3) .AND. (I .NE. 3)) THEN
         C0(I,J) = C(I,6)
        ELSEIF ((I .EQ. 3) .AND. (J .NE. 3)) THEN
         C0(I,J) = C(6,J)
        ENDIF
920   CONTINUE
      C0(3,3) = C(6,6)
      CALL DLINRG(5,C0,5,CPLR,5)   ! IMSL Library for matrix inversion
      RETURN
      END

      SUBROUTINE STROH(U)
* * * * * * * * * * * * * * * * * * * * * * * * * * * * * * * * * * * * * * *
*     The subroutine determines the Stroh eigenvalues from the reduced       *
*  structural compliance matrix.                                             *
*                                                                            *
*  --- Subroutine input: CPLR                                                *
*  --- Subroutine output: U,K2,P,Q                                           *
*                                                                            *
*  --- Definition of local variables:                                        *
*  A1(i)       Array for the 5 coefficients in solving the in-plane          *
*              characteristic equation.                                      *
*  U(m,n)      Array for the Stroh eigenvalues. m=1..3, 3 pairs of eigenvalues*
*              and m=3 indicates the out-of-plane eigenvalue. n=2 is the     *
*              conjugate of n=1.                                             *
*  Z(i)        Array for the 4 roots of the in-plane characteristic equation. *
* * * * * * * * * * * * * * * * * * * * * * * * * * * * * * * * * * * * * * *
      IMPLICIT DOUBLE PRECISION (A-H,O-Z)
      COMPLEX(8) U,Z,D2,K2,P,Q,UPLUS,UMINU,UPROD
      COMMON /MATL/ CPL(6,6),CPLR(5,5),EX,PR
      COMMON /MUS/ UPLUS,UMINU,UPROD,B,D,K2(3),P(2,2),Q(2,2)
      DIMENSION U(3,2),A1(5),Z(4)

C...Solve for 4 in-plane eigenvalues:
```

```
      A1(1) = CPLR(2,2)            ! coefficient for mu^0: "s'_22"
      A1(2) = -2*CPLR(2,3)         ! coefficient for mu^1: "-2*s'_26"
      A1(3) = 2*CPLR(1,2)+CPLR(3,3)     ! coefficient for mu^2
      A1(4) = -2*CPLR(1,3)         ! coefficient for mu^3: "-2*s'_16"
      A1(5) = CPLR(1,1)            ! coefficient for mu^4: "s'_11"
C...Use an IMSL Library to find the roots of a polynomial with real
C   coefficients by Laguerre's method:
      CALL DZPLRC(4,A1,Z)
      U(1,1) = Z(1)           ! "mu1"
      U(1,2) = Z(2)           ! "mu1_bar"
      U(2,1) = Z(3)           ! "mu2"
      U(2,2) = Z(4)           ! "mu2_bar"
      UMINU = U(1,1)-U(2,1)   ! "mu1-mu2"
C...Solve for 2 out-of-plane eigenvalues:
      A2 = CPLR(5,5)          ! coefficient for mu^2: "s'_55"
      B2 = -2*CPLR(4,5)       ! coefficient for mu^1: "-2*s'_45"
      C2 = CPLR(4,4)          ! coefficient for mu^0: "s'_44"
      D2 = B2**2-4*A2*C2
      U(3,1) = (-B2+SQRT(D2))/(2*A2)    ! "mu3"
      U(3,2) = (-B2-SQRT(D2))/(2*A2)    ! "mu3_bar"
C...Calculate p, q, and normalization factors k:
      DO 935 N = 1,2
       P(N,1) = CPLR(1,1)*U(N,1)**2-CPLR(1,3)*U(N,1)+CPLR(1,2)   ! "p1"
       P(N,2) = CONJG(P(N,1))                                    ! "p1_bar"
       Q(N,1) = CPLR(1,2)*U(N,1)-CPLR(2,3)+CPLR(2,2)/U(N,1)      ! "q1"
       Q(N,2) = CONJG(Q(N,1))                                    ! "q1_bar"
       K2(N) = 1/(2*(Q(N,1)-U(N,1)*P(N,1)))                      ! k1^2, k2^2
935   CONTINUE
      K2(3) = 1/(2*(CPLR(4,4)/U(3,1)-CPLR(4,5)))                 ! k3^2
990   RETURN
      END

      SUBROUTINE GUASS
* * * * * * * * * * * * * * * * * * * * * * * * * * * * * * * * * * * * * *
*     The subroutine defines the Gaussian integration point locations using   *
*  reduced 8-point rule.                                                      *
*                                                                             *
*  --- Subroutine input: none                                                 *
*  --- Subroutine output: RG,SG,TG                                            *
*                                                                             *
*  --- Definition of local variables:                                         *
*  PL1          Integration point location.                                   *
*  RI,SI,TI     Coeffecients for the integration point locations.             *
* * * * * * * * * * * * * * * * * * * * * * * * * * * * * * * * * * * * * *
      IMPLICIT DOUBLE PRECISION (A-H,O-Z)
      COMMON /GIP/ RG(8),SG(8),TG(8)
      DIMENSION SI(8),TI(8),RI(8)
      DATA RI /-1,1,1,-1,-1,1,1,-1/
      DATA SI /-1,-1,1,1,-1,-1,1,1/
      DATA TI /-1,-1,-1,-1,1,1,1,1/

      PL1 = 1/SQRT(3.0)       ! point location for integration
C...Set up 2x2x2 reduced Gaussian integration points:
      DO 10 K = 1,8
       RG(K) = PL1*RI(K)
       SG(K) = PL1*SI(K)
       TG(K) = PL1*TI(K)
10    CONTINUE
      RETURN
      END
```

```
      SUBROUTINE FERST(KS,KE)
* * * * * * * * * * * * * * * * * * * * * * * * * * * * * * * * * * * * * * *
*      The subroutine reads strain, stress, and nodal data from ANSYS results.*
*  Those data are stored in different arrays for later uses.                 *
*                                                                             *
*  --- Subroutine input: data files 1,2,3,4                                  *
*  --- Subroutine output: DISP,STRS,STRN,MIE,MNE,COORD,COORDL                *
*                                                                             *
*  --- Definition of local variables:                                        *
*  KE          The element number in the layer(segment).                     *
*  KS          The element layer(segment) number along the crack front.      *
*  THETA       Angular coordinate (in radians) of the nodal points.          *
* * * * * * * * * * * * * * * * * * * * * * * * * * * * * * * * * * * * * * *
      IMPLICIT DOUBLE PRECISION (A-H,O-Z)
      CHARACTER HEAD*40
      COMMON PI,PL,HEAD
      COMMON /FESOL/ DISP(21,3),STRS(8,6),STRN(8,6)
      COMMON /FEMOD/ MIE(50,24),MNE(50,24,20),COORD(21,3),COORDL(20,3)
C...Read element-nodal data and sort by local node numbers:
      READ (4,1001) MIE(KS,KE),(MNE(KS,KE,K),K=1,20)
1001  FORMAT (//////////////////2X,I6,TR21,8I6/TR29,8I6/TR29,
     +4I6/////////////////)       ! ANSYS 5.5 format
      II = 0
1002  READ (4,1003) NK,(COORD(21,J),J=1,3)   ! NK: node no. in the data file
1003  FORMAT (1X,I7,2X,3E12.5)
      II = II+1
      DO 1010 I = 1,20             ! I: local node no.
       NI = MNE(KS,KE,I)           ! NI: global node no.
       IF (NI .EQ. NK) THEN
        DO 1005 J =1,3
         COORD(I,J) = COORD(21,J)
1005    CONTINUE
        IF (II .LT. 20) GOTO 1002
       ENDIF
1010  CONTINUE

C...Convert local cylindrical nodal coordinates to local Cartesian coordinates:
      DO 1020 I = 1,20        ! I: local node no.
       THETA = COORD(I,2)*PI/180
       COORDL(I,1) = COORD(I,1)*COS(THETA)        ! x1-coordinate
       COORDL(I,2) = COORD(I,1)*SIN(THETA)        ! x2-coordinate
       COORDL(I,3) = COORD(I,3)                   ! x3-coordinate
1020  CONTINUE

C...Read stress data within an element:
      READ (1,1021) (STRS(1,J),J=1,6)
1021  FORMAT (////9X,6E12.5)       ! ANSYS 5.5 format
1023  FORMAT (9X,6E12.5)
      DO 1030 I = 2,8
       READ (1,1023) (STRS(I,J),J=1,6)
1030  CONTINUE

C...Read strain data within an element:
      READ (2,1021) (STRN(1,J),J=1,6)
      DO 1040 I = 2,8
       READ (2,1023) (STRN(I,J),J=1,6)
1040  CONTINUE

C...Sort stress and strain data in consistent with the stress and strain
```

```
C   vectors, i.e. [sigma]=[Sxx,Syy,Szz,Syz,Sxz,Sxy] and similar to strains:
      DO 1050 I =1,8
       SXY = STRS(I,4)
       STRS(I,4) = STRS(I,5)
       STRS(I,5) = STRS(I,6)
       STRS(I,6) = SXY
       EXY = STRN(I,4)
       STRN(I,4) = STRN(I,5)
       STRN(I,5) = STRN(I,6)
       STRN(I,6) = EXY
1050  CONTINUE

C...Read displacement data within an element and sort by local node numbers:
1051  READ (3,'(A40)') HEAD
      II = 0
1052  READ (3,1053) NK,(DISP(21,J),J=1,3)    ! NK: node no. in the data file
1053  FORMAT (1X,I7,1X,3E12.5)
      II = II+1
      DO 1060 I = 1,20        ! I: local node no.
       NI = MNE(KS,KE,I)      ! NI: global node no.
       IF (NK .EQ. NI) THEN
        DO 1055 J =1,3
         DISP(I,J) = DISP(21,J)
1055    CONTINUE
        IF (II .LE. 19) GOTO 1052
       ENDIF
1060  CONTINUE
1100  RETURN
      END

      SUBROUTINE AUXT13(U,AL,MAT)
* * * * * * * * * * * * * * * * * * * * * * * * * * * * * * * * * * * * * * *
*     The subroutine calculates the auxiliary stress, strain, and displacement*
*  fields under a line load f3 applying on the crack front, in order to       *
*  calculate the T13 stresses later.                                          *
*                                                                             *
*  --- Subroutine input: U,AL,MAT                                             *
*  --- Subroutine output: ASTRS13,ASTRN13,ADISP13                             *
*                                                                             *
*  --- Definition of local variables:                                         *
*  AL          Arc length (in degrees) of a single element.                   *
*  R           Radial coordinate of the integration or nodal points.          *
*  RE          Element size in r-direction.                                   *
*  SR3(i)      r-3 stresses on the 8 integration points.                      *
*  THETAD      Angular coordinate (in degrees) of the integration or nodal    *
*              points.                                                        *
*  U(i)        Stroh eigenvalues, i=1,2,3.                                    *
* * * * * * * * * * * * * * * * * * * * * * * * * * * * * * * * * * * * * * *
      IMPLICIT DOUBLE PRECISION (A-H,O-Z)
      COMPLEX(8) U(3,2),P,Q,XI3,OMEGA3,K2,UPLUS,UMINU,UPROD
      PARAMETER (FF = 1)
      COMMON PI,PL,HEAD
      COMMON /AUX13/ ASTRS13(8,6),ASTRN13(8,6),ADISP13(20,3)
      COMMON /FEMOD/ MIE(50,24),MNE(50,24,20),COORD(21,3),COORDL(20,3)
      COMMON /MATL/ CPL(6,6),CPLR(5,5),EX,PR
      COMMON /MUS/ UPLUS,UMINU,UPROD,B,D,K2(3),P(2,2),Q(2,2)
      DIMENSION JR(8),JS(8)
      DIMENSION SR3(8)
      DOUBLE PRECISION MU
      DATA JR /1,1,-1,-1,1,1,-1,-1/
```

```
      DATA JS /-1,1,1,-1,-1,1,1,-1/

      RE = COORD(1,1)-COORD(4,1)
      GOTO (1302,1351) MAT    ! determine anisotropic or isotropic material

C...For anisotropic material:
1302  MU = (CPLR(4,4)*CPLR(5,5)-CPLR(4,5)**2)**(-0.5)
      DO 1320 L = 1,8         ! L: counter for the integration points
       R = COORD(L,1)-(1-PL)*(RE/2)*JR(L)
       THETAD = COORD(L,2)-(1-PL)*(AL/2)*JS(L)
       XI3 = COSD(THETAD)+U(3,1)*SIND(THETAD)
       OMEGA3 = (-SIND(THETAD)+U(3,1)*COSD(THETAD))/XI3
       A1 = REAL(K2(3)*OMEGA3)
       SR3(L) = FF*A1/(PI*MU*R)              ! "Sr3"
C...Compute Cartesian stress components:
       ASTRS13(L,1) = 0                      ! "Sxx"
       ASTRS13(L,2) = 0                      ! "Syy"
       ASTRS13(L,3) = 0                      ! "Szz"
       ASTRS13(L,4) = SIND(THETAD)*SR3(L)    ! "Syz"
       ASTRS13(L,5) = COSD(THETAD)*SR3(L)    ! "Sxz"
       ASTRS13(L,6) = 0                      ! "Sxy"
C...Compute engineering strains:
       DO 1310 I = 1,6
        ASTRN13(L,I) = 0
        DO 1310 J = 1,6
         ASTRN13(L,I) = ASTRN13(L,I)+CPL(I,J)*ASTRS13(L,J)
1310   CONTINUE
C...Convert engineering strains to tensorial strains:
       ASTRN13(L,4) = ASTRN13(L,4)/2
       ASTRN13(L,5) = ASTRN13(L,5)/2
       ASTRN13(L,6) = ASTRN13(L,6)/2
1320  CONTINUE
C...Compute displacements:
      DO 1330 I = 1,20             ! I: counter for the local nodes
       R = COORD(I,1)
       THETAD = COORD(I,2)
       XI3 = COSD(THETAD)+U(3,1)*SIND(THETAD)
       ADISP13(I,1) = 0            ! "u1"
       ADISP13(I,2) = 0            ! "u2"
       ADISP13(I,3) = -FF*(LOG(R)+REAL(LOG(XI3)))/(2*PI*MU)      !"u3"
1330  CONTINUE
      GOTO 1400

C...For isotropic material:
1351  DO 1370 L = 1,8
       R = COORD(L,1)-(1-PL)*(RE/2)*JR(L)
       THETAD = COORD(L,2)-(1-PL)*(AL/2)*JS(L)
       SR3(L) = -FF/(2*PI*R)       ! "Sr3"
C...Compute Cartesian stress components:
       ASTRS13(L,1) = 0                          ! "Sxx"
       ASTRS13(L,2) = 0                          ! "Syy"
       ASTRS13(L,3) = 0                          ! "Szz"
       ASTRS13(L,4) = -FF*SIND(THETAD)/(2*PI*R)  ! "Syz"
       ASTRS13(L,5) = -FF*COSD(THETAD)/(2*PI*R)  ! "Sxz"
       ASTRS13(L,6) = 0                          ! "Sxy"
C...Compute tensorial strains:
       ASTRN13(L,1) = (ASTRS13(L,1)-PR*(ASTRS13(L,2)+ASTRS13(L,3)))/EX  ! "Exx"
       ASTRN13(L,2) = (ASTRS13(L,2)-PR*(ASTRS13(L,1)+ASTRS13(L,3)))/EX  ! "Eyy"
       ASTRN13(L,3) = (ASTRS13(L,3)-PR*(ASTRS13(L,1)+ASTRS13(L,2)))/EX  ! "Ezz"
       ASTRN13(L,4) = (1+PR)/EX*ASTRS13(L,4)     ! "Eyz"
```

```
       ASTRN13(L,5) = (1+PR)/EX*ASTRS13(L,5)      ! "Exz"
       ASTRN13(L,6) = (1+PR)/EX*ASTRS13(L,6)      ! "Exy"
1370  CONTINUE
      DO 1380 I = 1,20
       R = COORD(I,1)
       ADISP13(I,1) = 0                           ! "u1"
       ADISP13(I,2) = 0                           ! "u2"
       ADISP13(I,3) = -FF*(1+PR)*LOG(R)/(PI*EX)   ! "u3"
1380  CONTINUE

1400  RETURN
      END

      SUBROUTINE AUXAN(U,AL)
* * * * * * * * * * * * * * * * * * * * * * * * * * * * * * * * * * * * * * *
*     The subroutine calculates the auxiliary stress, strain, and displacement*
*  fields under a line load f1 applying on the crack front, for an anisotropic*
*  material according to the Stroh formalism with the normalization factor k. *
*  The auxiliary fields are later used to determine T11 stresses.            *
*                                                                             *
*  --- Subroutine input: U,AL                                                 *
*  --- Subroutine output: ASTRS,ASTRN,ADISP                                   *
*                                                                             *
*  --- Definition of local variables:                                         *
*  AL          Arc length (in degrees) of a single element.                   *
*  R           Radial coordinate of the integration or nodal points.          *
*  RE          Element size in r-direction.                                   *
*  SRR(i)      r-r stresses on the 8 integration points.                      *
*  THETAD      Angular coordinate (in degrees) of the integration or nodal    *
*              points.                                                        *
*  U(i)        Stroh eigenvalues, i=1,2,3.                                    *
* * * * * * * * * * * * * * * * * * * * * * * * * * * * * * * * * * * * * * *
      IMPLICIT DOUBLE PRECISION (A-H,O-Z)
      COMPLEX(8) U(3,2),P,Q,XI(2),OMEGA(2),K2,UPLUS,UMINU,
     +UPROD,DL(2,2),S(2,2)
      PARAMETER (FF = 1)
      COMMON PI,PL,HEAD
      COMMON /AUX/ ASTRS(8,6),ASTRN(8,6),ADISP(20,3)
      COMMON /FEMOD/ MIE(50,24),MNE(50,24,20),COORD(21,3),COORDL(20,3)
      COMMON /MATL/ CPL(6,6),CPLR(5,5),EX,PR
      COMMON /MUS/ UPLUS,UMINU,UPROD,B,D,K2(3),P(2,2),Q(2,2)
      DIMENSION JR(8),JS(8)
      DIMENSION SRR(8)
      DATA JR /1,1,-1,-1,1,1,-1,-1/
      DATA JS /-1,1,1,-1,-1,1,1,-1/

      RE = COORD(1,1)-COORD(4,1)
      DO 1320 L = 1,8         ! L: counter for the integration points
       R = COORD(L,1)-(1-PL)*(RE/2)*JR(L)
       THETAD = COORD(L,2)-(1-PL)*(AL/2)*JS(L)
       XI(1) = COSD(THETAD)+U(1,1)*SIND(THETAD)
       XI(2) = COSD(THETAD)+U(2,1)*SIND(THETAD)
       OMEGA(1) = (-SIND(THETAD)+U(1,1)*COSD(THETAD))/XI(1)
       OMEGA(2) = (-SIND(THETAD)+U(2,1)*COSD(THETAD))/XI(2)
       DL(1,1) = K2(1)*U(1,1)**2*OMEGA(1)+K2(2)*U(2,1)**2*OMEGA(2)
       DL(1,2) = -K2(1)*U(1,1)*OMEGA(1)-K2(2)*U(2,1)*OMEGA(2)
       DL(2,1) = DL(1,2)
       DL(2,2) = K2(1)*OMEGA(1)+K2(2)*OMEGA(2)
       A1 = REAL(COSD(THETAD)*(B*DL(1,1)+D*DL(1,2))+SIND(THETAD)*
     + (B*DL(2,1)+D*DL(2,2)))
```

```
      SRR(L) = FF*CPLR(1,1)*A1/(PI*R)                        ! "Srr"
C...Compute Cartesian stress components:
      ASTRS(L,1) = FF*CPLR(1,1)*COSD(THETAD)**2/(PI*R)*A1  ! "Sxx"
      ASTRS(L,2) = FF*CPLR(1,1)*SIND(THETAD)**2/(PI*R)*A1  ! "Syy"
      ASTRS(L,3) = -FF*CPLR(1,1)*(CPL(1,3)*COSD(THETAD)**2+CPL(2,3)
     + *SIND(THETAD)**2)/(PI*R*CPL(3,3))*A1                  ! "Szz"
      ASTRS(L,4) = 0                                         ! "Syz"
      ASTRS(L,5) = 0                                         ! "Sxz"
      ASTRS(L,6) = FF*CPLR(1,1)*SIND(THETAD)*COSD(THETAD)/(PI*R)*A1  ! "Sxy"
C...Compute engineering strains:
      DO 1310 I = 1,6
       ASTRN(L,I) = 0
       DO 1310 J = 1,6
        ASTRN(L,I) = ASTRN(L,I)+CPL(I,J)*ASTRS(L,J)
1310  CONTINUE
C...Convert engineering strains to tensorial strains:
      ASTRN(L,4) = ASTRN(L,4)/2
      ASTRN(L,5) = ASTRN(L,5)/2
      ASTRN(L,6) = ASTRN(L,6)/2
1320  CONTINUE
C...Compute displacements:
     DO 1330 I = 1,20            ! I: counter for the local nodes
      R = COORD(I,1)
      THETAD = COORD(I,2)
      XI(1) = COSD(THETAD)+U(1,1)*SIND(THETAD)
      XI(2) = COSD(THETAD)+U(2,1)*SIND(THETAD)
      S(1,1) = -K2(1)*U(1,1)*P(1,1)*LOG(XI(1))-K2(2)*U(2,1)*P(2,1)*
     + LOG(XI(2))
      S(1,2) = K2(1)*P(1,1)*LOG(XI(1))+K2(2)*P(2,1)*LOG(XI(2))
      S(2,1) = -K2(1)*U(1,1)*Q(1,1)*LOG(XI(1))-K2(2)*U(2,1)*Q(2,1)*
     + LOG(XI(2))
      S(2,2) = K2(1)*Q(1,1)*LOG(XI(1))+K2(2)*Q(2,1)*LOG(XI(2))
      ADISP(I,1) = -FF*CPLR(1,1)*(B*LOG(R)+2*REAL(B*S(1,1)+D*S(1,2)))/
     + (2*PI)                 ! "u1"
      ADISP(I,2) = -FF*CPLR(1,1)*(D*LOG(R)+2*REAL(B*S(2,1)+D*S(2,2)))/
     + (2*PI)                 ! "u2"
      ADISP(I,3) = 0          ! "u3"
1330  CONTINUE
1400  RETURN
      END

      SUBROUTINE AUXI(AL)
* * * * * * * * * * * * * * * * * * * * * * * * * * * * * * * * * * * * * *
*     The subroutine calculates the auxiliary stress, strain, and displacement*
*  fields under a line load applying on the crack front, for an isotropic     *
*  material. The auxiliary fields are later used to determine T11 stresses.   *
*                                                                              *
*  --- Subroutine input: AL                                                    *
*  --- Subroutine output: ASTRS,ASTRN,ADISP                                    *
*                                                                              *
*  --- Definition of local variables:                                          *
*  AL          Arc length (in degrees) of a single element.                    *
*  RE          Element size in r-direction.                                    *
*  THETA       Angular coordinate (in radians) of the integration or nodal     *
*              points.                                                         *
*  THETAD      Angular coordinate (in degrees) of the integration or nodal     *
*              points.                                                         *
* * * * * * * * * * * * * * * * * * * * * * * * * * * * * * * * * * * * * *
      IMPLICIT DOUBLE PRECISION (A-H,O-Z)
      PARAMETER (FF = 1)
```

```
      COMMON PI,PL,HEAD
      COMMON /AUX/ ASTRS(8,6),ASTRN(8,6),ADISP(20,3)
      COMMON /FEMOD/ MIE(50,24),MNE(50,24,20),COORD(21,3),COORDL(20,3)
      COMMON /MATL/ CPL(6,6),CPLR(5,5),EX,PR
      DIMENSION JX1(8),JX2(8)
      DATA JX1 /1,1,-1,-1,1,1,-1,-1/
      DATA JX2 /-1,1,1,-1,-1,1,1,-1/

      RE = COORD(1,1)-COORD(4,1)       ! element size in r-direction
      DO 1310 L = 1,8         ! L: counter for the integration points
       R = COORD(L,1)-(1-PL)*(RE/2)*JX1(L)
       THETAD = COORD(L,2)-(1-PL)*(AL/2)*JX2(L)
       ASTRS(L,1) = -FF*COSD(THETAD)**3/(PI*R)              ! "Sxx"
       ASTRS(L,2) = -FF*COSD(THETAD)*SIND(THETAD)**2/(PI*R) ! "Syy"
       ASTRS(L,3) = -FF*PR*COSD(THETAD)/(PI*R)              ! "Szz"
       ASTRS(L,4) = 0                                       ! "Syz"
       ASTRS(L,5) = 0                                       ! "Sxz"
       ASTRS(L,6) = -FF*COSD(THETAD)**2*SIND(THETAD)/(PI*R) ! "Sxy"
       ASTRN(L,1) = (ASTRS(L,1)-PR*(ASTRS(L,2)+ASTRS(L,3)))/EX   ! "Exx"
       ASTRN(L,2) = (ASTRS(L,2)-PR*(ASTRS(L,1)+ASTRS(L,3)))/EX   ! "Eyy"
       ASTRN(L,3) = (ASTRS(L,3)-PR*(ASTRS(L,1)+ASTRS(L,2)))/EX   ! "Ezz"
       ASTRN(L,4) = (1+PR)/EX*ASTRS(L,4)                    ! "Eyz"
       ASTRN(L,5) = (1+PR)/EX*ASTRS(L,5)                    ! "Exz"
       ASTRN(L,6) = (1+PR)/EX*ASTRS(L,6)                    ! "Exy"
1310  CONTINUE

      DO 1320 I = 1,20
       R = COORD(I,1)
       THETA = COORD(I,2)*PI/180
       ADISP(I,1) = -FF*(1-PR**2)*(LOG(R)+SIN(THETA)**2/(2*(1-PR)))/
     + (PI*EX)                ! "u1"
       ADISP(I,2) = -FF*(1+PR)*((1-2*PR)*THETA-SIN(THETA)*COS(THETA))/
     + (2*PI*EX)              ! "u2"
       ADISP(I,3) = 0         ! "u3"
1320  CONTINUE
1400  RETURN
      END

      SUBROUTINE INTEG(KR,KS,KE,VEDI,VII,VI2)
* * * * * * * * * * * * * * * * * * * * * * * * * * * * * * * * * * * * * *
*      The subroutine calculates the terms necessary for local interaction    *
*  integral and equivalent domain integral of each element.                   *
*                                                                             *
*  --- Subroutine input: KR,KS,KE                                             *
*  --- Subroutine output: VEDI,VII,VI2                                        *
*                                                                             *
*  --- Definition of local variables:                                         *
*  ADUX1(i,j)  Array for the derivatives of the j-th auxiliary displacement   *
*              component in calculating T11, w.r.t. the local x1 coordinate at*
*              the i-th integration point. j=1:u1; j=2:u2; j=3:u3.           *
*  ADUX113(i,j)     Array for the derivatives of the j-th auxiliary           *
*                   displacement component in calculating T13, w.r.t. the     *
*                   local x1 coordinate at the i-th integration point. j=1:u1;*
*                   j=2:u2; j=3:u3.                                           *
*  ASIGMA(i,j) 3x3 array for the auxiliary stress tensor of the element in    *
*              calculating T11.                                               *
*  ASIGMA13(i,j)    3x3 array for the auxiliary stress tensor of the element  *
*                   in calculating T13.                                       *
*  C1(i)       Coefficients for each of the 6 stress-work density terms in the*
*              calculation of the interaction integral.                       *
```

```
*  CEDI(i)      Coefficients for each of the 6 stress-work density terms in the*
*               calculation of the equivalent domain integral.                 *
*  DSHAP(i,j)   Array for the derivative of the i-th shape function w.r.t. the *
*               local coordinate j. j=1:x1; j=2:x2; j=3:x3.                    *
*  DSRST(i,j)   Array for the derivatives of the s-function w.r.t. the natural *
*               coordinates j at the i-th integration point. j=1:xi; j=2:eta;  *
*               j=3:zeta.                                                      *
*  DSX(i,j)     Array for the derivatives of the s-function w.r.t. the local   *
*               coordinates j at the i-th integration point. j=1:x1; j=2:x2;   *
*               j=3:x3.                                                        *
*  DUX1(i,j)    Array for the derivatives of the j-th displacement component   *
*               w.r.t. the local x1 coordinate at the i-th integration point.  *
*               j=1:u1; j=2:u2; j=3:u3.                                        *
*  KE           The element number in the ring.                                *
*  KR           The ring number.                                               *
*  KS           The element layer(segment) number along the crack front.       *
*  RX(i,j)      Inverse of the Jacobian. i=1..3; j=1..3                        *
*  SF(i)        s-function at the i-th integration point, i=1..8.              *
*  SIGMA(i,j)   3x3 array for the stress tensor of the element.                *
*  TERMEDI(i,j)      Array for the terms in the expression of the equivalent   *
*                    domain integral. i=1: 1st term; i=2: 2nd term.            *
*  TERMI2(i,j) Array for the terms in the expression of the interaction        *
*               integral I(2). i=1: 1st term; i=2: 2nd term.                   *
*  TERMII(i,j) Array for the terms in the expression of the interaction        *
*               integral I(1). i=1: 1st term; i=2: 2nd term.                   *
*  WEDI(k)      Array for the stress-work density at the k-th integration point*
*               for equivalent domain integral.                                *
*  WI2(k)       Array for the stress-work density at the k-th integration point*
*               in the calculation of the interaction integral I(2).           *
*  WII(k)       Array for the stress-work density at the k-th integration point*
*               in the calculation of the interaction integral I(1).           *
*  VEDI(i,j,k) Array for the value of the equivalent domain integral of the    *
*               k-th element in the (i+1)-th ring of the j-th layer(segment).  *
*  VI2(i,j,k)   Array for the value of the interaction integral I(2), for T13  *
*               stresses, of the k-th element in the (i+1)-th ring of the j-th *
*               layer(segment).                                                *
*  VII(i,j,k)   Array for the value of the interaction integral I(1), for T11  *
*               stresses, of the k-th element in the (i+1)-th ring of the j-th *
*               layer(segment).                                                *
*  XRJ          Determinant of the Jacobian.                                   *
* * * * * * * * * * * * * * * * * * * * * * * * * * * * * * * * * * * * * * * *
      IMPLICIT DOUBLE PRECISION (A-H,O-Z)
      COMMON PI,PL,HEAD
      COMMON /AUX/ ASTRS(8,6),ASTRN(8,6),ADISP(20,3)
      COMMON /AUX13/ ASTRS13(8,6),ASTRN13(8,6),ADISP13(20,3)
      COMMON /FESOL/ DISP(21,3),STRS(8,6),STRN(8,6)
      COMMON /FEMOD/ MIE(50,24),MNE(50,24,20),COORD(21,3),COORDL(20,3)
      COMMON /GIP/ RG(8),SG(8),TG(8)
      DIMENSION SF(8),DSRST(8,3),DSX(8,3),DUX1(8,3),SIGMA(3,3)
      DIMENSION DSHAP(20,3),RX(3,3)
      DIMENSION ASIGMA(3,3),ASIGMA13(3,3),ADUX1(8,3),ADUX113(8,3)
      DIMENSION CEDI(6),TERMEDI(8,2),VEDI(4,50,24),WEDI(8)
      DIMENSION C1(6),TERMII(8,2),VII(4,50,24),WII(8)
      DIMENSION TERMI2(8,2),VI2(4,50,24),WI2(8)
      DATA CEDI /0.5,0.5,0.5,1,1,1/
      DATA C1 /1,1,1,2,2,2/

C...Initialization:
      VEDI(KR,KS,KE) = 0
      VII(KR,KS,KE) = 0
```

```
      VI2(KR,KS,KE) = 0
      DO 1110 K = 1,8         ! K: counter for the integration points
       WEDI(K) = 0
       WII(K) = 0
       WI2(K) = 0
       TERMEDI(K,1) = 0
       TERMII(K,1) = 0
       TERMI2(K,1) = 0
       DO 1105 KI = 1,3       ! KI: counter for the local coordinates x1 to x3
        DSX(K,KI) = 0
        DUX1(K,KI) = 0
        ADUX1(K,KI) = 0
        ADUX113(K,KI) = 0
1105   CONTINUE
1110  CONTINUE

C...DO-Loop #1199 - Sum over 8 integration points:
      DO 1199 LI = 1,8        ! LI: counter for the integration point
       CALL SHPF(DSHAP,XRJ,RX,LI,RG,SG,TG)
C...Define s-function and its derivatives:
       SF(LI) = 0.5*(1+SG(LI))*(1-TG(LI)**2)      ! s(xi,eta,zeta)
       DSRST(LI,1) = 0.                           ! ds/d(xi)
       DSRST(LI,2) = 0.5*(1-TG(LI)**2)            ! ds/d(eta)
       DSRST(LI,3) = -1*(1+SG(LI))*TG(LI)         ! ds/d(zeta)
       DO 1120 KI = 1,3
        DO 1120 KJ = 1,3
         DSX(LI,KI) = DSX(LI,KI)+RX(KI,KJ)*DSRST(LI,KJ)
1120   CONTINUE
C...Calculate the stress-work density W for the equivalent domain integral and
C   the interaction integral:
       DO 1130 K = 1,6
        WEDI(LI) = WEDI(LI)+CEDI(K)*STRS(LI,K)*STRN(LI,K)
        WII(LI) = WII(LI)+C1(K)*STRS(LI,K)*ASTRN(LI,K)
        WI2(LI) = WI2(LI)+C1(K)*STRS(LI,K)*ASTRN13(LI,K)
1130   CONTINUE
C...Calculate [du/dx1] and [du/dx1]_a terms:
       DO 1140 KI = 1,3
        DO 1135 KN = 1,20     ! KN: counter for the local nodes
         DUX1(LI,KI) = DUX1(LI,KI)+DSHAP(KN,1)*DISP(KN,KI)
         ADUX1(LI,KI) = ADUX1(LI,KI)+DSHAP(KN,1)*ADISP(KN,KI)
         ADUX113(LI,KI) = ADUX113(LI,KI)+DSHAP(KN,1)*ADISP13(KN,KI)
1135    CONTINUE
1140   CONTINUE
C...Construct the stress tensors:
       DO 1150 KI = 1,3
        DO 1145 KJ = 1,3
         IF (KI .EQ. KJ) THEN
          SIGMA(KI,KJ) = STRS(LI,KI)
          ASIGMA(KI,KJ) = ASTRS(LI,KI)
          ASIGMA13(KI,KJ) = ASTRS13(LI,KI)
         ELSE
          SIGMA(KI,KJ) = STRS(LI,9-KI-KJ)
          ASIGMA(KI,KJ) = ASTRS(LI,9-KI-KJ)
          ASIGMA13(KI,KJ) = ASTRS13(LI,9-KI-KJ)
         ENDIF
1145    CONTINUE
1150   CONTINUE
C...Calculate the first terms of the equivalent domain integral and the
C   interaction integrals:
C   EDI- (du/dx1)*sigma*(dS/dx) <TERMEDI(LI,1)>
```

```
C   II - (du/dx1)_a*sigma*(dS/dx)+(du/dx1)*sigma_a*(dS/dx) <TERMII(LI,1)>
       DO 1160 KI = 1,3
        DO 1160 KJ = 1,3
         TERMEDI(LI,1) = TERMEDI(LI,1)+
     +   DUX1(LI,KI)*SIGMA(KI,KJ)*DSX(LI,KJ)
         TERMII(LI,1) = TERMII(LI,1)+(ADUX1(LI,KI)*SIGMA(KI,KJ)+
     +   DUX1(LI,KI)*ASIGMA(KI,KJ))*DSX(LI,KJ)
         TERMI2(LI,1) = TERMI2(LI,1)+(ADUX113(LI,KI)*SIGMA(KI,KJ)+
     +   DUX1(LI,KI)*ASIGMA13(KI,KJ))*DSX(LI,KJ)
1160   CONTINUE
C...Calculate the second terms of the equivalent domain integral and the
C   interaction integrals - W*(dS/dx1):
       TERMEDI(LI,2) = WEDI(LI)*DSX(LI,1)
       TERMII(LI,2) = WII(LI)*DSX(LI,1)
       TERMI2(LI,2) = WI2(LI)*DSX(LI,1)
C...Calculate the integrals for the element:
       VEDI(KR,KS,KE) = VEDI(KR,KS,KE)+(TERMEDI(LI,1)-TERMEDI(LI,2))*XRJ
       VII(KR,KS,KE) = VII(KR,KS,KE)+(TERMII(LI,1)-TERMII(LI,2))*XRJ
       VI2(KR,KS,KE) = VI2(KR,KS,KE)+(TERMI2(LI,1)-TERMI2(LI,2))*XRJ
1199  CONTINUE
1200  RETURN
      END

      SUBROUTINE SHPF(DSHP,XSJ,SX,L,RG,SG,TG)
* * * * * * * * * * * * * * * * * * * * * * * * * * * * * * * * * * * * *
*     The subroutine forms the shape functions and their derivatives for the  *
*  20-node 3-D solid element. The orientation of the local nodes 1 to 20 is   *
*  based on the ANSYS SOLID95 element type.                                   *
*  Ref.: I.M. Smith & D.V. Griffiths, Programming the Finite Element Method,  *
*        pp.432-433. John Wiley & Sons, 1988.                                 *
*                                                                             *
*  --- Subroutine input: L,RG,SG,TG                                           *
*  --- Subroutine output: DSHP,XSJ,SX                                         *
*                                                                             *
*  --- Definition of local variables:                                         *
*  DER(i,j)    Array for the derivative of the i-th shape function w.r.t. the *
*              natural coordinate j. j=1:xi; j=2:eta; j=3:zeta.               *
*  FUN(i)      Array for the shape function of the i-th node w.r.t. the       *
*              natural coordinates.                                           *
*  IR(i),IS(i),IT(i)     Arrays for the natural coodinates of the i-th node.  *
*  L           Counter for the integration points.                            *
*  SX(i,j)     The inverse of the Jacobian.                                   *
*  XS(i,j)     The Jacobian.                                                  *
*  XSJ         The determinant of the Jacobian.                               *
* * * * * * * * * * * * * * * * * * * * * * * * * * * * * * * * * * * * *
      IMPLICIT DOUBLE PRECISION (A-H,O-Z)
      COMMON /FEMOD/ MIE(50,24),MNE(50,24,20),COORD(21,3),COORDL(20,3)
      DIMENSION IS(20),IT(20),IR(20),SG(8),TG(8),RG(8)
      DIMENSION FUN(20),DER(20,3),XS(3,3),SX(3,3),DSHP(20,3)
      DATA IR /-1,1,1,-1,-1,1,1,-1,0,1,0,-1,0,1,0,-1,-1,1,1,-1/
      DATA IS /-1,-1,1,1,-1,-1,1,1,-1,0,1,0,-1,0,1,0,-1,-1,1,1/
      DATA IT /-1,-1,-1,-1,1,1,1,1,-1,-1,-1,-1,1,1,1,1,0,0,0,0/

C...Define shape functions and their derivatives for each node:
      DO 1205 I = 1,20        ! I: counter for the local node numbers
       R = RG(L)*IR(I)
       S = SG(L)*IS(I)
       T = TG(L)*IT(I)
       IF (IR(I) .EQ. 0) THEN           ! local nodes 9,11,13,15
        FUN(I) = 0.25*(1-RG(L)**2)*(1+S)*(1+T)
```

```
        DER(I,1) = -0.5*RG(L)*(1+S)*(1+T)
        DER(I,2) = 0.25*IS(I)*(1-RG(L)**2)*(1+T)
        DER(I,3) = 0.25*IT(I)*(1-RG(L)**2)*(1+S)
       ELSEIF (IS(I) .EQ. 0) THEN       ! local nodes 10,12,14,16
        FUN(I) = 0.25*(1+R)*(1-SG(L)**2)*(1+T)
        DER(I,1) = 0.25*IR(I)*(1-SG(L)**2)*(1+T)
        DER(I,2) = -0.5*SG(L)*(1+R)*(1+T)
        DER(I,3) = 0.25*IT(I)*(1+R)*(1-SG(L)**2)
       ELSEIF (IT(I) .EQ. 0) THEN       ! local nodes 17,18,19,20
        FUN(I) = 0.25*(1+R)*(1+S)*(1-TG(L)**2)
        DER(I,1) = 0.25*IR(I)*(1+S)*(1-TG(L)**2)
        DER(I,2) = 0.25*IS(I)*(1+R)*(1-TG(L)**2)
        DER(I,3) = -0.5*TG(L)*(1+R)*(1+S)
       ELSE                             ! local nodes 1,2,3,4,5,6,7,8
        FUN(I) = 0.125*(1+R)*(1+S)*(1+T)*(R+S+T-2)
        DER(I,1) = 0.125*IR(I)*(1+S)*(1+T)*(2*R+S+T-1)
        DER(I,2) = 0.125*IS(I)*(1+R)*(1+T)*(R+2*S+T-1)
        DER(I,3) = 0.125*IT(I)*(1+R)*(1+S)*(R+S+2*T-1)
       ENDIF
1205  CONTINUE
C...Construct the Jacobian, its determinant, and the inverse of the Jacobian:
      DO 1210 I = 1,3
       DO 1210 J = 1,3
        XS(I,J) = 0
        DO 1210 K = 1,20
         XS(I,J) = XS(I,J)+COORDL(K,J)*DER(K,I)   ! Jacobian
1210  CONTINUE
      CALL MINV(SX,XSJ,XS)
C...Form derivatives of the shape functions in global coordinates.
      DO 1230 I = 1,20
       DO 1230 J = 1,3
        DSHP(I,J) = 0
        DO 1230 K = 1,3
         DSHP(I,J) = DSHP(I,J)+SX(J,K)*DER(I,K)
1230  CONTINUE
1300  RETURN
      END

      SUBROUTINE MINV(AINV,DET,A)
* * * * * * * * * * * * * * * * * * * * * * * * * * * * * * * * * * * * * * *
*     The subroutine calculates the determinant of a 3x3 matrix, and forms its*
*  inverse matrix. A standard Gauss-Jordan elimination algorithm is used.     *
*  Ref.: G.J. Borse, FORTRAN 77 and Numerical Methods for Engineers, pp.429-  *
*        432. PWS Publishers, 1985.                                           *
*                                                                             *
*  --- Subroutine input: A                                                    *
*  --- Subroutine output: AINV,DET                                            *
*                                                                             *
*  --- Definition of local variables:                                         *
*  A           The input matrix.                                              *
*  AINV        The inverse of A.                                              *
*  DET         The determinant of A.                                          *
* * * * * * * * * * * * * * * * * * * * * * * * * * * * * * * * * * * * * * *
      IMPLICIT DOUBLE PRECISION (A-H,O-Z)
      DIMENSION A(3,3),AINV(3,3),B(3,3)
      DO 1 I = 1,3
       DO 1 J = 1,3
        B(I,J) = A(I,J)
         IF (I .EQ. J) THEN
         AINV(I,J) = 1
```

```
        ELSE
         AINV(I,J) = 0
        ENDIF
1     CONTINUE
      DO 10 IPASS = 1,3       ! IPASS: counter for the current pivot row
C...For each pass, find the maximum element in the pivot row:
       IMX = IPASS
       DO 2 IROW = IPASS,3
        IF (ABS(B(IROW,IPASS)) .GT. ABS(B(IMX,IPASS))) THEN
         IMX = IROW
        ENDIF
2      CONTINUE
C...Interchange the elements of row IPASS and row IMX in both B and AINV:
       IF (IMX .NE. IPASS) THEN
        DO 4 ICOL = 1,3
         TEMP = AINV(IPASS,ICOL)
         AINV(IPASS,ICOL) = AINV(IMX,ICOL)
         AINV(IMX,ICOL) = TEMP
         IF (ICOL .GE. IPASS) THEN
          TEMP = B(IPASS,ICOL)
          B(IPASS,ICOL) = B(IMX,ICOL)
          B(IMX,ICOL) = TEMP
         ENDIF
4       CONTINUE
       ENDIF
       PIVOT = B(IPASS,IPASS)           ! the current pivot
C...Normalize the pivot row by dividing across by the current pivot:
       DO 6 ICOL = 1,3
        AINV(IPASS,ICOL) = AINV(IPASS,ICOL)/PIVOT
        IF (ICOL .GE. IPASS) THEN
         B(IPASS,ICOL) = B(IPASS,ICOL)/PIVOT
        ENDIF
6      CONTINUE
C...Replace each row by the row plus a multiple of the pivot row with the
C   factor chosen so that the element of [B] in the pivot column is 0:
       DO 8 IROW = 1,3
        IF (IROW .NE. IPASS) THEN
         FACTOR = B(IROW,IPASS)         ! set the factor for this row
        ENDIF
        DO 7 ICOL = 1,3
         IF (IROW .NE. IPASS) THEN
          AINV(IROW,ICOL) = AINV(IROW,ICOL)-FACTOR*AINV(IPASS,ICOL)
          B(IROW,ICOL) = B(IROW,ICOL)-FACTOR*B(IPASS,ICOL)
         ENDIF
7       CONTINUE
8      CONTINUE
10    CONTINUE
      DET = A(1,1)*A(2,2)*A(3,3)-A(1,1)*A(2,3)*A(3,2)+
     +A(1,2)*A(2,3)*A(3,1)-A(1,2)*A(2,1)*A(3,3)+
     +A(1,3)*A(2,1)*A(3,2)-A(1,3)*A(2,2)*A(3,1)
      RETURN
      END

      SUBROUTINE STRN33(E33,KE)
* * * * * * * * * * * * * * * * * * * * * * * * * * * * * * * * * * * * * *
*     The subroutine calculates the average Ezz strain of a wedge-shaped      *
*  element from the finite element result.                                    *
*                                                                             *
*  --- Subroutine input: KE, data file 8                                      *
*  --- Subroutine output: E33                                                 *
```

```
*                                                                      *
*  --- Definition of local variables:                                 *
*  KE          The element number in the layer(segment).              *
*  E33(i)      Array for the average Ezz strain of the i-th element.  *
*  STRNZZ(i,j) Array for the FE result of strains within a wedge-shaped *
*              element, which is attached on the crack front. The i-th row *
*              stores strain components at the i-th Gaussian integration *
*              point, i=1..8. Strain components from 1st to 6th column are *
*              [Exx,Eyy,Ezz,Exy,Eyz,Exz], respectively.               *
* * * * * * * * * * * * * * * * * * * * * * * * * * * * * * * * * * * * *
      IMPLICIT DOUBLE PRECISION (A-H,O-Z)
      DIMENSION STRNZZ(8,6),E33(24)

C...Read strain data within a wedge-shaped element (the element attached on the
C   crack front):
      READ (8,1405) (STRNZZ(1,J),J=1,6)
1405  FORMAT (////9X,6(E12.5))          ! ANSYS 5.5 format
1406  FORMAT (9X,6(E12.5))
      DO 1410 I = 2,8
       READ (8,1406) (STRNZZ(I,J),J=1,6)
1410  CONTINUE
C...Calculate average strain_33 at the mid-side node on crack front:
      E33(KE) = (STRNZZ(4,3)+STRNZZ(8,3))/2
1500  RETURN
      END
```